

1977

Stability analysis of space stayed columns by the finite element method.

Ibrahim Abdel-Salam. Hathout
University of Windsor

Follow this and additional works at: <http://scholar.uwindsor.ca/etd>

Recommended Citation

Hathout, Ibrahim Abdel-Salam., "Stability analysis of space stayed columns by the finite element method." (1977). *Electronic Theses and Dissertations*. Paper 3568.

This online database contains the full-text of PhD dissertations and Masters' theses of University of Windsor students from 1954 forward. These documents are made available for personal study and research purposes only, in accordance with the Canadian Copyright Act and the Creative Commons license—CC BY-NC-ND (Attribution, Non-Commercial, No Derivative Works). Under this license, works must always be attributed to the copyright holder (original author), cannot be used for any commercial purposes, and may not be altered. Any other use would require the permission of the copyright holder. Students may inquire about withdrawing their dissertation and/or thesis from this database. For additional inquiries, please contact the repository administrator via email (scholarship@uwindsor.ca) or by telephone at 519-253-3000ext. 3208.



National Library of Canada

Cataloguing Branch
Canadian Theses Division

Ottawa, Canada
K1A 0N4

Bibliothèque nationale du Canada

Direction du catalogage
Division des thèses canadiennes

NOTICE

The quality of this microfiche is heavily dependent upon the quality of the original thesis submitted for microfilming. Every effort has been made to ensure the highest quality of reproduction possible.

If pages are missing, contact the university which granted the degree.

Some pages may have indistinct print especially if the original pages were typed with a poor typewriter ribbon or if the university sent us a poor photocopy.

Previously copyrighted materials (journal articles, published tests, etc.) are not filmed.

Reproduction in full or in part of this film is governed by the Canadian Copyright Act, R.S.C. 1970, c. C-30. Please read the authorization forms which accompany this thesis.

**THIS DISSERTATION
HAS BEEN MICROFILMED
EXACTLY AS RECEIVED**

AVIS

La qualité de cette microfiche dépend grandement de la qualité de la thèse soumise au microfilmage. Nous avons tout fait pour assurer une qualité supérieure de reproduction.

S'il manque des pages, veuillez communiquer avec l'université qui a conféré le grade.

La qualité d'impression de certaines pages peut laisser à désirer, surtout si les pages originales ont été dactylographiées à l'aide d'un ruban usé ou si l'université nous a fait parvenir une photocopie de mauvaise qualité.

Les documents qui font déjà l'objet d'un droit d'auteur (articles de revue, examens publiés, etc.) ne sont pas microfilmés.

La reproduction, même partielle, de ce microfilm est soumise à la Loi canadienne sur le droit d'auteur, SRC 1970, c. C-30. Veuillez prendre connaissance des formules d'autorisation qui accompagnent cette thèse.

**LA THÈSE A ÉTÉ
MICROFILMÉE TELLE QUE
NOUS L'AVONS REÇUE**

STABILITY ANALYSIS OF SPACE STAYED COLUMNS
BY THE FINITE ELEMENT METHOD

by

Ibrahim Abdel-Salam Hathout
B.Sc. (Honor)

A Thesis
submitted to the Faculty of Graduate Studies
through the Department of
Civil Engineering in Partial Fulfillment of the
requirements for the Degree
of Master of Applied Science at
the University of Windsor

Windsor, Ontario, Canada

1977

Ibrahim Abdel-Salam Hathout 1977 .

000000

DEDICATION

To My Father
Abdel-Salam Hathout
In his eleventh memory

ABSTRACT

This dissertation deals with the stability analysis of single-crossarm space stayed columns which are acted upon by a concentrated axial load. Two methods of predicting the critical load and the corresponding buckling mode are considered. The two methods are (1) the nonlinear analysis based on the stability functions, and (2) geometrically nonlinear analysis by the finite element method. In the first method the stiffness matrix is written in terms of the stability functions to account for the change in the bending stiffness as the axial load is increased. In the second method the geometric stiffness matrix in three dimensions was developed based on retaining the quadratic terms in the expression of strain energy and discarding the higher order terms. The two methods of predicting the critical load were programmed and were run on an IBM System/360 computer. The parameters of the single-crossarm stayed column with three and four crossarm members were varied to determine the effect on the predicted critical load, buckling mode and the relative efficiency. The influence of end conditions on the buckling behavior of a single-crossarm stayed column with three crossarm members were briefly

investigated. Three cases of end conditions are considered: (1) both ends fixed; (2) one end fixed and the other end hinged; and (3) one end fixed and the other end free.

The theoretical results indicate that the buckling behavior of the stayed columns is heavily dependent upon the stay properties and the crossarm member length. It has been found that the buckling strength of the stayed column with four crossarm members is always higher than that of three crossarm members regardless of the stay properties and the crossarm member length. Also, the single-crossarm stayed column with three crossarm members is generally more efficient than that of four crossarm members.

An important conclusion is that since in the finite element method the process is non-iterative it is therefore much more convenient for a computer solution. At the same time it should be pointed out that, in solving for critical loading as an eigenvalue problem, the presence of the geometric stiffness matrix is absolutely essential when using the finite element method. Finally, it can be said with great confidence that the stability analysis of any uniform space stayed column is now possible.

ACKNOWLEDGEMENTS

The author is greatly indebted to his thesis advisor, Dr. Murray C. Temple for his encouragement, advice, and valuable suggestions during the preparation of this dissertation. The guidance of Professors John B. Kennedy, George Abdel-Sayed and John S. Ellis, the members of the special committee discussing the author's work on November 28, 1975, is gratefully acknowledged. The author wishes to express his sincere gratitude to Professor G. R. Monforton for his help and advice.

Thanks are due to:

- The Computer Center at the University of Windsor for running the computer programs,
- The Defense Research Board whose financial assistance made this research possible.

The manuscript was typed with care by Mrs. Shirley V. Morgan, Miss Stella Hui and Mrs. Doreen Truant, their cooperation is appreciated.

TABLE OF CONTENTS

	<u>Page</u>
ABSTRACT	v
ACKNOWLEDGEMENTS	vii
LIST OF ILLUSTRATIONS	xii
LIST OF TABLES	xv
NOTATION	xvi
Chapter 1 INTRODUCTION	
1.1 General	1
1.2 Purpose of research	5
1.3 System to be studied	5
1.4 Previous work	7
Chapter 2 METHODS OF ANALYSIS	
2.1 Introduction	10
2.2 The nonlinear analysis based on the stability functions	11
2.2.1 General	11
2.2.2 Characteristic value problem	12
2.2.3 Generation of element stability stiffness matrix	15
2.3 Geometrically nonlinear analysis by the finite element method	19
2.3.1 General	19
2.3.2 General theories	19
2.3.3 Theoretical development	22

	<u>Page</u>
2.4 Calculating the Critical Load	33
2.5 Transformations	36
Chapter 3 COMPUTER PROGRAMS FOR THE ANALYSIS OF SPACE STAYED COLUMNS	
3.1 General	44
3.2 The first program based on the stability functions	45
3.2.1 Description of computer program	45
3.2.2 Subroutines	46
STAFUN	
STASM	
TRANS	
MULT	
BAKY	
EIGEN	
3.2.3 Main program	47
3.2.4 Critical loads other than the first	49
3.3 The second program based on the finite element method	51
3.3.1 Description of the program	51
3.3.2 Subroutines	51
ELAKM	
GEOKM	
TRANS	
MULT	
ARRAY	
NROOT	
DODY.	
3.3.3 Main program	52
Chapter 4 INFLUENCE OF THE CROSSARM MEMBER LENGTH ON THE BUCKLING BEHAVIOR	
4.1 General	54

	<u>Page</u>
4.2 Influence of crossarm member length	55
4.3 Modes of buckling	60
Chapter 5 INFLUENCE OF THE STAY PROPERTIES ON BUCKLING BEHAVIOR	
5.1 General	63
5.2 Influence of stay size	64
5.3 Influence of stay modulus of elasticity	70
Chapter 6 THE RELATIVE EFFICIENCY OF THE STAYED COLUMNS	
6.1 General	76
6.2 Influence of the crossarm member length	77
6.3 Effect of stay size	80
Chapter 7 INFLUENCE OF END CONDITIONS ON BUCKLING BEHAVIOR	
7.1 General	82
7.2 Influence of crossarm member length	83
7.3 Influence of stay size	85
7.4 The relative efficiency	88
7.5 Modes of instability	90
7.6 Numerical example	94
Chapter 8 SUMMARY, CONCLUSION AND RECOMMENDATIONS	
8.1 Summary	99
8.2 Conclusion	101
8.3 Recommendations	103

	<u>Page</u>
ILLUSTRATIONS	105
APPENDIX A LARGE DEFLECTION STRAIN DISPLACEMENT EQUATION IN THREE-DIMENSIONS ANALYSIS	149
APPENDIX B GENERATION OF DISPLACEMENT FUNCTIONS FOR A SPACE FRAME ELEMENT BY THE USE OF INTERPOLATION FORMULAS	153
APPENDIX C LISTING OF COMPUTER PROGRAMS	163
BIBLIOGRAPHY	180
VITA AUCTORIS	182

LIST OF FIGURES

		<u>Page</u>
Fig. 1-1	Single Crossarm Space Stayed Columns	105
Fig. 2-1	Stability Stiffness Matrix for Frame Element in 3-Dimensions	106
Fig. 2-2	The Conventional Small Deflection Stiffness Matrix for Frame Element in 3-Dimensions	107
Fig. 2-3	Geometric Stiffness Matrix for Frame Element in 3-Dimensions	108
Fig. 4-1	Influence of Crossarm Member Length on the Buckling Behavior ($\phi_{stay} = 3/16$ in.)	109
Fig. 4-2	The Additional Horizontal Force at the Crossarm Level	110
Fig. 4-3	Influence of Crossarm Member Length on the Buckling Behavior ($\phi_{stay} = 4/16$ in.)	111
Fig. 4-4	Influence of Crossarm Member Length on the Buckling Behavior ($\phi_{stay} = 5/16$ in.)	112
Fig. 4-5	Influence of Crossarm Member Length on the Buckling Behavior ($\phi_{stay} = 6/16$ in.)	113
Fig. 4-6	Influence of Crossarm Member Length on the Buckling Behavior ($\phi_{stay} = 7/16$ in.)	114
Fig. 4-7	Influence of Crossarm Member Length on the Buckling Behavior ($\phi_{stay} = 8/16$ in.)	115
Fig. 4-8	Influence of Crossarm Member Length on the Buckling Behavior ($\phi_{stay} = 9/16$ in.)	116
Fig. 4-9	Influence of Crossarm Member Length on the Buckling Behavior ($\phi_{stay} = 10/16$ in.)	117
Fig. 4-10	Influence of Crossarm Member Length on the Buckling Behavior ($\phi_{stay} = 12/16$ in.)	118

	<u>Page</u>
Fig. 4-11 Modes and Model of Buckling	119
Fig. 5-1 Influence of Stay Diameter on the Buckling Behavior ($L/lca = 10$)	120
Fig. 5-2 Model of Buckling and the Restraining Couple at the Crossarm Level	121
Fig. 5-3 Influence of Stay Diameter on the Buckling Behavior ($L/lca = 9$)	122
Fig. 5-4 Influence of Stay Diameter on the Buckling Behavior ($L/lca = 8$)	123
Fig. 5-5 Influence of Stay Diameter on the Buckling Behavior ($L/lca = 7$)	124
Fig. 5-6 Influence of Stay Diameter on the Buckling Behavior ($L/lca = 6$)	125
Fig. 5-7 Influence of Stay Diameter on the Buckling Behavior ($L/lca = 5$)	126
Fig. 5-8 Influence of Stay Diameter on the Buckling Behavior ($L/lca = 4$)	127
Fig. 5-9 Influence of Stay Diameter on the Buckling Behavior ($L/lca = 2$)	128
Fig. 5-10 Influence of Stay Modulus of Elasticity and Crossarm Member Length ($\phi = 0.25$ in.)	129
Fig. 5-11 Influence of Stay Modulus of Elasticity and Crossarm Member Length ($\phi = 0.5$ in.)	130
Fig. 5-12 Influence of Stay Modulus of Elasticity and Stay Size ($L/lca = 10$)	131
Fig. 5-13 Influence of Stay Modulus of Elasticity and Stay Size ($L/lca = 6$)	132
Fig. 5-14 Influence of Varying the Stay Modulus of Elasticity on Buckling Behavior	133
Fig. 6-1 Influence of Crossarm Member Length on the Relative Efficiency ($\phi = 3/16$ in.)	134
Fig. 6-2 Influence of Crossarm Member Length on the Relative Efficiency ($\phi = 4/16$ in.)	135

	<u>Page</u>	
Fig. 6-3	Influence of Crossarm Member Length on the Relative Efficiency ($\phi = 5/16$ in.)	135
Fig. 6-4	Influence of Crossarm Member Length on the Relative Efficiency ($\phi = 6/16$ in.)	136
Fig. 6-5	Influence of Crossarm Member Length on the Relative Efficiency ($\phi = 7/16$ in.)	136
Fig. 6-6	Influence of Crossarm Member Length on the Relative Efficiency ($\phi = 8/16$ in.)	137
Fig. 6-7	Influence of Crossarm Member Length on the Relative Efficiency ($\phi = 9/16$ in.)	137
Fig. 6-8	Influence of Crossarm Member Length on the Relative Efficiency ($\phi = 10/16$ in.)	138
Fig. 6-9	Influence of Crossarm Member Length on the Relative Efficiency ($\phi = 12/16$ in.)	138
Fig. 6-10	Influence of Stay Size on the Maximum Value of the Relative Efficiency	139
Fig. 7-1	Influence of Crossarm Member Length and End Conditions on the Buckling Behavior	140
Fig. 7-2	Modes of Buckling for three cases of End Conditions	141
Fig. 7-3	Influence of Stay Size and End Conditions on the Buckling Behavior	142
Fig. 7-4	Influence of Crossarm Member Length and End Conditions on the Relative Efficiency	143
Fig. 7-5	Model and possible Modes of Buckling for the case of two Fixed Ends	144
Fig. 7-6	Model and possible Modes of Buckling for the case of one End Fixed and the other Hinged	145
Fig. 7-7	Modes of Buckling for the case of one End Fixed and the other Free	146
Fig. 7-8	Triple Crossarm Space Stayed Column (Numerical Example)	147
Fig. 7-9	Modes of Buckling for the Triple Crossarm Stayed Column	148

LIST OF TABLES

		<u>Page</u>
Table 1.I	The Data Considered for the two Systems in the case of Hinged End Conditions	6
Table 1.II	The Data Considered for the Single Crossarm Stayed Column with three Crossarm Members with Different End Conditions	7
Table 4.I	Values of Length Parameter, L_p , for Various Values of the Crossarm Member Length , l_{ca}	58
Table 5.I	Values of the Denominator, D , (see Eq. 5.8) for Various Values of the Stay Diameter	68
Table 7.I	Data Considered for the Triple Cross-arm Stayed Column (Numerical Example)	95
Table 7.II	Stay Diameters and Modulus of Elasticity of the Stays for the four cases considered in the Numerical Example	96
Table 7.III	Results obtained by the Computer Program for the four cases considered in the Numerical Example	96

NOTATION

English Alphabet

A	= cross-sectional area
A_S	= stay cross-sectional area
a	= $\frac{F_d}{\Delta m_a}$
b	= distance
c	= carry-over factor, a stability function
c_1, c_2, c_3	= local coordinate axes
c'_1, c'_2, c'_3	= local coordinate axes (see Section 2.4)
D	= see Eq. (5.8)
d_S	= diameter of the stay
E	= modulus of elasticity
E_S	= stay modulus of elasticity
e_1, e_2, e_3	= unit vectors in the directions of c_1, c_2, c_3 respectively
F	= force
F_a	= horizontal component of the additional force in the stay
f(S)	= function (see Appendix B)
f_1, f_2	= values of function f(s) at o and b
G	= modulus of rigidity
$H_{ni}^{(N)}(s)$	= polynomials (see Appendix B)
I_1 to I_6	= integrals

I_x, I_y	= moment of inertia about x and y axes
I_{ca}	= moment of inertia of the crossarm
$[I_M]$	= unit matrix
I_z	= torsional constant
$\underline{i}, \underline{j}, \underline{k}$	= unit vectors along X, Y, Z axes
$[K]$	= stiffness matrix
$[K_E]$	= elastic stiffness matrix
$[\tilde{K}_E]$	= elastic stiffness matrix in local coordinates
$[K_G]$	= geometric stiffness matrix
$[\tilde{K}_G]$	= geometric stiffness matrix in local coordinates
$ K $	= determinant of stiffness matrix
k	= $\frac{EI}{L}$
k_{ij}	= an element of the stiffness matrix
L	= length
L_s	= length of the stay
L_1	= $(l_1^2 + n_1^2)^{1/2}$
L_p	= length parameter (see Eq. 4.6)
l_{ca}	= crossarm member length
l_1, m_1, n_1	= direction cosines
m_a	= inverse of magnification factor = $1 - \frac{P}{(P_{cr})_n}$
m	= sway stability function
N	= number of derivatives that the set can interpolate
$[N_1], [N_2]$	= see Section 2.3.2

n = order of stiffness matrix
 P_E = Euler load
 P_{cr} = critical load
 P = axial load
 P^* = unit load
 $\{P\}$ = vector of nodal forces in global coordinates
 $\{\bar{P}\}$ = vector of end forces in local coordinate
 $[R]$ = member orientation matrix
 REF = relative efficiency
 r = radius
 S = stiffness stability function
 T_a = additional force in the stay
 $[T]$ = transformation matrix
 U_s = strain energy
 $\{U\}$ = vector of nodal displacement in global coordinates
 $\{u\}$ = vector of end displacements in global coordinates
 $\{\bar{u}\}$ = vector of end displacements in local coordinates
 u, v, w = displacements in x, y, z directions
 $\bar{u}_p, \bar{u}_q, \bar{v}_p, \bar{v}_q,$
 \bar{w}_p, \bar{w}_q = end displacement in local coordinates
 V = volume
 V_a = vertical component of the additional force in the stay

x, y, z = local coordinates
 X, Y, Z = global coordinates

Greek Letters

α = angle (see Section 2.5)
 β = angle of rotation
 β_p, β_q = end rotations about the longitudinal axis
 γ = shear strain
 Δ = general displacements
 δ_c = displacement of the column at the crossarm level
 δ_{ca} = deflection at the end of the crossarm member
 ϵ = normal strain
 η = see Appendix B
 θ = angle = $\cos^{-1} \frac{l_{ca}}{L}$
 θ_p, θ_q = end rotation about y axis
 λ = eigenvalue
 λ_p, λ_q = end rotation about z axis
 μ = $\frac{P}{P^*}$
 ρ = $\frac{P}{P_E}$
 σ = normal stress
 τ = shear strain
 ϕ = diameter of the stay
 ψ = the angle of rotation of the buckled column at the crossarm
 ω = $\frac{\pi}{2} \sqrt{\rho}$

CHAPTER 1

INTRODUCTION

1.1 General

In the last few decades it has been widely recognized in the field of structural engineering that theory of buckling is an indispensable basis for design of structures. That is because of the fact that the strength of structures is heavily dependent upon structural instability. Numerous research articles have been published on various aspects of this vast subject. This work was greatly aided by the development of matrix methods of structural analysis for use on modern high speed digital computer.

One of the interesting problems that arose in the field of structural instability in the last decade was the stability analysis of stayed columns. It was found that the buckling strength of a concentrically loaded, pin-ended, slender metal column may be increased many

times by reinforcing it with rigidly connected crossarm members and pretensioned stays. These stayed columns can be used as 1) supports to hold plates in place during the erection of large plate structures, 2) side booms for the mast of a derrick, 3) masts for ships, etc.

In this thesis the study is focused on the stability analysis of the single-crossarm space stayed columns with three and with four crossarm members. It should be noted that in the space stayed column the buckling is not confined in a certain plane and hence must be treated as a three-dimensional structure. In general many alternative methods can be used to analyze the nonlinear problems. In this research the finite element method has been selected.

In the last decade the finite element method appears to offer many advantages, and its relatively simple logic makes it ideally suited for the computer. Now the finite element method is widely accepted as a method of stress analysis. Progress in the finite element method has been made in three fronts, all of which contribute to the strength and flexibility of the method. First, the relation of the finite element method to previous well-established methods in continuum mechanics has given it a firm foundation. Secondly, the search for and development of many consistent elements has given

it a wide area of application. Finally, extension of the method to the study of nonlinear behavior in both material and geometric nonlinearities has resulted in more realistic models and design methods.

In fact nonlinear theory is inevitably more complex than the corresponding linear theory. Consequently, the application of nonlinear theory to physical problems leads to mathematical problems which are usually intractable. This is not surprising since a similar situation often arises in connection with the intrinsically simpler linear problem. In fact, it was just this situation which led to the development of the finite element method in the first place.

At the present time, finite elements offer the greatest promise for solving complex nonlinear problems. The practical analyst has been aware of this for some time and has done much to lay down the foundations for providing such a capability. Progress and results achieved during the last decade indicate that significant advances can be expected during the decade which lies just ahead.

It should be emphasized here that material or physical nonlinearity is not considered in this study. Only geometric nonlinearity is considered which results in two classes of engineering problems, the large deflection problem and the problem of structural stability.

Two methods of determining the critical load and the corresponding buckling mode are investigated in Chapter 2. The two methods are (1) the nonlinear analysis based on the stability functions, and (2) geometrically nonlinear analysis by the finite element method.

The two methods of determining the critical loads were computerized for an IBM System/360 Computer. In Chapter 3 the two computer programs are discussed in detail.

In Chapter 4 the influence of the crossarm member length on the buckling behaviour of the single-crossarm stayed columns with three and four crossarm members is examined.

Investigation in Chapter 5 deals with the influence of stay properties on the buckling behavior of the single-crossarm stayed columns.

In Chapter 6 the influence of crossarm member length on the relative efficiency and the influence of the stay size on the maximum value of the relative efficiency are examined.

The effect of the end conditions on the buckling behaviour of the single-crossarm stayed column with three crossarm members are studied in Chapter 7. A numerical example is given to illustrate the power of the finite element method in the stability analysis of space stayed columns.

In Chapter 8 summary, conclusions and recommendations are presented.

1.2 Purpose of Research

The purpose of this research can be summarized as follows:

1) To establish an analytical method of predicting the critical load and the corresponding buckling mode for any three-dimensional stayed column.

2) To investigate the effect of varying certain parameters of the stayed column on the buckling behavior.

3) To compare the relative efficiency of the single-crossarm stayed columns with three and four crossarm members.

4) To investigate the effect of varying the end conditions of the stayed column on the buckling behavior.

1.3 System to be Studied

In this research two systems are considered: a single-crossarm stayed column with three crossarm members, and the other with four crossarm members as illustrated in Fig. 1-1.

In both systems it is assumed that:

1) The axial deformation of the column and the crossarms have a negligible effect on the buckling

behavior.

2) The connections between the crossarm members and the column are assumed perfectly rigid.

3) The stayed column is ideally concentrically loaded. This means that there is no initial eccentricity or crookedness and that there is no lateral deflection of the column prior to bifurcation.

4) The axial load in the crossarms is negligible compared to its critical load.

5) At the instant of buckling there is a small residual pretension force left in the stays. This implies that all stays are effective in resisting displacements of the stayed column.

In the analysis presented in Chapters 4 to 6 (i.e. hinged end conditions) it is assumed:

No. of System	(1)	(2)
	3 crossarms	4 crossarms
Elements	13	16
Elements with bending stiffness	7	8
Elements with significant axial load	4	4
Nodes	8	9
Nodes in columns	5	5
Degrees of freedom	37	43

Table 1.1

It is assumed that the displacement u, v, w and the rotation about the longitudinal axis are prevented at both ends of the column.

In the analysis presented in Chapter 7 (i.e. different end conditions) it is assumed:

No. of System	both ends fixed	one end fixed and the other end hinged	one end fixed and the other end free
Element's	13	13	13
Elements with bending stiffness	7	7	7
Elements with significant axial load	4	4	4
Nodes	8	8	8
Nodes in columns	5	5	5
Degrees of freedom	33	35	42

Table 1.II

1.4 Previous Work

In 1963, Chu and Berge⁽¹⁾ developed a general solution for the elastic buckling load of a slender, pin-ended column stayed with tension ties and multiple ideally pin-connected crossarms. The solution indicated that the maximum buckling load that could be achieved would be a four-fold strength increase over the Euler Load, regardless of the number of symmetrically placed

intermediate crossarm supports.

In 1967, Mauch and Felton⁽²⁾ continued the work of Chu and Berge by developing an analytical foundation for the rational design of these columns, such as exists for simple columns. Their analysis indicated that at low values of structural index (i.e. P/L^2) columns supported by tension ties offer potential savings of up to 50% of the weight of optimum simple tubular columns.

In 1970, as a design-build-test project, a single-crossarm stayed column was studied by the Civil Engineering undergraduate students at the Royal Military College of Canada as their fourth year project⁽³⁾. The crossarm member was rigidly connected, by means of welding, to the column. The test result was a sevenfold increase in the buckling strength of the column.

In 1971, Pearson⁽⁴⁾ examined the behavior of a single-crossarm stayed column with a high slenderness ratio when loaded to its buckling point. The effect on column strength of stay eccentricity and pretension force were examined experimentally only. The result indicated that buckling strength is directly proportional to stay eccentricity and pretension.

During 1971, at the Royal Military College of Australia, Ellis introduced a stayed column with three sets of crossarm members along its length. Buckling

strength increases of 20 and 23 times that of the unstayed column were achieved experimentally for the two pin-ended stayed columns tested. In 1972, four experiments on pin-ended triple-crossarm stayed columns were conducted at the Royal Military College of Canada by McCaffrey. Test results with strength increases ranging from 34 to 45 times that of the Euler buckling load of the unstayed column were obtained.

In January 1975, Smith, McCaffrey and Ellis⁽⁵⁾ published a paper in which they developed an analytical solution to predict the buckling load associated with each of two assumed modes of failure for single-crossarm stayed columns.

In 1976, Temple⁽⁶⁾ developed an analytical solution to predict the buckling load and the corresponding buckling shape for a single, double and triple-crossarm stayed column by the finite element method.

CHAPTER 2

ANALYTICAL METHODS FOR PREDICTION OF CRITICAL LOAD

2.1 Introduction

Two approaches have been selected for solving the present problem. The two approaches are 1) the analysis based on the stability functions, and 2) the analysis by the finite element method. The first approach requires an iterative solution. With the finite element approach, the buckling loads are obtained directly. Thus, the latter approach requires less computer time. For this reason the finite element approach is used to analyze the problem. The first approach is the so-called "exact" solution and is used to check the results obtained by the finite element approach. The two approaches will be discussed subsequently in detail. It should be noted that excellent results may be obtained by the finite element approach when a reasonable number of finite elements are used. Therefore the

finite element approach is believed to be the best solution for the present problem.

2.2 Method I: Analysis Based on the Stability Functions

2.2.1 General

One common method used to determine whether a structure containing axially loaded members is stable or unstable is to study the behavior of such a system under the effect of disturbing forces. If after removing the disturbing force, the structure goes back to its original position, it is in stable equilibrium. If the structure remains in its deflected configuration then it is in neutral equilibrium and the axial load is the critical load. If the deflection increases indefinitely when an infinitely small disturbing force is applied, then the structure was in a position of unstable equilibrium.

When the disturbing forces are applied the equilibrium equations may be written in matrix form as:

$$[K]\{\Delta\} = \{F_d\} \quad (2.1)$$

where $[K]$ is the stiffness matrix for the complete structure, $\{\Delta\}$ is the vector of displacements, and $\{F_d\}$ is the vector of disturbing forces. It will be shown later that the elements of the stiffness matrix will be written in terms of stability functions to account for the change in bending

stiffness as the axial load is increased.

For the most part, stability analysis has been transformed into an eigenvalue problem that predicts the buckling load and the buckling mode. This approach will be discussed subsequently in detail.

2.2.2 Characteristic Value Problem

Eqs.2.1 can be expanded as follows:

$$\begin{bmatrix} k_{11} & k_{12} & \dots & \dots & \dots & k_{1n} \\ k_{21} & k_{22} & \dots & \dots & \dots & k_{2n} \\ \cdot & \cdot & & & & \cdot \\ \cdot & \cdot & & & & \cdot \\ \cdot & \cdot & & & & \cdot \\ k_{n1} & k_{n1} & \dots & \dots & \dots & k_{nn} \end{bmatrix} \begin{Bmatrix} \Delta_1 \\ \Delta_2 \\ \cdot \\ \cdot \\ \cdot \\ \Delta_n \end{Bmatrix} = \begin{Bmatrix} F_{d1} \\ F_{d2} \\ \cdot \\ \cdot \\ \cdot \\ F_{dn} \end{Bmatrix} \quad (2.2)$$

The displacements may be written as (7,8)

$$\begin{aligned} \Delta_1 &= \frac{\Delta_{d1}}{1 - \frac{P}{(P_{cr})_1}} = \frac{\Delta_{d1}}{m_a} = \frac{F_{d1}}{a_1 m_a} \\ \cdot & \\ \cdot & \\ \Delta_j &= \frac{\Delta_{dj}}{1 - \frac{P}{(P_{cr})_j}} = \frac{\Delta_{dj}}{m_a} = \frac{F_{dj}}{a_j m_a} \\ \cdot & \\ \cdot & \\ \Delta_n &= \frac{F_{dn}}{a_n m_a} \end{aligned} \quad (2.3)$$

Eqs. 2.3 can be written as follows:

$$\begin{Bmatrix} F_{d1} \\ \cdot \\ \cdot \\ \cdot \\ F_{dn} \end{Bmatrix} = \begin{Bmatrix} \Delta_1 a_1 m_a \\ \cdot \\ \cdot \\ \cdot \\ \Delta_n a_n m_a \end{Bmatrix}, \quad (2.4)$$

Substituting Eqs. 2.4 into Eqs. 2.2 and rearranging, the following system of equations is obtained:

$$\begin{bmatrix} k_{11} - a_1 m_a & k_{12} & \cdot & \cdot & \cdot & k_{1n} \\ k_{21} & k_{22} - a_2 m_a & \cdot & \cdot & \cdot & k_{2n} \\ \cdot & \cdot & \cdot & \cdot & \cdot & \cdot \\ \cdot & \cdot & \cdot & \cdot & \cdot & \cdot \\ \cdot & \cdot & \cdot & \cdot & \cdot & \cdot \\ k_{n1} & k_{n2} & \cdot & \cdot & \cdot & k_{nn} - a_n m_a \end{bmatrix} \begin{Bmatrix} \Delta_1 \\ \Delta_2 \\ \cdot \\ \cdot \\ \cdot \\ \Delta_n \end{Bmatrix} = \begin{Bmatrix} 0 \\ 0 \\ \cdot \\ \cdot \\ \cdot \\ 0 \end{Bmatrix} \quad (2.5)$$

Since $m_a = 1 - P/(P_{cr})_j$, m_a approaches zero as P approaches any of the critical loads. Thus, at the critical load, the term $a m_a$ goes to zero regardless of the value of the constants a_1 to a_n . The terms $a m_a$ can thus be replaced with a single term λ .

Eqs. 2.5 can be written as follows:

$$\begin{bmatrix} k_{11} - \lambda & k_{12} & \dots & k_{1n} \\ k_{21} & k_{22} - \lambda & \dots & k_{2n} \\ \vdots & \vdots & \ddots & \vdots \\ k_{n1} & k_{n2} & \dots & k_{nn} - \lambda \end{bmatrix} \begin{Bmatrix} \Delta_1 \\ \Delta_2 \\ \vdots \\ \Delta_n \end{Bmatrix} = \begin{Bmatrix} 0 \\ 0 \\ \vdots \\ 0 \end{Bmatrix} \quad (2.6)$$

Since Eqs. 2.6 are homogeneous, they are consistent and always have a trivial solution ($\Delta = 0$). However, it is the nontrivial solutions that are of interest, and they will exist only if the determinant of the coefficient matrix is zero. Therefore

$$\begin{vmatrix} k_{11} - \lambda & k_{12} & \dots & k_{1n} \\ k_{21} & k_{22} - \lambda & \dots & k_{2n} \\ \vdots & \vdots & \ddots & \vdots \\ k_{n1} & k_{n2} & \dots & k_{nn} - \lambda \end{vmatrix} = 0 \quad (2.7)$$

This is a typical eigenvalue problem. The load must be varied until the minimum eigenvalue goes to zero. There are n eigenvalues and there may be as many as n critical loads. The eigenvector associated with each eigenvalue gives the relative value of the displacement components, that is, the buckled shape (9,10).

2.2.3 Generation of Element Stability Stiffness Matrix

The difficulty in the nonlinear structural analysis or the analysis in the presence of significant axial forces arises from the fact that the axial forces in the elements are themselves unknowns. Since the axial force in the elements of a structure varies, their individual stiffnesses change and so does the master stiffness matrix of the structure.

The stiffness matrix will be developed for an element in which the shear center and the centroid of its cross-section coincide⁽⁷⁾. Such a section is shown in Fig. 2.I.

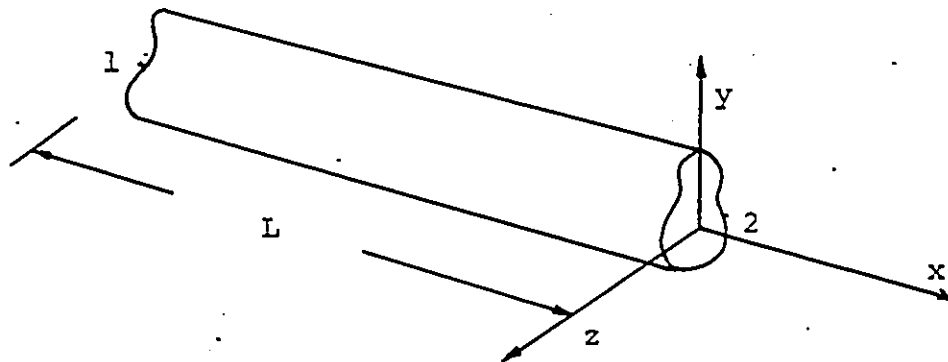


Fig. 2.I

To develop the stiffness matrix four types of deformations are required. They are:

1) axial - the AE/L terms, where A is the cross-sectional area, E the modulus of elasticity and L the length of the element,

- 2) torsion - the $I_x G/L$ terms, where I_x is the torsional constant, and G is the modulus of rigidity, and
- 3) translation of one end with respect to the other as shown below.

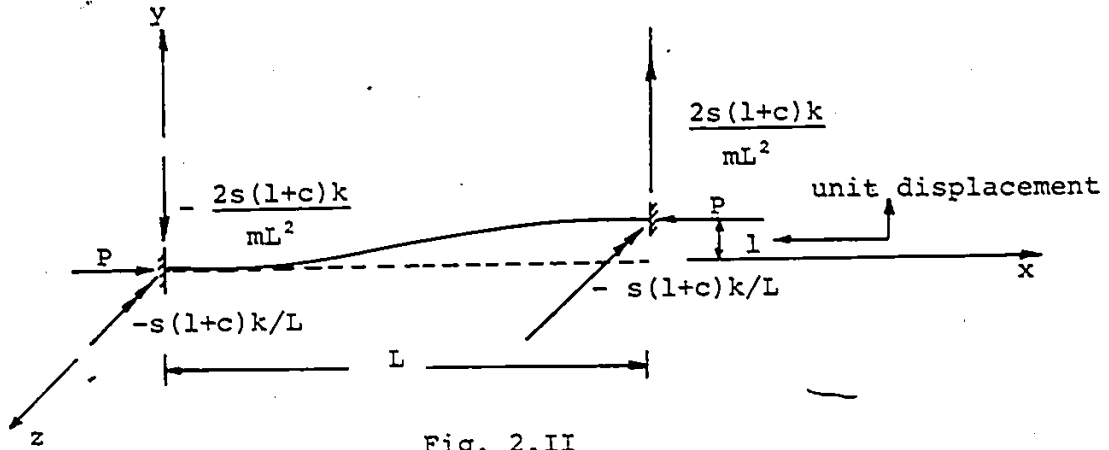


Fig. 2.II

- 4) rotation of one end,

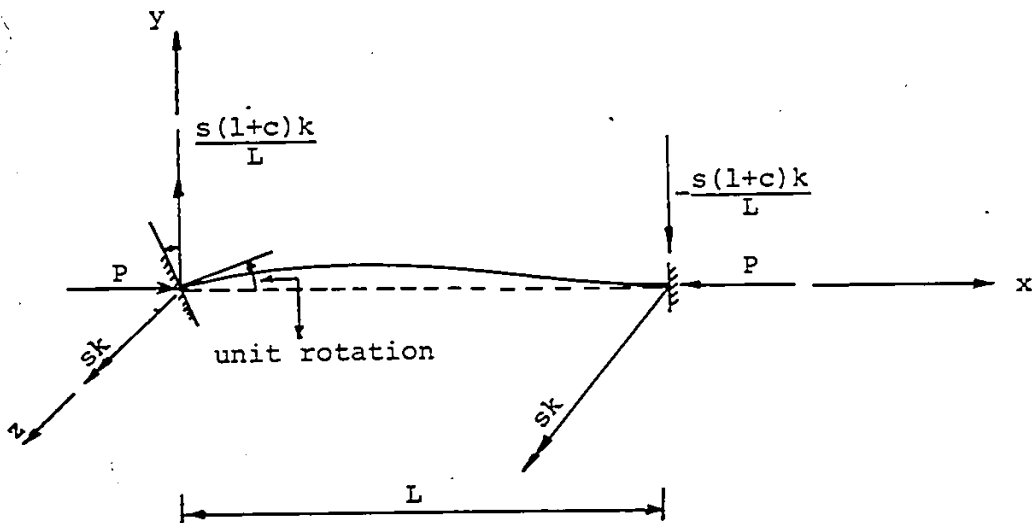


Fig. 2.III

where,*

$$k = EI_z/L$$

$$c = \frac{2\omega - \sin(2\omega)}{\sin(2\omega) - 2\omega \cos(2\omega)}$$

$$s = \frac{\omega(1 - 2\omega \cot(2\omega))}{\tan(\omega) - \omega}$$

$$m = \frac{2s(1+c)}{2s(1+c) - \pi^2 \rho} \quad (2.8)$$

and,

$$\omega = \frac{\pi}{2} \sqrt{\rho}$$

$$\rho = \frac{P}{P_E} \quad (2.9)$$

$$P_E = \frac{\pi^2 EI}{L^2}, \text{ the Euler load for the column.}$$

The expressions listed above which have been represented, for convenience, as $s, c,$ and m are called stability functions. This is not the complete listing of stability functions[†] used in structural problems but are the only ones required in this dissertation.

The complete element stability stiffness matrix

*Details of these stability functions can be found in Horne, M.R. and Marchant, W. (11)

[†]For detailed information and explanation refer to Majid (12).

is shown in Fig. 2-1. When the axial force is zero, $s = 4.0$, $c = 0.5$ and $m = 1.0$ and the element stability stiffness matrix becomes the familiar elastic stiffness matrix shown in Fig. 2-2.

2.3 Method II: Finite Element Analysis

2.3.1 General

As mentioned before geometric nonlinearity results in two classes of problems: the large deflection problem, and the problem of structural stability. The term "large deflections" is misleading since problems falling within this category need not have actual deflections which are in any sense large; in fact they can be, and often are, as small as those arising for the linear case. However, and this is important, the deformed configuration of the structure must be used when writing the equilibrium equations for the large deflection problem. In addition, the strain displacement equations must now include the appropriate higher order, nonlinear terms. Each of these effects introduces nonlinearity into the problem.

2.3.2 General Theories

In Ref. 13, the finite element theory for the geometrically nonlinear problem was established in terms of the Lagrangian strain tensor, and the principle of virtual displacements. Theoretical developments since then have occurred along several paths.

The development in Ref. 13 retained quadratic terms in nodal displacements in the expression for the strain

energy but discarded higher order terms. Although this formulation permitted large deflection and stability analyses to be undertaken, it left unanswered the question as to the possible importance of the discarded terms.

P.V. Marcal and R. Mallett presented an alternative development which retained these higher order terms. This led to a hierarchy of stiffness matrices which Mallett and Marcal called the initial displacement stiffness matrices*. These involve only three basic matrices, namely, $[K]$, $[N1]$ and $[N2]$. Matrix $[K]$ has been identified as the conventional linear stiffness matrix. Matrix $[N1]$ is a linear function of the displacements. The terms in this first order stiffness matrix represent the membrane and flexure actions of the element. Terms in the $[N2]$ matrix are quadratic and are confined to the flexure region of the matrix. The second-order stiffness matrix is essential to accurate predictions of behavior in the presence of significant nonlinearity. Mallett and Marcal emphasized that no post-buckled solutions exist in the absence of this matrix.

A third formulation due to Purdy and Przemieniecki showed that an alternative formulation was possible which also retained the higher order terms. This formulation is

*For detailed formulation and explanation refer to Mallett and Marcal⁽¹⁴⁾. Some comments by Martin on this approach can be found in Ref. 17. ³

very interesting in that it leads to the same stiffness matrices as in Ref. 13, which was developed on the basis of retaining only the quadratic terms; however, an additional generalized load vector is introduced to account for the higher order terms in the strain energy. A detailed formulation of this approach can be found in Refs. 16 and 17. In Ref. 17 Martin solved the nonlinear problem shown in Fig. 2.IV using several theories. These include the exact solution, the solution using the higher

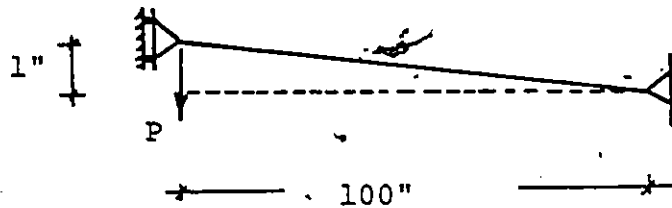


Fig. 2.IV

order initial displacement matrix of Mallett and Marcal, and the solution of Purdy and Przemieniecki. In addition, the solution based on the first order geometric stiffness matrix of Martin is also done. This analysis indicates surprising agreement between the exact solution and the solution by Purdy and Przemieniecki, and also indicates that the solution by Mallett and Marcal is extremely close to the solution by Martin and very close to the exact solution.

It should be emphasized here that the general theories mentioned above deal with a nonlinear analysis of plane structures.

2.3.3 Theoretical Development

To develop the geometric stiffness matrix for a three-dimensional element, consider the general prismatic space frame element with end displacements

$$\{\bar{u}\}^T = \{\bar{u}_p, \bar{v}_p, \bar{w}_p, \bar{\beta}_p, \bar{\theta}_p, \bar{\lambda}_p, \bar{u}_q, \bar{v}_q, \bar{w}_q, \bar{\beta}_q, \bar{\theta}_q, \bar{\lambda}_q\}$$

as shown in Fig. 2.V.

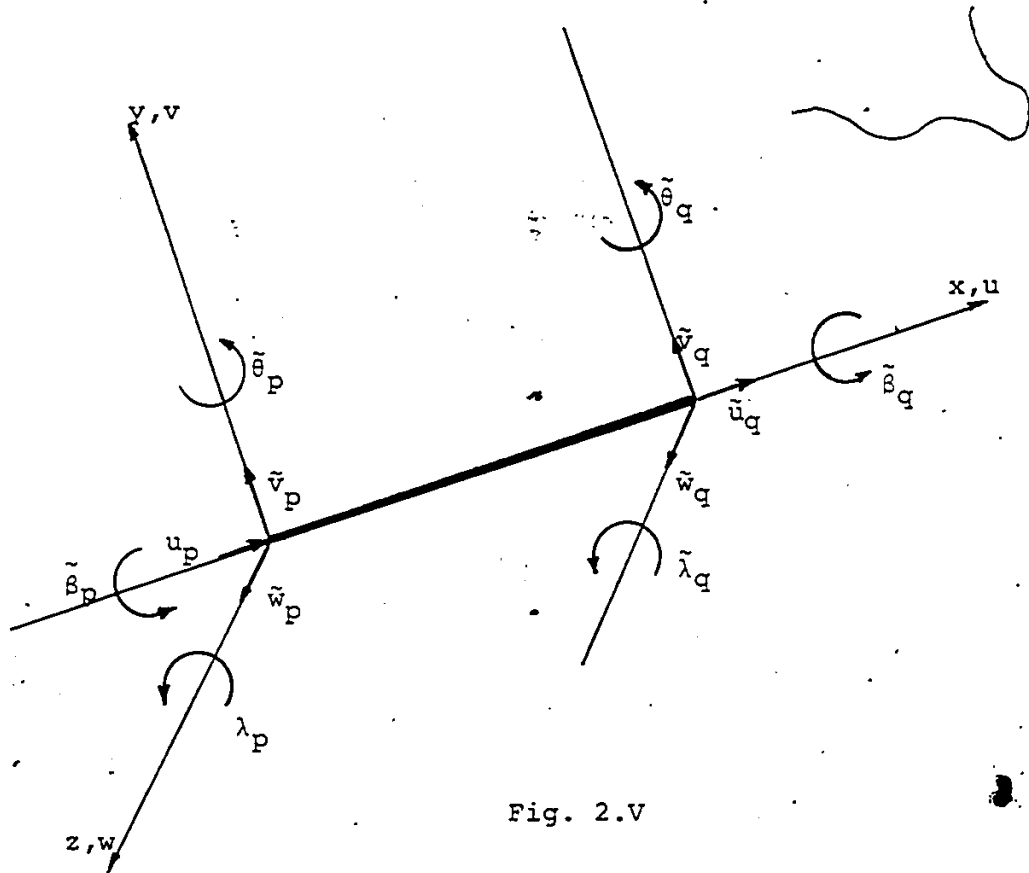


Fig. 2.V

The total strain energy is the sum of the strain energy due to the normal strain and shear strain.

$$U_s = U_{sn} + U_{ss} \quad (2.10)$$

in which U_s is the total strain energy, U_{sn} is the strain energy due to normal strain and U_{ss} is the strain energy due to shear strain.

And,

$$U_{sn} = \int_v \left(\int_0^{\epsilon_{xx}} \sigma d\epsilon \right) dv$$

$$U_{ss} = \int_v \left(\int_0^{\gamma} \tau d\gamma \right) dv \quad (2.11)$$

where σ and τ are the normal and shear stress respectively.

Introducing Hooke's Law $\sigma = E\epsilon$, $\tau = G\gamma$ and substituting into Eq. 2.11 and then into Eq. 2.10 leads to

$$U_s = \frac{E}{2} \int_v \epsilon_{xx}^2 dv + \frac{G}{2} \int_v \gamma^2 dv \quad (2.12)$$

in which E is the modulus of elasticity, ϵ_{xx} is the normal strain and γ is the shear strain.

Referring to Appendix A, the normal strain can be written as

$$\epsilon_{xx} = \frac{d\tilde{u}}{dx} - y \frac{d^2\tilde{v}}{dx^2} - z \frac{d^2\tilde{w}}{dx^2} + \frac{1}{2} \left(\frac{d\tilde{v}}{dx} \right)^2 + \frac{1}{2} \left(\frac{d\tilde{w}}{dx} \right)^2 \quad (2.13)$$

$$\begin{aligned}
\epsilon_{xx}^2 &= \left(\frac{d\tilde{u}}{dx}\right)^2 + y^2 \left(\frac{d^2\tilde{v}}{dx^2}\right)^2 + \frac{1}{4} \left(\frac{d\tilde{v}}{dx}\right)^4 + z^2 \left(\frac{d^2\tilde{w}}{dx^2}\right)^2 + \frac{1}{4} \left(\frac{d\tilde{w}}{dx}\right)^4 \\
&\quad - 2y \left(\frac{d\tilde{u}}{dx}\right) \left(\frac{d^2\tilde{v}}{dx^2}\right) - 2z \left(\frac{d\tilde{u}}{dx}\right) \left(\frac{d^2\tilde{w}}{dx^2}\right) + y \left(\frac{d^2\tilde{v}}{dx^2}\right) \left(\frac{d\tilde{w}}{dx}\right)^2 - z \left(\frac{d\tilde{v}}{dx}\right)^2 \left(\frac{d^2\tilde{w}}{dx^2}\right) \\
&\quad + \frac{1}{2} \left(\frac{d\tilde{v}}{dx}\right)^2 \left(\frac{d\tilde{w}}{dx}\right)^2 \quad (2.14)
\end{aligned}$$

The shear strain can be written as a function of rotation of the cross section about the x axis as shown in Fig. 2.VI.

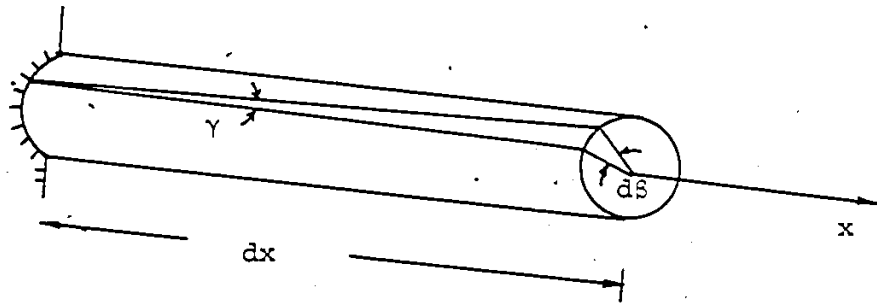


Fig. 2.VI

$$\tan \gamma = r \frac{d\tilde{\theta}}{dx} = \gamma$$

$$\gamma^2 = r^2 \left(\frac{d\tilde{\theta}}{dx}\right)^2 \quad (2.15)$$

Substituting Eqs. 2.14 and 2.15 into Eq. 2.12 leads to

$$\begin{aligned}
U_s = \frac{E}{2} \int_0^L \left[\int_A \left[\left(\frac{d\tilde{u}}{dx} \right)^2 + y^2 \left(\frac{d^2\tilde{v}}{dx^2} \right)^2 + z^2 \left(\frac{d^2\tilde{w}}{dx^2} \right)^2 + \frac{1}{4} \left(\frac{d\tilde{v}}{dx} \right)^4 \right. \right. \\
+ \frac{1}{4} \left(\frac{d\tilde{w}}{dx} \right)^4 - 2y \left(\frac{d\tilde{u}}{dx} \right) \left(\frac{d^2\tilde{v}}{dx^2} \right) - 2z \left(\frac{d\tilde{u}}{dx} \right) \left(\frac{d^2\tilde{w}}{dx^2} \right) + \left(\frac{d\tilde{u}}{dx} \right) \left(\frac{d\tilde{v}}{dx} \right)^2 \\
+ \left(\frac{d\tilde{u}}{dx} \right) \left(\frac{d\tilde{w}}{dx} \right)^2 + 2yz \left(\frac{d^2\tilde{v}}{dx^2} \right) \left(\frac{d^2\tilde{w}}{dx^2} \right) - y \left(\frac{d^2\tilde{v}}{dx^2} \right) \left(\frac{d\tilde{v}}{dx} \right)^2 \\
- y \left(\frac{d^2\tilde{v}}{dx^2} \right) \left(\frac{d\tilde{w}}{dx} \right)^2 - z \left(\frac{d^2\tilde{w}}{dx^2} \right) \left(\frac{d\tilde{v}}{dx} \right)^2 - z \left(\frac{d^2\tilde{w}}{dx^2} \right) \left(\frac{d\tilde{w}}{dx} \right)^2 \\
\left. \left. + \frac{1}{4} \left(\frac{d\tilde{v}}{dx} \right)^2 \left(\frac{d\tilde{w}}{dx} \right)^2 \right] dA \right] dx + \frac{G}{2} \int_0^L \left[\int_A r^2 \left(\frac{d\tilde{\theta}}{dx} \right)^2 dA \right] dx
\end{aligned} \tag{2.16}$$

But

$$\int_A dA = A$$

$$\int_A y^2 dA = I_z$$

$$\int_A z^2 dA = I_y$$

$$\int_A r^2 dA = I_x$$

$$\int_A y dA = \int_A z dA = \int_A zy dA = 0$$

y and z are the principal axes. (2.17)

Substituting Eqs. 2.17 into the strain energy expression Eq. 2.16 and then neglecting the higher-order term $\left(\frac{d\tilde{v}}{dx} \right)^4$ and $\left(\frac{d\tilde{w}}{dx} \right)^4$ leads to

$$\begin{aligned}
U_s = & \frac{EA}{2} \int_0^L \left(\frac{d\tilde{u}}{dx} \right)^2 dx + \frac{EI_z}{2} \int_0^L \left(\frac{d^2\tilde{v}}{dx^2} \right)^2 dx + \frac{EI_y}{2} \int_0^L \left(\frac{d^2\tilde{w}}{dx^2} \right)^2 dx \\
& + \frac{EA}{2} \int_0^L \left(\frac{d\tilde{u}}{dx} \right) \left(\frac{d\tilde{v}}{dx} \right)^2 dx + \frac{EA}{2} \int_0^L \left(\frac{d\tilde{u}}{dx} \right) \left(\frac{d\tilde{w}}{dx} \right)^2 dx + \frac{GI_x}{2} \int_0^L \left(\frac{d\tilde{\beta}}{dx} \right)^2 dx
\end{aligned}
\tag{2.18}$$

The displacement distribution on a space frame element is given by (see Appendix B).

$$\tilde{u}(x) = \tilde{u}_p + (\tilde{u}_q - \tilde{u}_p) \frac{x}{L} \quad *$$

$$\begin{aligned}
\tilde{v}(x) = & \left[1 - 3\left(\frac{x}{L}\right)^2 + 2\left(\frac{x}{L}\right)^3 \right] \tilde{v}_p + \left[\left(\frac{x}{L}\right) - 2\left(\frac{x}{L}\right)^2 + \left(\frac{x}{L}\right)^3 \right] L\tilde{\lambda}_p \\
& + \left[3\left(\frac{x}{L}\right)^2 - 2\left(\frac{x}{L}\right)^3 \right] \tilde{v}_q + \left[-\left(\frac{x}{L}\right)^2 + \left(\frac{x}{L}\right)^3 \right] L\tilde{\lambda}_q
\end{aligned}$$

$$\begin{aligned}
\tilde{w}(x) = & \left[1 - 3\left(\frac{x}{L}\right)^2 + 2\left(\frac{x}{L}\right)^3 \right] \tilde{w}_p - \left[\left(\frac{x}{L}\right) - 2\left(\frac{x}{L}\right)^2 + \left(\frac{x}{L}\right)^3 \right] L\tilde{\theta}_p \\
& + \left[3\left(\frac{x}{L}\right)^2 - 2\left(\frac{x}{L}\right)^3 \right] \tilde{w}_q - \left[-\left(\frac{x}{L}\right)^2 + \left(\frac{x}{L}\right)^3 \right] L\tilde{\theta}_q
\end{aligned}$$

$$\tilde{\beta}(x) = \tilde{\beta}_p + (\tilde{\beta}_q - \tilde{\beta}_p) \frac{x}{L} \tag{2.19}$$

* since $\tilde{u}(x) = \tilde{u}_p + (\tilde{u}_q - \tilde{u}_p) \frac{x}{L}$

$$\frac{d\tilde{u}}{dx} = \left(\frac{\tilde{u}_q - \tilde{u}_p}{L} \right) = \text{constant}$$

i.e. Eq. 2:18 contains only the quadratic terms.

From Eqs. 2.19

$$\frac{d\tilde{u}}{dx} = (\tilde{u}_q - \tilde{u}_p) / L$$

$$\begin{aligned} \frac{d\tilde{v}}{dx} = \frac{1}{L} & \left[(-6\left(\frac{x}{L}\right) + 6\left(\frac{x}{L}\right)^2)\tilde{v}_p + (1 - 4\left(\frac{x}{L}\right) + 3\left(\frac{x}{L}\right)^2) L\tilde{\lambda}_p \right. \\ & \left. + (6\left(\frac{x}{L}\right) - 6\left(\frac{x}{L}\right)^2)\tilde{v}_q + (-2\left(\frac{x}{L}\right) + 3\left(\frac{x}{L}\right)^2)L\tilde{\lambda}_q \right] \end{aligned}$$

$$\begin{aligned} \frac{d^2\tilde{v}}{dx^2} = \frac{1}{L^2} & \left[6(-1 + 2\frac{x}{L})\tilde{v}_p + (-4 + 6\frac{x}{L})L\tilde{\lambda}_p \right. \\ & \left. + 6(1 - 2\frac{x}{L})\tilde{v}_q + (-2 + 6\frac{x}{L})L\tilde{\lambda}_q \right] \end{aligned}$$

$$\begin{aligned} \frac{d\tilde{w}}{dx} = \frac{1}{L} & \left[6\left(\frac{x}{L} + \left(\frac{x}{L}\right)^2\right)\tilde{w}_p + (1 - 4\left(\frac{x}{L}\right) + 3\left(\frac{x}{L}\right)^2)L\tilde{\theta}_p \right. \\ & \left. + 6\left(\frac{x}{L} - \left(\frac{x}{L}\right)^2\right)\tilde{w}_q + (-2\left(\frac{x}{L}\right) + 3\left(\frac{x}{L}\right)^2)L\tilde{\theta}_q \right] \end{aligned}$$

$$\begin{aligned} \frac{d^2\tilde{w}}{dx^2} = \frac{1}{L^2} & \left[6(-1 + 2\frac{x}{L})\tilde{w}_p + (-4 + 6\frac{x}{L})L\tilde{\theta}_p \right. \\ & \left. + 6(1 - 2\frac{x}{L})\tilde{w}_q + (-2 + 6\frac{x}{L})L\tilde{\theta}_q \right] \end{aligned}$$

$$\frac{d\tilde{\beta}}{dx} = (\tilde{\beta}_q - \tilde{\beta}_p) / L \quad (2.20)$$

Eq. 2.18 can be rewritten as follows:

$$U_s = I_1 + I_2 + I_3 + I_4 + I_5 + I_6 \quad (2.18a)$$

where,

$$\begin{aligned}
 I_1 &= \frac{EA}{2} \int_0^L \left(\frac{d\tilde{u}}{dx} \right)^2 dx \\
 I_2 &= \frac{EI_z}{2} \int_0^L \left(\frac{d^2\tilde{v}}{dx^2} \right)^2 dx \\
 I_3 &= \frac{EI_y}{2} \int_0^L \left(\frac{d^2\tilde{w}}{dx^2} \right)^2 dx \\
 I_4 &= \frac{EA}{2} \int_0^L \left(\frac{d\tilde{u}}{dx} \right) \left(\frac{d\tilde{v}}{dx} \right)^2 dx \\
 I_5 &= \frac{EA}{2} \int_0^L \left(\frac{d\tilde{u}}{dx} \right) \left(\frac{d\tilde{w}}{dx} \right)^2 dx \\
 I_6 &= \frac{GI_x}{2} \int_0^L \left(\frac{d\tilde{\beta}}{dx} \right)^2 dx
 \end{aligned}$$

(2.21)

Substituting Eqs. 2.20 into Eqs. 2.21 and integrating lead to

$$1) \quad I_1 = \frac{EA}{2} \int_0^L \left(\frac{d\tilde{u}}{dx} \right)^2 dx = \frac{EA}{2L} (\tilde{u}_q - \tilde{u}_p)^2 \quad (2.22)$$

$$2) \quad I_2 = \frac{EI_z}{2} \int_0^L \left(\frac{d^2\tilde{v}}{dx^2} \right)^2 dx$$

$$\begin{aligned}
 I_2 &= \frac{EI_z}{2L^4} \left[12L\tilde{v}_p^2 + 4L^3\tilde{\lambda}_p^2 + 12L\tilde{v}_q^2 + 4L^3\tilde{\lambda}_q^2 + 12L^2\tilde{v}_p\tilde{\lambda}_p \right. \\
 &\quad \left. - 24L\tilde{v}_p\tilde{v}_q + 12L^2\tilde{v}_p\tilde{\lambda}_q - 12L^2\tilde{\lambda}_p\tilde{v}_q + 4L^3\tilde{\lambda}_p\tilde{\lambda}_q - 12L^2\tilde{v}_q\tilde{\lambda}_q \right]
 \end{aligned}$$

(2.23)

$$3) \quad I_3 = \frac{EI_Y}{2} \int_0^L \left(\frac{d^2 \tilde{w}}{dx^2} \right)^2 dx$$

$$I_3 = \frac{EI_Y}{2L^4} \left[12L\tilde{w}_p^2 + 4L^3\tilde{\theta}_p^2 + 12L\tilde{w}_q^2 + 4L^3\tilde{\theta}_q^2 - 12L^2\tilde{w}_p\tilde{\theta}_p \right. \\ \left. - 24L\tilde{w}_p\tilde{w}_q - 12L^2\tilde{w}_p\tilde{\theta}_q + 12L^2\tilde{\theta}_p\tilde{w}_q + 4L^3\tilde{\theta}_p\tilde{\theta}_q + 12L^2\tilde{w}_q\tilde{\theta}_q \right] \quad (2.24)$$

$$4) \quad I_4 = \frac{EA}{2} \int_0^L \left(\frac{d\tilde{u}}{dx} \right) \left(\frac{d\tilde{v}}{dx} \right)^2 dx$$

since $\frac{d\tilde{u}}{dx} = \frac{1}{L} (\tilde{u}_q - \tilde{u}_p) = \text{constant}$

$$I_4 = \frac{EA}{2L} (\tilde{u}_q - \tilde{u}_p) \int_0^L \left(\frac{d\tilde{v}}{dx} \right)^2 dx$$

But $\epsilon = \frac{\tilde{u}_q - \tilde{u}_p}{L}$

and, $E\epsilon A = \sigma A = F$

where F is the axial load in the member

$$F = \frac{EA}{L} (\tilde{u}_q - \tilde{u}_p)$$

$$I_4 = \frac{F}{2} \int_0^L \left(\frac{d\tilde{v}}{dx} \right)^2 dx$$

$$I_4 = \frac{F}{2L^2} \left[\frac{6}{5} L\tilde{v}_p^2 + \frac{2}{15} L^3\tilde{\lambda}_p^2 + \frac{6}{5} L\tilde{v}_q^2 + \frac{2}{15} L^3\tilde{\lambda}_q^2 + \frac{L^2}{5}\tilde{\lambda}_p\tilde{v}_p \right. \\ \left. - \frac{12}{5} L\tilde{v}_p\tilde{v}_q + \frac{L^2}{5}\tilde{v}_p\tilde{\lambda}_q - \frac{L^2}{5}\tilde{\lambda}_p\tilde{v}_q - \frac{L^3}{15}\tilde{\lambda}_p\tilde{\lambda}_q - \frac{L^2}{5}\tilde{\lambda}_q\tilde{v}_q \right] \quad (2.25)$$

$$5) \quad I_5 = \frac{EA}{2} \int_0^L \left(\frac{d\tilde{u}}{dx} \right) \left(\frac{d\tilde{w}}{dx} \right)^2 dx$$

$$I_5 = \frac{F}{2} \int_0^L \left(\frac{d\tilde{w}}{dx} \right)^2 dx$$

$$\begin{aligned}
I_5 = & \frac{F}{2L^2} \left[\frac{6}{5} L\tilde{w}_p^2 + \frac{2}{15} L^3 \tilde{\theta}_p^2 + \frac{6}{5} L\tilde{w}_q^2 + \frac{2}{15} L^3 \tilde{\theta}_q^2 - \frac{L^2}{5} \tilde{w}_p \tilde{\theta}_p \right. \\
& \left. - \frac{12}{5} L\tilde{w}_p \tilde{w}_q - \frac{L^2}{5} \tilde{w}_p \tilde{\theta}_q + \frac{L^2}{5} \tilde{\theta}_p \tilde{w}_q - \frac{L^3}{15} \tilde{\theta}_p \tilde{\theta}_q + \frac{L^2}{12} \tilde{w}_q \tilde{\theta}_q \right] \\
& (2.26)
\end{aligned}$$

$$\begin{aligned}
6) \cdot I_6 &= \frac{GI_x}{2} \int_0^L \left(\frac{d\tilde{\beta}}{dx} \right)^2 dx \\
I_6 &= \frac{GI_x}{2L} (\tilde{\beta}_q - \tilde{\beta}_p)^2 \\
& (2.27)
\end{aligned}$$

Substituting Eqs. 2.22 to 2.27 into Eq. 2.18a leads to

$$\begin{aligned}
U_s = & \frac{EA}{2L} (\tilde{u}_q - \tilde{u}_p)^2 + \frac{EI_z}{2L^4} \left[12L\tilde{v}_p^2 + 4L^3 \tilde{\lambda}_p^2 + 12L\tilde{v}_q^2 + 4L^3 \tilde{\lambda}_q^2 \right. \\
& + 12L^2 \tilde{v}_p \tilde{\lambda}_p - 24L\tilde{v}_p \tilde{v}_q + 12L^2 \tilde{v}_p \tilde{\lambda}_q - 12L^2 \tilde{\lambda}_p \tilde{v}_q + 4L^3 \tilde{\lambda}_p \tilde{\lambda}_q \\
& \left. - 12L^2 \tilde{v}_q \tilde{\lambda}_q \right] + \frac{EI_y}{2L^4} \left[12L\tilde{w}_p^2 + 4L^3 \tilde{\theta}_p^2 + 12L\tilde{w}_q^2 + 4L^3 \tilde{\theta}_q^2 \right. \\
& - 12L^2 \tilde{w}_p \tilde{\theta}_p - 24L\tilde{w}_p \tilde{w}_q - 12L^2 \tilde{w}_p \tilde{\theta}_q + 12L^2 \tilde{\theta}_p \tilde{w}_q + 4L^3 \tilde{\theta}_p \tilde{\theta}_q \\
& \left. + 12L^2 \tilde{w}_q \tilde{\theta}_q \right] + \frac{F}{2L^2} \left[\frac{6}{5} L\tilde{v}_p^2 + \frac{2}{15} L^3 \tilde{\lambda}_p^2 + \frac{6}{5} L\tilde{v}_q^2 + \frac{2}{15} L^3 \tilde{\lambda}_q^2 \right. \\
& + \frac{L^2}{5} \tilde{\lambda}_p \tilde{v}_p - \frac{12}{5} L\tilde{v}_p \tilde{v}_q + \frac{L^2}{5} \tilde{v}_p \tilde{\lambda}_q - \frac{L^2}{5} \tilde{\lambda}_p \tilde{v}_q - \frac{L^3}{15} \tilde{\lambda}_p \tilde{\lambda}_q \\
& - \frac{L^2}{5} \tilde{\lambda}_q \tilde{v}_q + \frac{6}{5} L\tilde{w}_p^2 + \frac{2}{15} L^3 \tilde{\theta}_p^2 + \frac{6}{5} L\tilde{w}_q^2 + \frac{2}{15} L^3 \tilde{\theta}_q^2 \\
& - \frac{L^2}{5} \tilde{w}_p \tilde{\theta}_p - \frac{12}{5} L\tilde{w}_p \tilde{w}_q - \frac{L^2}{5} \tilde{w}_p \tilde{\theta}_q + \frac{L^2}{5} \tilde{\theta}_p \tilde{w}_q - \frac{L^3}{15} \tilde{\theta}_p \tilde{\theta}_q \\
& \left. + \frac{L^2}{12} \tilde{w}_q \tilde{\theta}_q \right] + \frac{GI_x}{2L} (\tilde{\beta}_q - \tilde{\beta}_p)^2 \\
& (2.28)
\end{aligned}$$

Applying Castigliano's theorem (Part I) ⁽¹⁸⁾ to the strain energy expression Eq. 2.28, leads to the following element force-displacement equations.

$$P_1 = \frac{\partial U_s}{\partial \tilde{u}_p} = \frac{EA}{L} (\tilde{u}_p - \tilde{u}_q)$$

$$P_2 = \frac{\partial U_s}{\partial \tilde{v}_p} = \frac{EI_z}{2L^4} \left[24L\tilde{v}_p + 12L^2\tilde{\lambda}_p - 24L\tilde{v}_q + 12L^2\tilde{\lambda}_q \right] \\ + \frac{F}{2L^2} \left[\frac{12}{5} L\tilde{v}_p + \frac{L^2}{5} \tilde{\lambda}_p - \frac{12}{5} L\tilde{v}_q + \frac{L^2}{5} \tilde{\lambda}_q \right]$$

$$P_3 = \frac{\partial U_s}{\partial \tilde{w}_p} = \frac{EI_y}{2L^4} \left[24L\tilde{w}_p - 12L^2\tilde{\theta}_p - 24L\tilde{w}_q - 12L^2\tilde{\theta}_q \right] \\ + \frac{F}{2L^2} \left[\frac{12}{5} L\tilde{w}_p - \frac{L^2}{5} \tilde{\theta}_p - \frac{12}{5} L\tilde{w}_q - \frac{L^2}{5} \tilde{\theta}_q \right]$$

$$P_4 = \frac{\partial U_s}{\partial \tilde{\beta}_p} = \frac{GI_x}{L} (\tilde{\beta}_p - \tilde{\beta}_q)$$

$$P_5 = \frac{\partial U_s}{\partial \tilde{\theta}_p} = \frac{EI_y}{2L^4} \left[8L^3\tilde{\theta}_p - 12L^2\tilde{w}_p + 12L^2\tilde{w}_q + 4L^3\tilde{\theta}_q \right] \\ + \frac{F}{2L^2} \left[\frac{4}{15} L^3\tilde{\theta}_p - \frac{L^2}{5} \tilde{w}_p + \frac{L^2}{5} \tilde{w}_q - \frac{L^3}{15} \tilde{\theta}_q \right]$$

$$P_6 = \frac{\partial U_s}{\partial \tilde{\lambda}_p} = \frac{EI_z}{2L^4} \left[8L^3\tilde{\lambda}_p + 12L^2\tilde{v}_p - 12L^2\tilde{v}_q + 4L^3\tilde{\lambda}_q \right] \\ + \frac{F}{2L^2} \left[\frac{4}{15} L^3\tilde{\lambda}_p + \frac{L^2}{5} \tilde{v}_p - \frac{L^2}{5} \tilde{v}_q - \frac{L^3}{15} \tilde{\lambda}_q \right]$$

$$P_7 = \frac{\partial U_s}{\partial \tilde{u}_q} = \frac{EA}{L} (\tilde{u}_q - \tilde{u}_p)$$

$$P_8 = \frac{\partial U_s}{\partial \tilde{v}_q} = \frac{EI_z}{2L^4} \left[24L\tilde{v}_q - 24L\tilde{v}_p - 12L^2\tilde{\lambda}_p - 12L^2\tilde{\lambda}_q \right] \\ + \frac{F}{2L^2} \left[\frac{12}{5} L\tilde{v}_q - \frac{12}{5} L\tilde{v}_p - \frac{L^2}{5} \tilde{\lambda}_p - \frac{L^2}{5} \tilde{\lambda}_q \right]$$

$$\begin{aligned}
P_9 &= \frac{\partial U_S}{\partial \tilde{w}_q} = \frac{EI_Y}{2L^4} \left[24L\tilde{w}_q - 24L\tilde{w}_p + 12L^2\tilde{\theta}_p + 12L^2\tilde{\theta}_q \right] \\
&\quad + \frac{F}{2L^2} \left[\frac{12}{5} L\tilde{w}_q - \frac{12}{5} L\tilde{w}_p + \frac{L^2}{5} \tilde{\theta}_p + \frac{L^2}{5} \tilde{\theta}_q \right] \\
P_{10} &= \frac{\partial U_S}{\partial \tilde{\beta}_q} = \frac{GJ}{L} (\tilde{\beta}_q - \tilde{\beta}_p) \\
P_{11} &= \frac{\partial U_S}{\partial \tilde{\theta}_q} = \frac{EI_Y}{2L^4} \left[8L^3\tilde{\theta}_q - 12L^2\tilde{w}_p + 4L^3\tilde{\theta}_p + 12L^2\tilde{w}_q \right] \\
&\quad + \frac{F}{2L^2} \left[\frac{4}{15} L^3\tilde{\theta}_q - \frac{L^2}{5} \tilde{w}_p - \frac{L^3}{15} \tilde{\theta}_p + \frac{L^2}{5} \tilde{w}_q \right] \\
P_{12} &= \frac{\partial U_S}{\partial \tilde{\lambda}_q} = \frac{EI_Z}{2L^4} \left[8L^3\tilde{\lambda}_q + 12L^2\tilde{v}_p + 4L^3\tilde{\lambda}_p - 12L^2\tilde{v}_q \right] \\
&\quad + \frac{F}{2L^2} \left[\frac{L^2}{5} \tilde{v}_p - \frac{L^3}{15} \tilde{\lambda}_p - \frac{L^2}{5} \tilde{v}_q + \frac{4}{15} L^3\tilde{\lambda}_q \right]
\end{aligned} \tag{2.29}$$

Eqs. 2.29 can be rewritten in matrix form as follows:

$$\{\tilde{P}\} = [\tilde{K}_E] \{\tilde{u}\} + [\tilde{K}_G] \{\tilde{u}\} \tag{2.30}$$

where $[\tilde{K}_E]$ is the conventional small deflection theory stiffness matrix shown in Fig. 2-2, $[\tilde{K}_G]$ is called geometric stiffness matrix, $\{\tilde{P}\}$ is the vector of end forces and $\{\tilde{u}\}$ is the vector of end displacements. All of these matrices are written with reference to the local coordinates.

Notice that $[\tilde{K}_G]$ depends not only on the geometry but also on the initial load F as shown in Fig. 2-3.

For an arbitrarily oriented space element, the stiffness matrix in the global coordinates may be obtained from the local stiffness matrix by the transformation $[T]^T [\tilde{K}] [T]$. The transformation matrix $[T]$ is developed in detail in section 2.5.

2.4 Calculating the Critical Load

Two fundamental types of nonlinear analysis method exist: iterative and incremental. The iterative approach is a direct attack on the nonlinear problem, it is also valid in all methods of analysis. The incremental approach is also valid in all methods of analysis but unfortunately it breaks down with the first occurrence of an instability. Therefore the incremental method should be used only to determine the critical load.

In the post-buckling analysis, iterative method should be used. It should be re-emphasized that the method of analysis used in this thesis cannot analyze the post-buckling phenomenon. To analyze this phenomenon, the higher order terms in the expression of strain energy should be retained.

The equilibrium equations are

$$[K_E + K_G] \{U\} = \{P\} \quad (2.31)$$

where, $[K_E]$ is the master elastic stiffness matrix for the stayed column, $[K_G]$ is the master geometric stiffness

matrix assembled only for the column elements, $\{U\}$ is the vector of nodal displacements, and $\{P\}$ is the vector of nodal loads.

In Eq. 2.31 the external loading P is expressed as

$$P = \mu P^* \quad (2.32)$$

where μ is a constant and P^* represent the relative magnitude of the applied loads which can be conveniently taken as unity. Also, since the geometrical stiffness matrix is proportional to the internal forces at the start of the loading step, it follows that

$$[K_G] = \mu [K_G^*] \quad (2.33)$$

where $[K_G^*]$ is the geometrical stiffness matrix for unit value of applied loading ($\mu=1$). The elastic stiffness matrix $[K_E]$ can be treated as a constant for quite a wide range of displacements $\{U\}$. Hence we may write.

$$[K_E + \mu K_G^*] \{U\} = \mu \{P^*\} \quad (2.34)$$

The displacements $\{U\}$ may therefore be determined from,

$$\{U\} = [K_E + \mu K_G^*]^{-1} \mu \{P^*\} \quad (2.35)$$

From the formal definition of the matrix inverse, the adjoint matrix divided by the determinant of the coefficients, it can be noted that the displacements tends to infinity when

$$| K_E + \mu K_G^* | = 0 \quad (2.36)$$

the lowest value of μ multiplied by P^* gives the critical load for the stayed column. Since the relative value of the applied load P^* is chosen as unity then the

lowest value of μ is the first buckling load, the second lowest value is the second buckling load, etc. The eigenvector associated with each eigenvalue gives the relative value of the displacement, that is the buckling shape. The disadvantage of this direct approach is the need to solve a set of nonlinear algebraic equations, consequently a relatively long computer time.

The incremental approach is generally more efficient in determining the critical load. In this approach Eq. 2.31 can be rewritten in linear incremental form as follows

$$[K_E + \Delta\mu K_G] \{\Delta U\} = \{\Delta\mu P^*\} \quad (2.37)$$

By taking incremental values of $\Delta\mu$, it is easy to determine the corresponding incremental displacements $\{\Delta U\}$.

Continue increasing the incremental load and computing the corresponding incremental displacements $\{\Delta U\}$.

If at the n^{th} step the incremental displacements tends to go to infinity it means that the applied load at this step is the critical load, and the buckling shape just before the instant of buckling is (18).

$$\{U_{n-1}\} = \sum_{i=1}^{n-1} \{\Delta U_i\} \quad (2.38)$$

There is another approach (6) to calculate the buckling load and the corresponding buckling mode without using an iterative or incremental procedure. This can be done by using Subroutine NROOT from IBM System/360

Scientific Subroutine Package (20). Eq. 2.36 should be rearranged to read

$$| \lambda [I_M] + [K_E]^{-1} [K_G^*] | = 0 \quad (2.39)$$

where λ is $\frac{1}{\mu}$ and $[I_M]$ is an unit matrix. Subroutine NROOT calculates the eigenvalues of the matrix $[K_E]^{-1} [K_G^*]$ which are λ . To obtain the desired buckling load, μ , the values of λ are simply inverted. To obtain the first buckling load the smallest value of μ is required and hence the largest eigenvalue, λ , is inverted to obtain this critical load. Other buckling loads are obtained in a similar manner.

The last approach is the most efficient for determining the critical load. Unfortunately, this approach is only valid when the quadratic terms in the expression of strain energy have been retained. No knowledge of post-buckling behavior can be obtained from this approach.

2.5 Transformations *

The displacements associated with the space frame element in local coordinates (c_j , $j=1,2,3$) can be expressed in terms of displacement components in the global X, Y and Z coordinate system as

* For more details refer to Gerstle (19).

$$\{\bar{u}\} = [T] \{u\} \quad (2.40)$$

where,

$$\{u\}^T = \{u_p, v_p, w_p, \beta_p, \theta_p, \lambda_p, u_q, v_q, w_q, \beta_q, \theta_q, \lambda_q\}$$

are the end displacement components in global coordinates.

And,

$$[T] = \begin{bmatrix} R & 0 & 0 & 0 \\ 0 & R & 0 & 0 \\ 0 & 0 & R & 0 \\ 0 & 0 & 0 & R \end{bmatrix} \quad (2.41)$$

12x12

in which

$$[R]_{3 \times 3} = \begin{bmatrix} \ell_1 & m_1 & n_1 \\ \ell_2 & m_2 & n_2 \\ \ell_3 & m_3 & n_3 \end{bmatrix}_{3 \times 3} \quad (2.42)$$

where ℓ_j, m_j, n_j are the direction cosines of the angles between the c_j axis and X, Y and Z axes respectively.

To determine the matrix [R], consider the general member of length L shown in Fig. 2.VII. The principal member axes are shown as $c_j, j=1,2,3$ and the global axes as X, Y, and Z with unit vectors $\underline{i}, \underline{j}$ and \underline{k} . The member end coordinates are x_1, y_1 and z_1 at end 1, and x_2, y_2 and z_2 at end 2.

The direction cosines of the longitudinal axis c_1 of the member are determined by the geometry of Fig. 2.VI as follows,

$$l_1 = \frac{x_2 - x_1}{L}$$

$$m_1 = \frac{y_2 - y_1}{L}$$

$$n_1 = \frac{z_2 - z_1}{L}$$

(2.43)

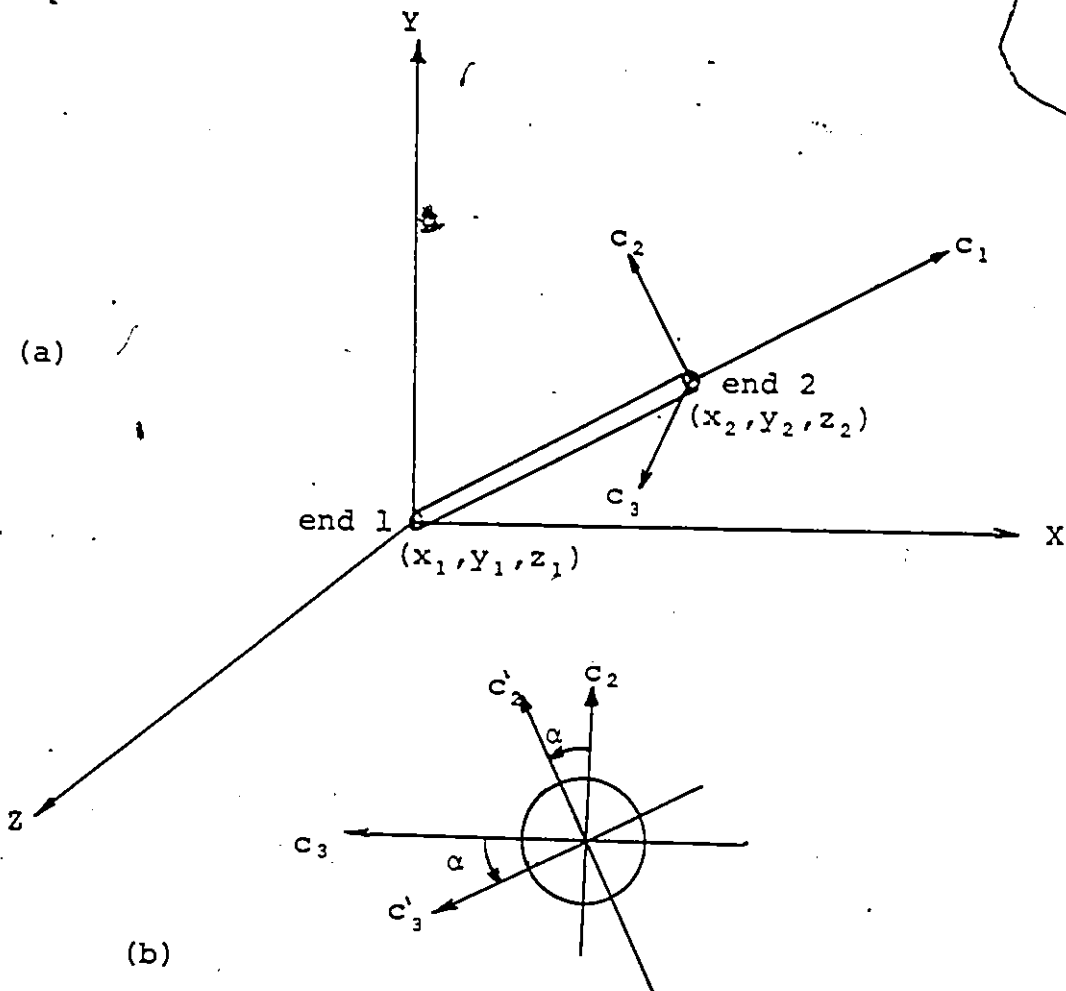


Fig. 2.VII

In the special case of a circular cross section the principal cross-sectional axes are considered to be any two perpendicular diameters. Consequently, one can assume c_3 is parallel to xz -plane, or horizontal, that is normal to the vertical global axis Y . In this case, a unit vector e_3 along this cross-sectional axis, denoted by c_3 , in Fig. 2.VI is determined according to the rules of vector analysis (19). Since e_3 is normal to both vectors \underline{j} and $e_1 (l_1 \underline{i}, m_1 \underline{j}, n_1 \underline{k})$,

$$e_3 = \frac{e_1 \times \underline{j}}{|e_1 \times \underline{j}|} = \frac{1}{(l_1^2 + n_1^2)^{\frac{1}{2}}} \begin{vmatrix} \underline{i} & \underline{j} & \underline{k} \\ l_1 & m_1 & n_1 \\ 0 & 1 & 0 \end{vmatrix}$$

$$e_3 = \frac{-n_1 \underline{i} + l_1 \underline{k}}{(l_1^2 + n_1^2)^{\frac{1}{2}}}$$

Calling the denominator quantity $(l_1^2 + n_1^2)^{\frac{1}{2}} \equiv L_1$

$$l_3 = -\frac{n_1}{L_1}$$

$$m_3 = 0$$

$$n_3 = \frac{l_1}{L_1}$$

(2.44)

The other bending axis c_2 is normal to the unit vectors along c_1 and c_3 . Therefore the unit vector e_2 along c_2 is obtained by

$$e_2 = e_3 \times e_1 = \frac{1}{L_1} \begin{vmatrix} \underline{i} & \underline{j} & \underline{k} \\ -n_1 & 0 & l_1 \\ l_1 & m_1 & n_1 \end{vmatrix}$$

$$e_2 = \frac{1}{L_1} \left[\underline{i}(-l_1 m_1) - \underline{j}(-n_1^2 - l_1^2) + \underline{k}(-m_1 n_1) \right]$$

The direction cosines of c_2 are

$$l_2 = \frac{-1}{L_1} (l_1 m_1)$$

$$m_2 = \frac{1}{L_1} (l_1^2 + n_1^2)$$

$$n_2 = \frac{-1}{L_1} (m_1 n_1) \quad (2.45)$$

From Eqs. 2.43, 2.44 and 2.45, the direction cosines are assembled into the $[R_1]$ matrix for the case in which c_3 local is normal to Y global.

$$[R_1] = \begin{bmatrix} l_1 & m_1 & n_1 \\ \frac{-l_1 m_1}{L_1} & \frac{l_1^2 + n_1^2}{L_1} & \frac{-m_1 n_1}{L_1} \\ \frac{-n_1}{L_1} & 0 & \frac{l_1}{L_1} \end{bmatrix}_{3 \times 3} \quad (2.46)$$

In the most general case the local axis c_3 is not perpendicular to the global Y axis. Assuming a new set of local axis (c'_1 , c'_2 and c'_3) in which c'_3 makes an angle α

with the previously defined c_3 , as shown in Fig. 2.VIb. The longitudinal member axis c'_1 is identical with the c_1 axis.

It is essential now to transform from the c_j to c'_j axes ($j = 1, 2, 3$) as follows

$$\{c'\} = [R_2] \{c\}$$

where,

$$[R_2] = \begin{bmatrix} 1 & 0 & 0 \\ \rho & \cos\alpha & \sin\alpha \\ 0 & -\sin\alpha & \cos\alpha \end{bmatrix} \quad (2.47)$$

The resultant transformation now consists of two successive transformations, first from (X,Y,Z) axes to (c_j , $j=1,2,3$) axes by Eq. 2.46, then from the (c_j , $j=1,2,3$) axes to the (c'_j , $j=1,2,3$) axes by Eq. 2.47.

$$\text{i.e. } \{c'\} = [R_2][R_1] \begin{Bmatrix} x \\ y \\ z \end{Bmatrix}$$

$$\{c'\} = [R] \begin{Bmatrix} x \\ y \\ z \end{Bmatrix}$$

where,

$$[R] = [R_2][R_1] \quad (2.48)$$

In the special case when the element longitudinal axis is vertical, the transformation by Eq. 2.46 breaks down, since the direction cosines l_1 and n_1 are both zero, and some of the terms in the transformation $[R_1]$ become

indeterminate ($L_1=0$, see Eq. 2.46). The angle α can be redefined, however, as the angle in the horizontal xz -plane between the global Z and the local c_3 axes, positive when turning from the global Z to global X axis (19) as shown in Fig. 2.VIII.

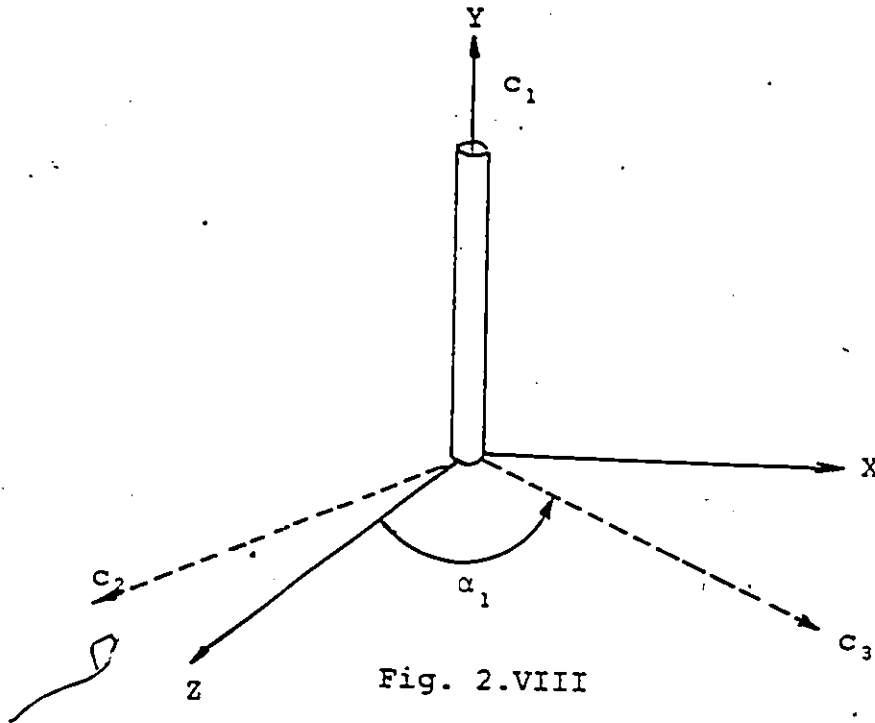


Fig. 2.VIII

Direction cosines for the longitudinal axis are,

$$l_1 = 0$$

$$m_1 = \frac{Y_2 - Y_1}{L}$$

$$n_1 = 0$$

(2.49)

Referring to Fig. 2.VIII one can easily determine the direction cosines of axis c_3 as follows,

$$\begin{aligned}
 l_3 &= \sin\alpha \\
 m_3 &= 0 \\
 n_3 &= \cos\alpha
 \end{aligned} \tag{2.50}$$

The unit vector along axis c_2 is normal to the unit vectors along c_1 and c_3 axes. Therefore the unit vector e_2 along c_2 is obtained by,

$$\begin{aligned}
 e_2 &= e_3 \times e_1 = \begin{vmatrix} \underline{i} & \underline{j} & \underline{k} \\ \sin\alpha & 0 & \cos\alpha \\ 0 & m_1 & 0 \end{vmatrix} \\
 e_2 &= -(m_1 \cos\alpha)\underline{i} + (m_1 \sin\alpha)\underline{k}
 \end{aligned}$$

or the direction cosines of c_2 are

$$\begin{aligned}
 l_2 &= -m_1 \cos\alpha \\
 m_2 &= 0 \\
 n_2 &= m_1 \sin\alpha
 \end{aligned} \tag{2.51}$$

$$[R]_{3 \times 3} = \begin{bmatrix} 0 & m_1 & 0 \\ -m_1 \cos\alpha & 0 & m_1 \sin\alpha \\ \sin\alpha & 0 & \cos\alpha \end{bmatrix} \tag{2.52}$$

Eq. 2.52 is valid only in case of vertical members, and in this case $m_1 = 1.0$ and the same Eq. becomes,

$$[R] = \begin{bmatrix} 0 & 1 & 0 \\ -\cos\alpha & 0 & \sin\alpha \\ \sin\alpha & 0 & \cos\alpha \end{bmatrix}_{3 \times 3} \tag{2.53}$$

CHAPTER 3

COMPUTER SOLUTION3.1 General

Two methods of determining the critical load and the corresponding buckling mode for the space stayed columns were outlined in Chapter 2. The two methods were (1) the nonlinear analysis based on the stability functions, and (2) geometrically nonlinear analysis by the finite element method.

The procedures of Chapter 2 could hardly be applied in a meaningful way without a computer program. For this reason, two programs were written to handle the calculations required to investigate the buckling behavior of the space stayed columns. One is based on the stability functions, and the other on the finite element method and are listed in Appendix C.

The process of determining the critical load in the first method is iterative since many of the elements of

the stiffness matrix are dependent upon the value of the axial load. A highly sophisticated iterative technique is used in the second program based on geometrically nonlinear analysis by the finite element method. This technique will allow the user to find the critical load in one computer run.

In the subsequent sections the general layout of the two programs will be discussed in some detail.

3.2 The First Program (stability functions)

3.2.1 Description of Computer Program

A computer program of approximately 450 cards was written to handle the calculation required to find the critical load and the corresponding buckling mode. The program is written in FORTRAN IV and will run on IBM System/360 Computer. This program iteratively determines the critical load based on the arithmetic minimum eigenvalue method. The program consists of a main program and six subroutines. Below is a description of each component of the program. Since most of the work is accomplished by the subroutines they will be discussed first, followed by a description of the main program.

3.2.2 Subroutines

STAFUN This subroutine calculates the stability functions as shown in Chapter 2, Section 2.2.3.

STASM This subroutine sets up the master stability stiffness matrix for the three-dimensional stayed column. The element stiffness matrices in local coordinates and the transformation matrices are generated by this subroutine. With the assistance of subroutines: TRANS and MULT, the element stiffness matrices in global coordinates are assembled according to the relation,

$$[K] = [T]^T [\tilde{K}] [T]$$

Then the master stability stiffness matrix is assembled using the variable correlation table.

TRANS This subroutine transposes a matrix.

MULT This subroutine determines the product of two matrices.

BAKY This subroutine stores the upper triangular elements of the master stability stiffness matrix as a column vector. This form of the stiffness matrix is required for use in subroutine EIGEN.

EIGEN EIGEN is a subroutine from IBM System/360 Scientific Subroutine Package⁽²⁰⁾. This subroutine calculates the eigenvalues and eigenvectors of a real symmetric matrix. The eigenvalues are developed on the diagonal elements of the matrix. A matrix of eigen-

vectors is also generated. The final arrangement of eigenvalues is in descending order on the diagonal. The eigenvectors are arranged by column in the same order as the eigenvalues.

3.2.3 Main Program

The MAIN program can be divided into several main parts that outline the steps in the iterative process used to obtain the critical load for the structure. Comments on operations are given for clarification or emphasis.

The steps are:

- 1 - Read input data. The input data consists of,
 - a) number of elements (M)
 - b) number of nodes (N)
 - c) number degree of freedom (NDF)
 - d) number of elements with bending stiffness (NBS)
 - e) number of elements with significant axial load (NKG)
 - f) number of buckling loads required (NM)
 - g) dimension of the problem (NN)
 - h) variable correlation table (IVC)
 - i) Coordinates of nodal points (CN)
 - j) outer and inner diameters (D22 and D11)
 - k) modulus of elasticity (E) and modulus

of rigidity (G).

- l). the angle α (ALPHAI) has been defined in Chapter 2, Section 2.4.
- m). the initial load (P1) and the load increment (DP).

2 - Calculate element properties. The properties of element consists of,

- a) area (AA)
- b) moment of inertia (MI)
- c) direction cosines (DC)
- d) Euler load for elements with significant axial load (PE)

3 - Write the input data and the element properties.

Thus, the results of the analysis will be accompanied by the input data and the elements properties. This makes checking easier if some mistakes have been inadvertently introduced. Also, this data will generally be useful for future reference.

4 - Calculate the stability functions using subroutine (STAFUN).

5 - Set up the master stability stiffness matrix through subroutine (STASM).

6 - Store the upper triangular portion of the stability stiffness matrix as a linear array, using subroutine (BAKY).

7 - Calculate the eigenvalues and the corresponding eigenvectors through subroutine (EIGEN).

8 - Iteration. The minimum eigenvalue is found in the $[n(n+1)/2]^{\text{th}}$ element of the matrix, where n is the order of the master stability stiffness matrix. Based on the sign of the minimum eigenvalue the load is incremented, the new system stability stiffness matrix is assembled, and the eigenvalues are calculated again. If the sign of the minimum eigenvalue changes, the load increment or decrement is reset at minus one-fourth of its previous value.

9 - The iteration continues until the critical load is obtained within certain limits.

10 - Write the critical load and the corresponding buckling mode.

3.2.4 Critical Loads Other Than the First

To determine a critical load other than the first, the corresponding eigenvalue must be used as a basis of iteration. The eigenvalues are generated on the diagonal of the matrix which was the master stability stiffness matrix. This is illustrated in Fig. 3-I. The elements of the upper triangular portion of the master stability stiffness matrix are stored, by BAKY, in a linear array in which the elements are numbered as shown in Fig. 3-I.

After EIGEN calculates the eigenvalues these appear on the diagonal, as elements $1, 3, 6, 10, 15, \dots, \{j \times (j+1)\}/2, \dots, \{n \times (n+1)\}/2$, where j is the j^{th} eigenvalue and n is the order of the two dimensional stiffness matrix. The eigenvalues are stored in descending order. Thus the eigenvalue in the $\{n \times (n+1)\}/2$ th position is used to obtain the first critical load. To obtain the i^{th} critical load ($i = 2, 3, 4, 5, \dots, n$) the eigenvalue that must be used as a basis of iteration is the $j^{\text{th}} = n - i + 1$. The storage location of this eigenvalue is the element $\{(n - i + 1)(n - i + 2)\}/2$ th. Thus any of the critical load may be determined

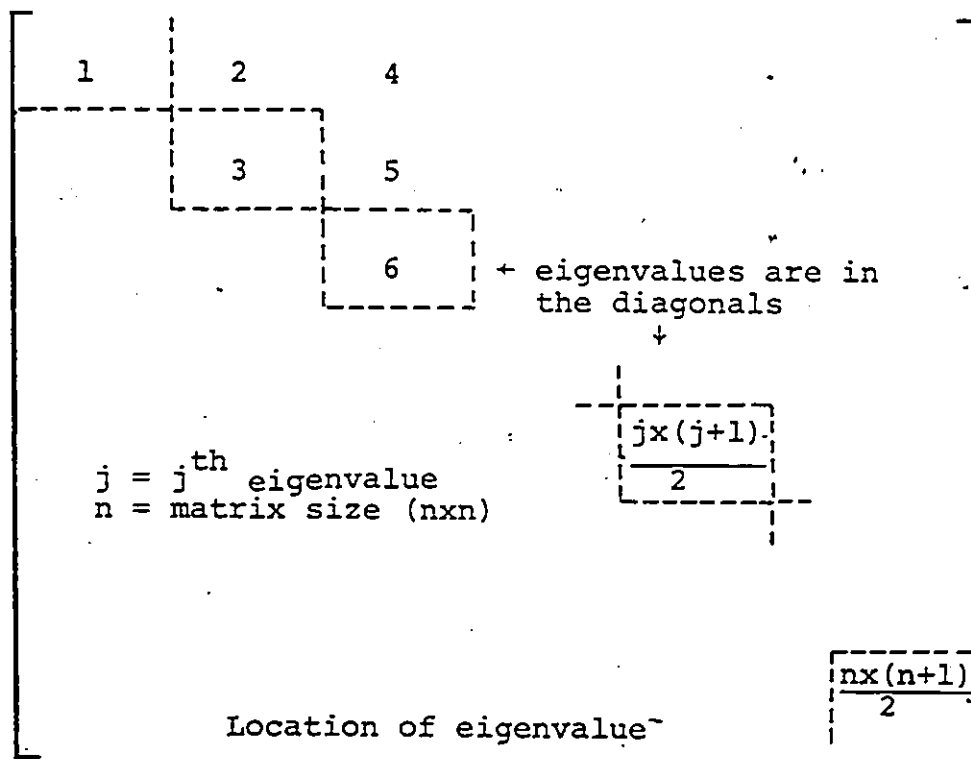


Fig. 3.I

3.3 The Second Program (The finite element method)

3.3.1 Description of the Program

A computer program of approximately 550 cards was written to calculate the critical load and the corresponding buckling mode in one computer run using the geometric nonlinear analysis by the finite element method. The program is written in FORTRAN IV and will run on the IBM System/360 Computer. The program consists of a main program and seven subroutines. As mentioned previously most of the work is accomplished by the subroutines, therefore they will be discussed first, followed by a discussion of the main program.

3.3.2 Subroutines

ELAKM This subroutine sets up the master elastic stiffness matrix by a similar procedure as subroutine STASM in Section 3.2.2.

GEOKM This subroutine sets up the master geometric stiffness matrix in 3-dimension by the same procedure as subroutine ELAKM.

TRANS and MULT These subroutines have been defined in Section 3.2.2.

ARRAY ARRAY is a subroutine from IBM System/360 Scientific Subroutine Package⁽²⁰⁾. This subroutine converts the data matrix from double to single dimension.

This form of matrix (Array) is required for use in subroutine NROOT.

NROOT NROOT is also a subroutine from IBM System/360 Scientific Subroutine Package⁽²⁰⁾. This subroutine calculates the eigenvalues, λ_i , and the matrix eigenvectors, V , of a real square non-symmetric matrix of a special form $B^{-1}A$, where both B and A are real symmetric matrices and B is positive definite.

DODY This subroutine calculates the weight and the relative efficiency of the stayed column.

3.3.3 Main Program

The MAIN program can best be described by a series of statements that outline the steps used to obtain the critical load for the space stayed column in one computer run. Where applicable, comments on operations have been added for clarification or emphasis. The steps are:

1 - Read input data. The input data are exactly the same as in the first program, Section 3.2.3, except step (1-m), the initial load P_1 and the load increment (DP) are omitted.

2 - Calculate element properties. The same as in the first program, Section 3.2.3, except step (2-d), the Euler load (PE) is not required.

3 - Write the input data and the element properties. As in the first program.

4 - Set up the master elastic stiffness matrix through subroutine (ELAKM).

5 - Set up the master geometric stiffness matrix using subroutine (GEOKM).

6 - Convert the matrices ELAKM and GEOKM from double to single dimension or array through subroutine (ARRAY).

7 - Calculate the eigenvalues and the corresponding eigenvectors using subroutine (NROOT). As explained in Chapter 2, Section 2.2.5.

8 - Calculate the weight and the relative efficiency using subroutine (DODY).

9 - Write the output data which consists of the

- a) Critical load and the corresponding buckling mode.
- b) Weight and the relative efficiency of the stayed column.

10 - A new data set is now read and the process continues. The only data cards that need be included in the new data set are those on which some or all the data has been changed. This is convenient and saves time when the effect on the critical load of changing a parameter is being investigated.

CHAPTER 4

INFLUENCE OF CROSSARM MEMBER LENGTH ON BUCKLING BEHAVIOR

4.1 General

As mentioned in Chapter 1, the elastic buckling load of a concentrically loaded, pin-ended, slender metal column may be increased several times by reinforcing it with rigidly connected crossarm members and pretensioned stays. The purpose of the pretensioned stays and the crossarm members is to introduce, at several points along the length of the column, restraint against translation and rotation. The effect is to decrease the effective unsupported buckling length of the column. One of the most interesting problems associated with this research is that of influence of crossarm length on buckling behavior of the stayed columns. The investigation in this chapter is focused on the following problems:

- 1) Influence of crossarm length on the buckling

strength of a single-crossarm stayed column.

2) Comparing the buckling behavior of the single-crossarm stayed columns with three and four crossarm members, due to the changing of crossarm member length.

3) Influence of crossarm length on the modes of instability for the two systems under consideration.

4.2 Influence of Crossarm Member Length

The influence of crossarm member length on the buckling behavior for the two systems mentioned previously in Chapter 1 are explored here. The stay diameters, which must remain constant, during the varying of crossarm member length were selected as 3/16, 4/16, 5/16, 6/16, 7/16, 8/16, 9/16, 10/16 and 12/16 ins. Then, for various ratios of half column length, L , to crossarm member length, l_{ca} , and with the aid of the computer program based on the finite element method, the buckling load and the corresponding buckling mode were calculated.

An important feature of the problem is that there are two practical possible modes of instability: a type of triple curvature and double curvature buckling. Consequently, it was of interest to study the influence of crossarm member length on these modes of buckling. The two modes of buckling will be discussed subsequently in some detail.

The theoretical results obtained from the computer program are illustrated in Figs. 4-1 and 4-3 to 4-10. Each of these diagrams corresponds to a constant value of the stay diameter. The ratio of half column length to crossarm length is the abscissa and the values of the critical loads corresponding the two buckling modes are the ordinates in these diagrams.

The curved lines in Fig. 4-1 reveal that for large ratios of half column length to crossarm member length, instability in both systems results in Mode I buckling, a type of triple curvature buckling. As the ratio of L to l_{ca} became smaller, in this case by increasing l_{ca} , a ratio was reached where Mode II, double curvature buckling, becomes the controlling instability mode at bifurcation. This behavior was expected since, as the crossarm member length is increased, the rotational restraint of the crossarm at the column is decreased and the translational restraint at the same point is increased. These results can be supported mathematically as follows. Referring to Fig. 4-2, the change in the stay length due to deflection, δ_c , at the crossarm level is Δ_s , and

$$\Delta_s = \delta_c \cos\theta \quad (4.1)$$

The additional force in the stay T_a due to the change in length is given by,

$$T_a = E_s (\Delta_s) A_s / L_s \quad (4.2)$$

substituting Eq. 4.1 into Eq. 4.2 leads to

$$T_a = \delta_c \frac{E_s A_s}{L_s} \cos\theta \quad (4.3)$$

where,

A_s is the stay cross-sectional area,

L_s is the stay length, and,

E_s is the modulus of elasticity of the stay.

also,

$$\cos\theta = l_{ca} / L_s$$

$$A_s = \pi d_s^2 / 4$$

in which d_s is the stay diameter.

Eq. 4.3 can be rewritten as follows:

$$T_a = \frac{\delta_c l_{ca}}{L_s^2} E_s \frac{\pi^2 d_s^2}{4} \quad (4.4)$$

but,

$$L_s^2 = L^2 + l_{ca}^2 \quad (4.5)$$

in which L and l_{ca} has been defined previously.

When Eq. 4.5 is substituted into Eq. 4.4, the

result is:

$$T_a = \delta_c L_p E_s \pi^2 d_s^2 / 4 \quad (4.6)$$

in which $L_p = 1 / (L^2 / l_{ca} + l_{ca})$

It is obvious from Eq. 4.6 that the additional force in the stay T_a is proportional to the parameters δ_c , E_s , d_s^2 and L_p . Investigation is now focusing on the length parameter L_p .

To examine the influence of crossarm member length on T_a , the length parameter L_p is calculated for various values of crossarm member length l_{ca} . The half column length, L , is considered constant and equal to 120 ins. The results are given in Table 4.I.

l_{ca}	$L_p \times 10^3$
12	0.83
15	1.0
20	1.35
24	1.6
30	2.0
60	3.3
120	4.2

Table 4.I

It is obvious from Table 4.I that as the crossarm member length is increased, the length parameter L_p also increases. Consequently the additional force in the stay T_a , which is directly proportional to the length parameter L_p , is also increased.

Referring to Fig. 4-2, from geometry:

$$F_a = T_a \cos\theta \quad (4.7)$$

in which F_a is the horizontal component of the additional force in the stay. This is the force which resists translation. Eq. 4.7 reveals that as the crossarm member length is increased, the translational restraint is also increased.

As for the rotational restraint, it is a well-known fact that the bending stiffness of an element is inversely proportional to the length of the element. Therefore, it is expected that the bending stiffness, and consequently the rotational restraint decrease with the increase of the crossarm member length.

It is also apparent in Fig. 4-1 that as the ratio of L to l_{ca} is increased, and when instability is controlled by Mode I buckling, there is a rapid increase in buckling strength. When Mode II buckling controls, the strength decreases slowly. This diagram also indicated that for the two systems the maximum strength of the stayed column will be in the vicinity of the intersection of the two buckling curves. It should be noted that the strength of the stayed column with four crossarm members is higher than that with three crossarm members. It should be emphasized that a higher strength does not always lead to higher efficiency. This will be discussed in Chapter 6.

The curved lines in Fig. 4-3 and Fig. 4-4 indicate that as the stay diameter is increased the strength of the two systems was increased and the region in which Mode I buckling controlled is narrowed. These results were expected because of the effects of stay size as will be discussed in some detail in the next chapter.

In Fig. 4-5 it should be noted that the buckling behavior is totally controlled by Mode II buckling for the stayed column with four crossarm members. The region controlled by Mode I buckling narrowed for the stayed column with three crossarm members.

Figs. 4-6 to 4-10 indicate that Mode II buckling controls the buckling behavior in both systems regardless of the crossarm member length. It can also be recognized that the second buckling load, which corresponds to Mode I buckling, became closer to the maximum theoretical buckling load* of the stayed column. It is also seen that the rate of increase of the second buckling load is very small. This behavior can also be expected because of the influence of the stay size.

4.3 Modes of Buckling

Two realistic buckling modes are possible, for the

*Maximum theoretical buckling load is defined as the critical load for column of length L with one end fixed and the other hinged.

pin-ended single-crossarm stayed column. These are (1) a type of triple curvature buckling or symmetrical buckling, and (2) double curvature buckling or anti-symmetrical buckling. They are shown in Figs. 4-11a and 4-11b as Mode I buckling and Mode II buckling respectively.

To simplify the phenomenon of instability modes, the stayed column can be replaced by the model* shown in Fig. 4-11c. It consists of a pin-ended column of length $2L$, in which the stays and crossarm members have been replaced by an elastic spring that resists lateral translation of the column.

The resistance of the linear spring reflects the properties of the stays and the length of the crossarm member. Now, if there are no stays, the resistance of the linear spring will vanish and consequently the expected shape of instability will be a half sine wave or a single curvature buckling as shown in Fig. 4-11d. If the stays are light and the length of the crossarm members are small, the resistance of the spring will be small and the expected buckling mode will be a type of triple curvature as shown in Fig. 4-11a'. In the case of heavy stays and long crossarm members, the resistance of the spring will be enough to prevent translation.

*For detailed information refer to Smith, McCaffrey and Ellis⁽⁵⁾.

Thus the rotation of the column at the crossarm will either be equal to zero or have a certain value as shown in Figs. 4-11a" and 4-11b respectively. One can observe that the buckling strength in case of zero rotation at the crossarm is higher than that with a certain rotation at the crossarm. That is because the effective buckling length for the case where the rotation of the column at the crossarm occurs is longer than the case where the rotation at the crossarm is zero.

CHAPTER 5

INFLUENCE OF THE STAY PROPERTIES ON THE BUCKLING BEHAVIOR

5.1 General

In Chapter 4 the influence of the crossarm member length on buckling behavior was investigated. Through this investigation many questions arose concerning the influence of stay properties on buckling behavior. In this chapter the investigation is focused on the following problems:

- 1) Influence of the stay size on the buckling behavior of the single-crossarm stayed columns (Section 5.2).
- 2) Comparing the buckling behavior of the single-crossarm stayed columns with three and four crossarm members, due to the changing of the stay size (Section 5.2).
- 3) Influence of stay modulus of elasticity on the

buckling behavior of the single-crossarm stayed column with three crossarm members only (Section 5.3).

5.2 Influence of Stay Size

The influence of stay size on buckling behavior for the two systems under consideration and previously described in Chapter 1 are explored here. The ratio of half column length to crossarm member length, (L/l_{ca}) , which must remain constant during the varying of the stay size, were selected from 10 to 2 in unit increments. Then, for various values of stay size and with the aid of the computer program, based on the finite element method and previously described in Chapter 3, the buckling load and the corresponding buckling mode were calculated.

It should be noted that when the stay size or the modulus of elasticity of the stay is varied the modes of buckling will still be one of the two modes previously discussed in Chapter 4, Section 4.3. But it should be re-emphasized that the presence of the stays is extremely essential to the creation of these particular modes of instability.

The theoretical results obtained from the computer program are illustrated in Figs. 5-1 and 5-3 to 5-8. Each of these diagrams corresponds to a constant value of the

ratio (L/l_{ca}). In plotting these diagrams, the value of the stay diameter is the abscissa and the values of the critical loads corresponding the two modes of instability are the ordinates.

The curves in Fig. 5-1 indicate that for small stay diameters, instability in both systems were controlled by Mode I buckling (a type of triple curvature buckling). For larger stay diameter, Mode II buckling (double curvature buckling), became the controlling instability mode at bifurcation. This behavior was expected because the translational restraint of the column at the level of the crossarm increases as the stay diameter is increased.

The results seen in Fig. 5-1 also reveal that as the stay size was increased and when instability was controlled by Mode I buckling, the buckling strength of the stayed column increased rapidly. However, when Mode II buckling controlled, the increase in buckling strength comparatively was very small. These results can be supported mathematically as follows. Eq. 4.7 in Chapter 4 can be rewritten as follows:

$$F_a = \pi \delta_c L_p E_s d_s^2 \cos\theta / 4 \quad (5.1)$$

in which δ_c , L_p , E_s and d_s have been defined in Chapter 4, Section 4.2.

It is obvious from Eq. 5.1 that the horizontal

force F_a , which resists translation, is directly proportional to the square of the stay diameter. Then, for constant values of the crossarm member length and modulus of elasticity of the stay, the horizontal force F_a and consequently the translational restraint at the crossarm increase rapidly as the stay diameter increases.

The point of intersection of the two buckling curves reveal that both Mode I buckling and Mode II buckling are equally possible for the stayed column. Thereafter, as the stay diameter becomes larger, a value is reached where the stays become heavy enough to prevent the translation at the crossarm. At this point, Mode II buckling will be the governing instability mode at bifurcation.

As mentioned previously, the increase in buckling strength was relatively small when Mode II buckling controlled the instability behavior. This can be explained and supported mathematically as follows: Mode II buckling can be represented by the model* shown in Fig. 5-2a, in which the restraint of the stays has been replaced, in Fig. 5-2b, by a vertical elastic spring. In Fig. 5-2d the change in the stay length, Δ_s , due to vertical deformation, δ_{ca} , at the end of the crossarm member is shown

*For detailed information about this model refer to Smith, McCaffrey & Ellis (5).

to be

$$\Delta_s = \delta_{ca} \sin\theta \quad (5.2)$$

Consequently, the additional force in the stay T_a , due to the change in length is given by

$$T_a = E_s \delta_{ca} \frac{\sin\theta}{L_s} \frac{\pi d_s^2}{4} \quad (5.3)$$

in which E_s , d_s and L_s have been defined previously in Chapter 4.

In Ref. 5, the value of δ_{ca} was calculated, and the result was

$$\delta_{ca} = \frac{l_{ca} \psi}{\left(1 + \frac{\pi}{6} \frac{d_s^2 E_s}{E_{ca} I_{ca}} l_{ca}^2 \sin^2 \theta \cos \theta\right)} \quad (5.4)$$

in which ψ is the angle of rotation of the buckled column at the crossarm and I_{ca} is the moment of inertia of the crossarm member.

Substitution of δ_{ca} from Eq. 5.4 into Eq. 5.3 leads to

$$T_a = \frac{E_s \sin\theta}{L_s} \frac{\psi l_{ca}}{\frac{4}{\pi d_s^2} + \frac{2}{3} \frac{E_s}{E_{ca} I_{ca}} l_{ca}^2 \sin^2 \theta \cos \theta} \quad (5.5)$$

It is obvious from Eq. 5.5 that as the stay size increases the additional force in the stay also increases. Referring to Fig. 5-2a, the vertical component of the additional force in the stay, V_a , is given by

$$V_a = T_a \sin\theta \quad (5.6)$$

Eq. 5.6 reveals that the vertical force V_a is directly proportional to the additional force in the stay T_a , since the crossarm member length is considered constant. Referring to Fig. 5-2b the two vertical forces V_a consist of a couple which resists the rotation at the crossarm and consequently increases the buckling strength. To prove that the increase in buckling strength will be small as the stay diameter is increased, Eq. 5.6 can be rewritten as follows

$$V_a = \frac{(E_s \sin^2 \theta \cos \theta) \psi}{D} \quad (5.7)$$

where

$$D = \left(\frac{4}{\pi d_s^2} + \frac{2}{3} \frac{E_s}{E_{ca} I_{ca}} l_{ca}^2 \sin^2 \theta \cos \theta \right) \quad (5.8)$$

To examine the influence of stay diameter on the vertical force V_a , the denominator, D , defined by Eq. 5.8 is calculated for various values of stay diameter. The results are given in Table 5.I.

d_s	D
0.3750	20.91
0.4375	18.50
0.5000	16.94
0.5625	15.87
0.6250	15.11
0.6875	14.54
0.7500	14.11

Table 5.I

It is obvious from Table 5.I that as the stay diameter is increased, the value of the denominator D is slowly decreased. Consequently the vertical force V_a at the end of the crossarm member is increased at a slow rate. This leads to a slow increase in the restraining moment and consequently to a slow increase in the buckling strength.

Figs. 5-3 to 5-6 indicate that for the two systems as L/l_{ca} decreases the buckling strength is increased when instability is controlled by Mode I buckling. Similarly when Mode II instability controls, the buckling strength is slightly decreased. This result was expected because, as mentioned previously, the rotational restraint of the column at the crossarm is decreased and the translational restraint of the column at the crossarm is increased as the crossarm member length is increased. The results shown in these diagrams also indicate that the region in which Mode I buckling controlled is narrowed as L/l_{ca} decreases. This behavior was also expected due to the effect of the crossarm member length as discussed in Chapter 4.

In Figs. 5-7 to 5-9 it should be noted that, for the stay sizes studied, the buckling behavior for the two systems is totally controlled by Mode II buckling. It can also be recognized that the buckling strength of the stayed column is decreased as the crossarm member increases

71

in length. It can also be seen that the rate of increase of the second buckling load became smaller and closer to the maximum theoretical buckling load for the stayed column.

It should be noted that the strength of the stayed column with four crossarm members is higher than that of three crossarm members regardless of the stay size and the crossarm member length. As mentioned previously, and as will be discussed in detail in the next chapter, a higher strength does not mean a higher efficiency.

5.3 Influence of Stay Modulus of Elasticity

In this section investigation is focused on the influence of the stay modulus of elasticity on buckling behavior of the single-crossarm stayed column with three crossarm members. Two types of stayed columns are considered. In type I the stays are considered to be steel rods with a modulus of elasticity of 29600 ksi. In type II the stays are considered to be steel cables with modulus of elasticity of 9400 ksi. The main purpose of this study is to emphasize that the buckling behavior of the stayed columns previously discussed is heavily dependent upon the stay modulus of elasticity.

In Figs. 5-10 and 5-11 the influence of the crossarm member length on buckling behavior is examined

for the two types under consideration. The curved lines in Fig. 5-10 reveal that for large ratios of L to l_{ca} and when Mode I is the controlling mode, the buckling strength of the stayed column with high stay modulus of elasticity is higher than that of low stay modulus of elasticity or type II. It can also be seen from the curved lines in the same Fig. that the region in which Mode I controls is comparatively narrow for the stayed column (type I). Also, the buckling strength for the two types becomes closer for small ratios of L to l_{ca} and when Mode II buckling is the controlling mode at bifurcation. These results were expected and can be supported mathematically as follows. Eq. 5.1 can be rewritten as follows:

$$F_a = C L_p E_s \quad (5.9)$$

and

$$C = \frac{\pi}{4} \delta_c d_s^2 \cos\theta$$

in which L_p , E_s , δ_c and d_s have been defined previously.

It is obvious from Eq. 5.9 that the horizontal force F_a which resists the translation is directly proportional to the modulus of elasticity of the stays and the length parameter L_p for a constant stay size. Then, for the same crossarm member length, it is expected that the force F_a and consequently the translational restraint

for the stayed column with high stay modulus of elasticity (type I) will be higher than that of low stay modulus of elasticity (type II). This explains why the buckling strength of the stayed column of type I is higher than that of type II, when Mode I controls the buckling behavior for both types. It can also be seen from Eq. 5.9 that as the length parameter increases by increasing the crossarm member length, a value for F_a and consequently the translation restraint is reached where both Mode I and Mode II buckling configurations are equally possible for the stayed column. Thereafter, Mode II buckling becomes the controlling mode at bifurcation. Since the translational restraint of the stayed column of type I is greater than that of type II due to the influence of stay modulus of elasticity. It is therefore expected that the region controlled by Mode I buckling for the stayed column of type I is narrower than that of type II.

It can be seen from Eq. 5.7 that the vertical force V_a at the end of the crossarm member increases with the increase of the stay modulus of elasticity. Therefore, it is expected that the restraining couple for the stayed column of type I is greater than that of type II. This explains why the buckling strength of the stayed column of type I is higher than that of type II, when Mode II buckling was the controlling mode for both types at bifurcation.

The curved lines in Fig. 5-11 reflect the great effect of the stay modulus of elasticity on the buckling behavior of the stayed column. It can be seen from the curved lines Fig. 5-11 that the buckling behavior of the stayed column with high stay modulus of elasticity is totally controlled by Mode II buckling. Also, the buckling behavior for the stayed column with low stay modulus of elasticity is controlled by two modes of instability: Mode I controls for large ratios of L to l_{ca} while Mode II controls for small ratios of L to l_{ca} .

In Figs. 5-12 and 5-13 the influence of the stay size on the buckling behavior is shown for the two types under consideration. It is obvious from the curved lines in Fig. 5-12 that the buckling behavior is greatly affected by the stay modulus of elasticity. The curved lines in that Fig. indicate that the buckling strength of the stayed column of type I increases with a comparatively higher rate than that of type II when Mode I controls the buckling behavior in both types. Also, the region controlled by Mode I buckling for the stayed column of type II is wider. It can also be recognized that the buckling strength of the stayed column with high stay modulus of elasticity (type I) is higher than that of low stay modulus of elasticity (type II). These results are expected because of the influence of stay modulus of elasticity explained before.

It can also be seen from Fig. 5-13 that for the stayed column of type I the region controlled by Mode I buckling is narrowed. It can also be seen from the curved lines in Fig. 5-13 that the buckling strength of the stayed column with high stay modulus of elasticity (type I) increases rapidly in the region governed by Mode I buckling. These results are expected due to the effect of stay modulus of elasticity on buckling behavior.

In Fig. 5-14 the influence of varying the stay modulus of elasticity on buckling behavior for the single crossarm stayed column with three crossarm members is examined. The curved lines in that Fig. indicate that for small values of the stay modulus of elasticity, instability was controlled by Mode I buckling. For large values of the stay modulus of elasticity Mode II buckling became the controlling mode at bifurcation. This behavior was expected because the translational restraint of the stayed column at the crossarm increases as the stay modulus of elasticity is increased. This can be confirmed mathematically using Eq. 5.9. It can also be seen in the same Fig. that the buckling strength of the stayed column increased rapidly as the stay modulus of elasticity was increased and when Mode I buckling was the controlling mode at bifurcation. However, when Mode II buckling controlled, the increase in buckling strength

was comparatively small. These results can be confirmed mathematically by using Eqs. 5.7 and 5.9.

CHAPTER 6

THE RELATIVE EFFICIENCY OF THE STAYED COLUMNS

6.1 General

In the last two chapters the influence of the crossarm member length and stay properties on the buckling behavior of the single-crossarm stayed column were investigated. It was obvious through these investigations that the buckling strength of the stayed columns with four crossarm members was always higher than that of three crossarm members regardless of the stay properties and the crossarm member length. However, based on these results it cannot be said that the stayed column with four crossarm members is always more efficient than that of three crossarm members. It is of interest to explore the relative efficiency which will be defined as the strength of the stayed column relative to its total weight. In this chapter the influence of the crossarm member length on the relative efficiency and the

influence of the stay diameter on the maximum value of the relative efficiency will be examined in some detail.

6.2 Influence of the Crossarm Member Length

The influence of crossarm member length on the relative efficiency for the two systems under consideration, and previously described in Chapter 1, are examined here. The stay diameters, which must remain constant during the varying of crossarm member length were selected as 3/16 to 10/16 in. in 1/16 in. increments, plus 12/16 in. Then, for various ratios of L to l_{ca} and with the aid of the same computer program previously used for the analysis in the last two chapters, the relative efficiency was calculated. It should be noted that the total weight of the stayed column consisted of the weights of the column, crossarm members and stays. It did not include any additional weight due to connections.

The theoretical results obtained from the computer program are illustrated in Figs. 6-1 to 6-9. Each of these diagrams is plotted for a constant value of the stay size. The curves are plotted in these Figs. to represent the relative efficiency as a function of the ratio L to l_{ca} . It should be noted that the stay modulus of elasticity is considered to be a constant and was selected as 29600 ksi.

Fig. 6-1 reveals that the relative efficiency (REF)

of the stayed columns in both systems varied as the ratio of L to l_{ca} was changed. Also, for large ratios of L to l_{ca} , the relative efficiency of the stayed column with four crossarm members is higher than that of the three crossarm members. As the ratio of L to l_{ca} becomes smaller, by increasing the crossarm member length, a ratio was reached where the relative efficiency of the stayed column with three crossarm members becomes higher than that of the four crossarm members. It can also be seen from the same Fig. that the relative efficiency of the stayed column in both systems increased with the increase of the crossarm member length until it reached its maximum value. Thereafter, it decreased with the increase of the crossarm member length. These results were expected and can be fully understood by referring to Fig. 4-1. It can be recognized from Figs. 6-1 and 4-1 that the maximum value of the relative efficiency (REF) in both systems was obtained in the region where the two corresponding buckling curves of Fig. 4-1 intersect. It can also be seen from the same Figs. that for large ratios of L to l_{ca} , the rate of increase of buckling strength is higher than the corresponding rate of increase of the relative efficiency. Also, for small ratios of L to l_{ca} , the rate of decrease of the buckling strength is less than the corresponding rate of decrease of the relative efficiency. That is because the

weight of the stayed column was continually increasing with the increase of the crossarm member length. Fig. 4-1 reveals that for large ratios of L to l_{ca} the buckling strength of the stayed column with four crossarm members was higher than that of the three crossarm members. The difference in the strength becomes less for small ratios of L to l_{ca} . The weight of the stayed column with four crossarm members is higher than that of the three crossarm members and the difference in weight between the two systems becomes larger for small ratios of L to l_{ca} . This explains why the relative efficiency of the stayed column with four crossarm members is higher than that of the three crossarm members for large ratios of L to l_{ca} while the stayed column of three crossarm members is more efficient for small ratios of L to l_{ca} .

Figs. 6-2 and 6-3 indicates that for large ratios of L to l_{ca} the stayed column with four crossarm members is still more efficient than that of the three crossarm members. It can also be seen from the same Figs. that the region in which the stayed column with four crossarm members is more efficient becomes narrower. This result was expected and can be fully understood by going back to the corresponding Figs. in Chapter 4.

Figs. 6-4 to 6-9 indicates that the relative efficiency of the stayed column with three crossarm members

was higher than that of the four crossarm members regardless of the crossarm member length. It can also be seen from these Figs. that the relative efficiency for the two systems decreased with the increase of the stay size. These results were expected because at a certain stay size the translational restraint was enough to prevent the translation at the crossarm. Thereafter, the increase in the stay size will cause a slight increase in the buckling strength as explained previously in Chapter 5. At the same time the weight of the stayed column increases at a relatively higher rate than the increase in the buckling strength of the column as the stay size is increased.

6.3 Effect on the Stay Size

The influence of the stay size on the maximum value of the relative efficiency is examined here. It can be recognized from Figs. 6-1 to 6-9 that for each stay diameter there exists a stayed column configuration in both systems for which the relative efficiency will be a maximum. The maximum values of the relative efficiency obtained from Figs. 6-1 to 6-9 for the two systems under consideration are illustrated in Fig. 6-10. In plotting this diagram, the stay diameter is the abscissa and the maximum values of the relative efficiency are the ordinates. It should be noted that the points on the

two curves in Fig. 6-10 represent the maximum values of the relative efficiency (REF) for each diameter of the stay investigated. The numerical ratio beside each point indicates the ratio of L to l_{ca} for which the maximum value was obtained.

Fig. 6-10 reveals that the maximum values of REF for the stayed column with three crossarm members is higher than that of the four crossarm members regardless of the stay size. It can also be seen from the same Fig. that for small values of the stay size, the crossarm member length for which the maximum value of REF is obtained is relatively long. As the stay size becomes larger the corresponding crossarm member length decreases. Also, one can recognize that for a small stay size the crossarm member length for the stayed column with three crossarm members is longer than that of the four crossarm members. It is also apparent from the same Fig. that the maximum value of the REF increases as the stay size is increased until it reaches its maximum value. Thereafter it decreases as the stay size is increased.

It should be re-emphasized that changing the material properties of the column, crossarm members or stays generally would alter the shape of the curved lines in Fig. 6-10.

CHAPTER 7

INFLUENCE OF END CONDITIONS ON BUCKLING BEHAVIOR

7.1 General

In the last three chapters the studies have been directed towards the buckling behavior of the single-crossarm stayed columns with hinged ends. The analysis of the stayed columns with different end conditions is desirable since the previous work published on the stayed columns was confined to the case of hinged ends. It is the purpose of this chapter to present a summary and general survey of the buckling behavior of an arbitrary three-dimensional stayed columns with different end conditions. Attention will be focused on the analysis of a single-crossarm stayed column with three different boundary conditions: 1) both ends fixed, 2) one end fixed and the other end hinged, and 3) one end fixed and the other end free. First, the influence of crossarm

member length and the stay size on buckling behavior of the three cases under consideration will be examined. Next the influence of crossarm member length on the relative efficiency will be examined. Finally, a numerical example will be presented to illustrate the power of the finite element method in nonlinear analysis.

7.2 Influence of Crossarm Member Length

The influence of the crossarm member length on the buckling behavior of the three cases under consideration are explored here. The stay diameter, which must remain constant during the varying of crossarm member length, was selected as 0.25 in. Then, for various ratios of L to l_{ca} , and with the aid of the same computer program used previously, the buckling load and the corresponding buckling mode were calculated. The results obtained from the computer program are illustrated in Fig. 7-1. In this Fig. the value of L to l_{ca} is the abscissa and the values of the critical loads is the ordinate. It should be noted that the buckling behavior of the three cases under consideration is illustrated on the same Fig. to clarify the influence of end conditions. It can be seen from this Fig. that the buckling strength of the stayed column with one end fixed and the other end free is comparatively low. Also, for this case the buckling

strength changes slightly with the increase of the cross-arm member length. It can also be recognized that the buckling behavior in this case is controlled by only one mode of instability (Mode III buckling) shown in Fig. 7-2a. This mode will be discussed subsequently in some detail.

For the case of one end fixed and the other end hinged the buckling behavior is controlled by two modes of instability: Mode IV and Mode V buckling shown in Figs. 7-2b and 7-2c respectively. One can observe from Fig. 7-1 that Mode IV buckling controls for large ratios of L to l_{ca} . For small ratios of L to l_{ca} , Mode V buckling becomes the controlling mode at bifurcation. It can also be seen from the same Fig. that when Mode IV buckling is the controlling mode, the buckling strength of the stayed column is increased as the crossarm member length is increased. When Mode V buckling controls, the buckling strength decreases as the crossarm member length increases. This behavior was expected because as the crossarm member length is increased the translational restraint at the crossarm is increased and the rotational restraint at the crossarm is decreased. It is also apparent from the same Fig. that the buckling strength increases and decreases slowly when Mode IV and Mode V buckling controls respectively.

It can be seen from the same Fig. that the buckling

strength is the highest in the case of the stayed column with both ends fixed. Also, for large ratios of L to l_{ca} , the buckling strength increases rapidly and the buckling behavior is controlled by Mode VI buckling. It can also be seen that when Mode VII buckling is the controlling mode, the buckling strength decreases slowly with the increase of the crossarm member length. This behavior was expected because as the crossarm member length is increased the translational restraint increases and the rotational restraint decreases. It should be noted that the modes of instability mentioned here will be discussed subsequently in some detail. The curves in Fig. 7-1 reflect the great influence of the end conditions on the buckling behavior of a single-crossarm stayed column.

7.3 Influence of Stay Size

In this section the influence of the stay size on buckling behavior is investigated for the three cases under consideration. The ratio of L to l_{ca} , which must remain constant during the varying of the stay size, is selected as 7. Also, the stay modulus of elasticity is selected as 29600 ksi. Then, for various values of the stay size and with the aid of the computer program, the buckling load and the corresponding buckling mode were calculated. The results obtained from the computer program are illustrated

in Fig. 7-3. The curved lines in this Fig. represent the buckling strength of the stayed column as a function of the stay size. The curves in that Fig. illustrate the buckling behavior of the three cases under consideration and the influence of end conditions on buckling behavior. It can be observed from the same Fig. that the buckling strength of the three cases under consideration always increase with an increase in the stay size. For the case of one end fixed and the other end free, the buckling strength is only slightly increased with the increase of the stay size. It should also be noted that the buckling behavior in this case, is only controlled by one mode of instability (Mode III buckling). Also, the buckling strength is comparatively low as can be seen from the same Fig.

As for the second case where one end is fixed and the other end hinged, the buckling strength is controlled by two modes of instability: Mode IV and V buckling. For a small stay diameter the buckling behavior is controlled by Mode IV buckling, while Mode V buckling controls for larger stay diameters. It can be seen from the same Fig. that the buckling strength is slightly increased when Mode V buckling controls. Also, the rate of increase in buckling strength is comparatively high when Mode IV buckling is the controlling mode at bifurcation. These

results were expected because the horizontal component of the additional* force in the stay is increased as the stay size is increased. At a certain diameter the horizontal force at the crossarm is enough to prevent translation at the crossarm. At this point, the rotation of the column at the crossarm may equal zero or have a certain value. Mode V buckling will occur when the rotation has a certain value while Mode IV buckling occurs for zero rotation at the crossarm. It is obvious that the buckling strength corresponding to zero rotation at the crossarm is higher than that of a certain rotation at the crossarm. Consequently, it is expected that the buckling behavior will be controlled by Mode V buckling.

In the case of both ends fixed, the buckling strength is also controlled by two modes of instability: Mode VI and Mode VII buckling. For small stay diameter, Mode VI buckling controls the instability behavior. Also, the buckling behavior is controlled by Mode VII buckling for larger stay diameters. It can be observed from the same Fig. that the buckling strength increases rapidly when Mode VI buckling controls the instability behavior.

*At the instant of buckling, when Mode IV buckling occurs, the displacement at the crossarm causes elongations in the stays at the convex side. This creates additional force in these stays which resists the translation at the crossarm. At the same time the stays in the concave side slacks. A similar case explained in Chapter 4.

However, the buckling strength increases slowly when Mode VII buckling controls. It can also be seen from that Fig. that the buckling strength for this case is the highest.

7.4 The Relative Efficiency

The influence of the crossarm member length on the relative efficiency for the three cases under consideration is explored here. As defined previously the relative efficiency is the ratio of the critical load, P_{cr} , to the total weight of the stayed column. The results obtained from the computer program are illustrated in Fig. 7-4. The curved lines in this Fig. represent the relative efficiency of the stayed column as a function of the ratio L to L_{ca} . It should be noted that each of the three curves in that Fig. corresponds to one of the three cases under consideration. It should also be emphasized that the stay diameter and the stay modulus of elasticity are considered to be constant and are selected as 0.25 in. and 29600 ksi respectively. The curved line corresponding to the case of one end fixed and the other end free indicates that the relative efficiency is only slightly changed as the crossarm member length varies. It can be observed that the relative efficiency is slightly increased with the increase of the crossarm member length until it

reaches its maximum value. Thereafter, it slightly decreases as the crossarm member length is increased. This behavior is expected and can be fully understood by going back to the corresponding curve in Fig. 7-1. It is also apparent from this Fig. that the stayed column with one end fixed and the other end free is the least efficient.

As for the case of one end fixed and the other end hinged, it can be seen from the same Fig. that the relative efficiency increases normally as the crossarm member length is increased until it reaches its maximum value. Thereafter it decreases at a comparatively fast rate. This behavior can be fully understood by comparing the corresponding curves in Figs. 7-1 and 7-4. It can be observed that the relative efficiency increases when Mode IV buckling controls the instability behavior. It decreases when Mode V buckling is the controlling mode at bifurcation.

For the third case of both ends fixed it can be seen from the corresponding curve in the same Fig. that the relative efficiency in this case is the highest. It can also be seen that for large ratios of L to l_{ca} the relative efficiency increases rapidly with the increase of the crossarm member length until it reaches its maximum value. Thereafter it decreases rapidly as the crossarm member length is increased. It can be noted that the maximum value of the relative efficiency is obtained in the vicinity

where the two corresponding buckling curves of Fig. 7-1 intersect. The behavior can be truly understood by comparing the corresponding curves in Figs. 7-1 and 7-4. It can be observed that the relative efficiency in this case increases when Mode VI buckling controls the buckling behavior while it decreases when Mode VII buckling controls. The curved lines in this Fig. reflect the tremendous effect of the end conditions on the efficiency of the stayed columns.

7.5 Modes of Instability

In this chapter five modes of instability corresponding to the three cases under consideration have been mentioned. Quite naturally, attention has been directed toward the investigation of these modes. That is because the interpretation of the buckling phenomenon discussed in the previous sections is only possible when those modes of instability are fully understood by the analyst.

In the case of both ends fixed, the buckling behavior is found to be controlled by two modes of instability: Mode VI and Mode VII buckling. These modes are illustrated in Figs. 7-5a and 7-5b respectively. To simplify the phenomenon of buckling modes, the stayed column can be replaced by the model shown in Fig. 7-5c. It consists of a fixed ended column of length $2L$, in which

the stays and crossarm members have been replaced by an elastic spring that resists the lateral translation of the column at the crossarm. It is obvious that the resistance of the linear spring reflects the stay properties and the length of the crossarm members. If there are no stays, the resistance of the elastic spring will vanish and the expected mode of instability will be the symmetric buckling of the simple column with both ends fixed as illustrated in Fig. 7-5d. In case of light stays and small crossarm members, the resistance of the spring will be small. The expected mode of instability is illustrated in Fig. 7-5a (Mode VI buckling). For heavy stays and long crossarm members, the resistance of the spring will be enough to prevent the translation at the crossarm. As mentioned previously, the rotation of the column at the crossarm may have a certain value Fig. 7-5b (Mode VII buckling) or equal zero as illustrated in Fig. 7-5e. The two modes shown in Figs. 7-5b and 7-5e represent the possible modes of instability when the translation of the column at the crossarm is prevented. As can be seen from this Fig. the two modes can be referred to as a symmetric buckling in which the rotation of the column at the crossarm is prevented (Fig. 7-5e) and antisymmetric buckling in which the rotation of the column at the crossarm has a certain value (Fig. 7-5b). One can observe

that the effective buckling length in the case of anti-symmetric buckling is longer than that of symmetric buckling. Consequently the buckling load corresponding to the symmetric buckling is higher than that of the antisymmetric buckling. Therefore it is expected that for heavy stays and long crossarm members the antisymmetric buckling (Mode VII instability) will be the controlling mode at bifurcation.

In the case of one end fixed and the other end hinged, the buckling behavior is controlled by two modes of instability: Mode IV and Mode V buckling. These modes are shown in Figs. 7-6a and 7-6b. In this case the stayed column can also be replaced by the model illustrated in Fig. 7-6c. It consists of a column of length $2L$, with one end fixed and the other end hinged. The stays and the crossarm members are replaced by an elastic spring to resist the translation of the column at the crossarm. As mentioned previously, the resistance of the elastic spring will vanish if there are no stays and the expected buckling mode is shown in Fig. 7-6d. In the case of light stays and small crossarm members, the resistance of the elastic spring will be small and the expected mode of instability is shown in Fig. 7-6a (Mode IV buckling). Again, for heavy stays and long crossarm members, the resistance of the elastic spring will be enough to prevent the translation of

of the column at the crossarm. As mentioned previously, the rotation of the column at the crossarm at this point will either equal to zero (Fig. 7-6e) or have a certain value (Fig. 7-6b). It can be recognized that the occurrence of a certain rotation of the column at the crossarm is more probable. That is because the rotational restraint of the column at the crossarm decreases as the crossarm member length is increased. Also, one can see that the effective buckling length for the case where the rotation of the column at the crossarm occurs (Mode V buckling) is longer than the case where the rotation is prevented (Mode IV buckling). Consequently, it is expected that for heavy stays and long crossarm members, Mode V buckling controls the buckling behavior.

As for the case where one end of the stayed column is fixed and the other end free, the buckling behavior is controlled by only one mode of instability (Mode III buckling) as illustrated in Fig. 7-7a. It can be recognized that the main function of the stays and the crossarm members is to reduce the effective buckling length and consequently increase the buckling load. This can be observed by comparing this mode (Mode III buckling) to the mode of buckling for the simple column with one end fixed and the other end free shown in Fig. 7-7b.

7.6 Numerical Example

The finite element method was used to analyze the stayed column shown in Fig. 7-8 in order to gain insight into the power of the method in the analysis of space stayed columns. Special care is given to the buckling behavior of a three-dimensional triple-crossarm stayed column. However, it should be emphasized that the power of the computer program used here is not limited to a certain type of space stayed column.

In this example, the column and the crossarm members were assumed to be circular steel tubes with an outside diameter of 2.25 in. and an inside diameter of 1.75 in. The length of the column was selected to be 100/3 ft. The modulus of elasticity of the column and crossarm members were taken to be 29600 ksi. Two types of stays were considered in this example: 1) steel rods, with modulus of elasticity of 29600 ksi and 2) wire ropes, with modulus of elasticity of 9400 ksi. The stay diameters were selected as 0.25 in. and/or 0.375 in. This will illustrate how the buckling behavior of the stayed column is heavily dependent on the stay properties. Since the main purpose of the numerical example presented here is to emphasize that the method of analysis used in this thesis is capable of analyzing any space stayed column. No attempt has been made to optimize the load carrying capacity of the

triple crossarm space stayed column under consideration.

As can be observed from Fig. 7-8, there are three levels of crossarms. Each of the first and third level contains three crossarm members having a length of 14.3 in. as shown in Fig. 7-8b. The intermediate level contains four crossarm members having a length of 28.6 in. as illustrated in Fig. 7-8c. The stays connected to the ends of the crossarm members in the intermediate level and the ends of the column will be denoted as the outer stays (8 stays). All other stays will be referred to as the inner stays (12 stays). In this analysis it is considered that (table 7.I):

Number of:	
Elements	38
Element with bending stiffness	18
Elements with significant axial load	8
Nodes	19
Nodes in column	9
Degrees of freedom	99
Outer stays	8
Inner stays	12

Table 7.I

Four cases are examined here. In these cases the dimensions and the properties of the column and the crossarm members remain constant. Only, the stay properties are changed as illustrated in Table 7.II.

	Diameter		Modulus of Elasticity	
	inner stays	outer stays	inner stays	outer stays
Case I	0.25	0.25	9400	29600
Case II	0.25	0.25	29600	29600
Case III	0.25	0.375	29600	29600
Case IV	0.375	0.375	29600	29600

Table 7.II


The critical load, the corresponding buckling mode, the weight and the relative efficiency for the four cases under consideration were calculated using the computer program. The results are shown in Table 7.III.

	Case I	Case II	Case III	Case IV
Critical Load (kps)	21.5	37.0	37.0	42.9
Weight (lbs)	300.0	306.0	334.0	355.0
Relative efficiency	71.6	120.9	110.9	120.8

Table 7.III

The buckling mode corresponding to the critical load in case I is illustrated in Fig. 7-9.

The theoretical results illustrated in Table 7.III indicate the following points:



1 - When the modulus of elasticity of the inner stays changes from 9400 ksi in case I to 29600 ksi in case II, the buckling strength increases significantly from 21.5k to 37k. That is because as the modulus of elasticity of the inner stays is increased, the translational restraint at the first and third crossarm levels is increased. Consequently the buckling strength is increased. This reflects the influence of stay modulus of elasticity on the buckling behavior of the stayed column.

2 - From case II and case III, it can be observed that the buckling strength does not change with the change in the diameter of the outer stays from 0.25 in. in case II to 0.375 in. in case III. This result was expected because the crossarm member length and the stay properties in case II were sufficient to prevent the translation at the intermediate crossarm. Therefore the increase in the diameter of the outer stays will not cause any change in the buckling shape and consequently no change in the buckling strength.

3 - The buckling strength in case IV increased when the diameter of the inner stay changed from 0.25 in. in

case III to 0.375 in. in case IV. That was because the crossarm member length and the stay properties of the inner stays in case III were not sufficient to prevent the translation at the first and third crossarm levels. Therefore any increase in the stay size or the modulus of elasticity of the inner stays reduces the translation at the first and third levels. Consequently will increase the buckling strength.

CHAPTER 8

SUMMARY, CONCLUSIONS AND RECOMMENDATIONS

8.1 Summary

This dissertation deals with the stability of three-dimensional stayed columns which are acted upon by a concentrated load. Two systems are considered in this study: a single-crossarm stayed column with three crossarm members, and the other with four-crossarm members. The following problems are included in the investigation:

- 1) Method of analysis for structures with geometrically nonlinear behavior (due to axial forces).
- 2) Influence of certain parameters of a single-crossarm stayed column on buckling behavior.
- 3) Efficiency of single-crossarm stayed columns.
- 4) Comparing the buckling behavior and the efficiency of the single-crossarm stayed column with three crossarm members and the other with four crossarm members.
- 5) Buckling of a stayed column with various end

conditions.

Problem number 1 has been investigated in detail in Chapter 2. In Chapters 4 and 5 the problems numbers 2 and 4 have been examined for the two systems under consideration. The relative efficiency for the two systems was explored in Chapter 6. The buckling behavior of a single-crossarm stayed column with three crossarm members was investigated briefly in Chapter 7 for three cases of end conditions.

The contributions contained in this dissertation may be summarized as follows:

- 1) The development of the geometric stiffness matrix in three-dimensions is believed to be the first extension of the geometric stiffness matrix from two dimensions to three dimensions.
- 2) The influence of varying certain parameters on buckling behavior of a single-crossarm space stayed column.
- 3) The comparison of the buckling behavior and the relative efficiency of the single-crossarm stayed column with three and that having four crossarm members. One can gain insight into the influence of the number of crossarm members on the buckling behavior and the relative efficiency.
- 4) A general survey of the buckling behavior of

a single-crossarm stayed column with various end conditions.

5) A computer program to analyze any space stayed column.

8.2 Conclusions

The methods of predicting the critical loads based on the finite element method and the stability functions were reviewed. It was concluded that for a computer solution the analysis based on the finite element method was much more convenient due to its non-iterative process. As mentioned previously the parameters of the single-crossarm stayed column were varied to determine their effect on the buckling behavior and the relative efficiency. At this point some of the important conclusions are summarized as follows:

1) It is possible to predict the buckling load and the corresponding buckling mode for any three dimensional stayed column by the finite element method.

2) The analysis based on the stability function is more accurate but needs more computer time due to its iterative process. Excellent results may be obtained by the finite element method when a reasonable number of finite elements are used.

3) The load carrying capacity of a column may be increased several times by reinforcing it with a system

of rigidly connected crossarms and pretensioned stays.

4) The load carrying capacity of the stayed column with four crossarm members is always higher than that of three crossarm members regardless of the stayed properties or the crossarm member length.

5) The crossarm member length has a significant effect on buckling behavior. The optimum length is that sufficient to make Mode I and Mode II buckling equally possible for the stayed column.

6) The buckling load increases continuously as the stay size is increased. The rate of increase of the buckling load when Mode I buckling controls is higher than that when Mode II buckling is the controlling mode.

7) For small stay diameters and small crossarm member lengths, the stayed column with four crossarm members is more efficient. For small stay sizes and longer crossarm members the stayed column with three crossarm members is more efficient. For heavy stays the stayed column with three crossarm members is more efficient.

8) For the stayed column with three crossarm members the maximum value of the relative efficiency is higher than that of four crossarm members regardless of the stay size.

9) For the single-crossarm stayed column with one end fixed and the other end either fixed or hinged,

the buckling behavior is controlled by two modes of instability. However, in the case where one end is fixed and the other end is free, the buckling behavior is controlled by only one mode of instability.

10) The buckling strength of the single-crossarm stayed column with one end fixed and the other end free changes slightly with the varying of the crossarm member length and the stay size.

11) For the single crossarm stayed column with one end fixed and the other end either fixed or hinged, the modes of instability are heavily dependent upon the stay properties and the crossarm member length.

12) The buckling strength and the relative efficiency of the single-crossarm stayed column with both ends fixed are the highest and those for a column with one end fixed and the other end free are the smallest.

8.3 Suggestions for Future Investigations

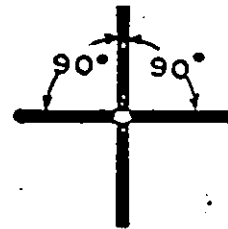
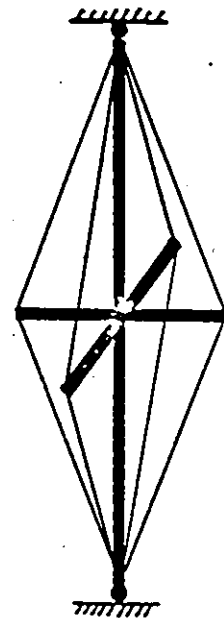
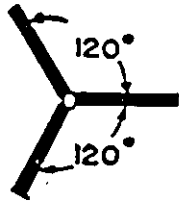
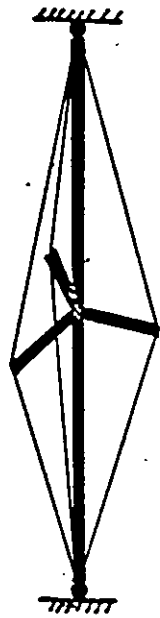
The theoretical studies presented in this dissertation constitute the firm foundation for obtaining solutions to the buckling of any space stayed columns. Further problems that need be studied in future are:

1) Extension of the analysis to the most general case in which both geometric nonlinearity and material nonlinearity are present.

2) Stability analysis at non-uniform stayed columns.

3) Pretension of space stayed columns. This will include the theoretical formulation required to determine the optimum pretension in the stays.

4) Experimental verification of the theoretical results obtained.



a) Single-crossarm stayed column
with three crossarm members

b) Single-crossarm stayed
column with four cross-
arm members

Fig.1-1 STAYED COLUMNS

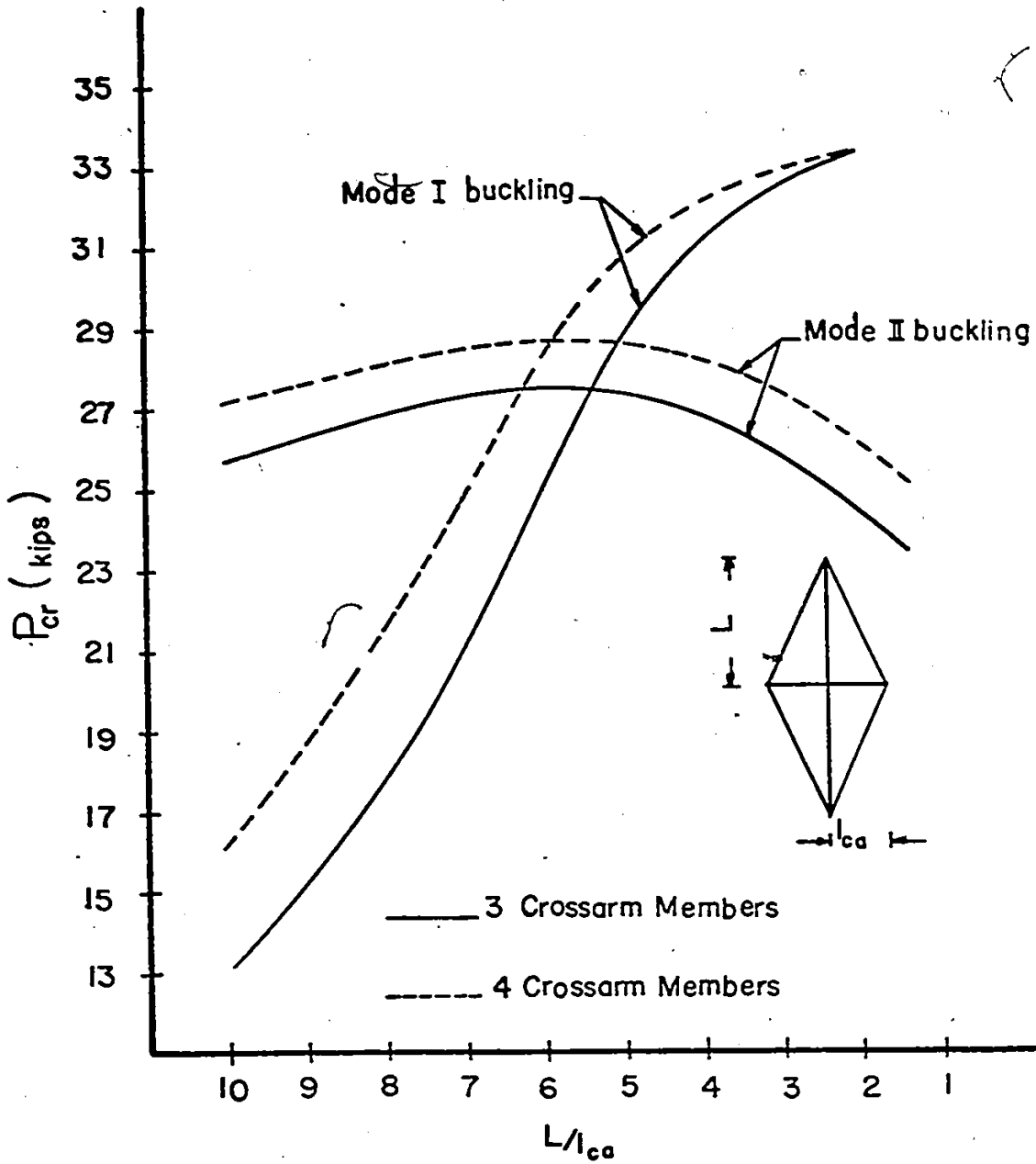
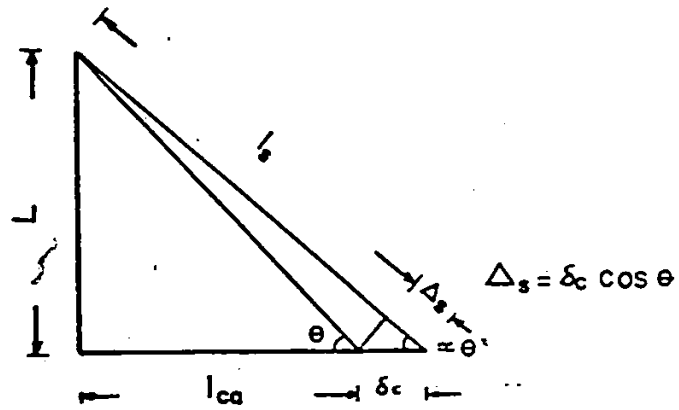
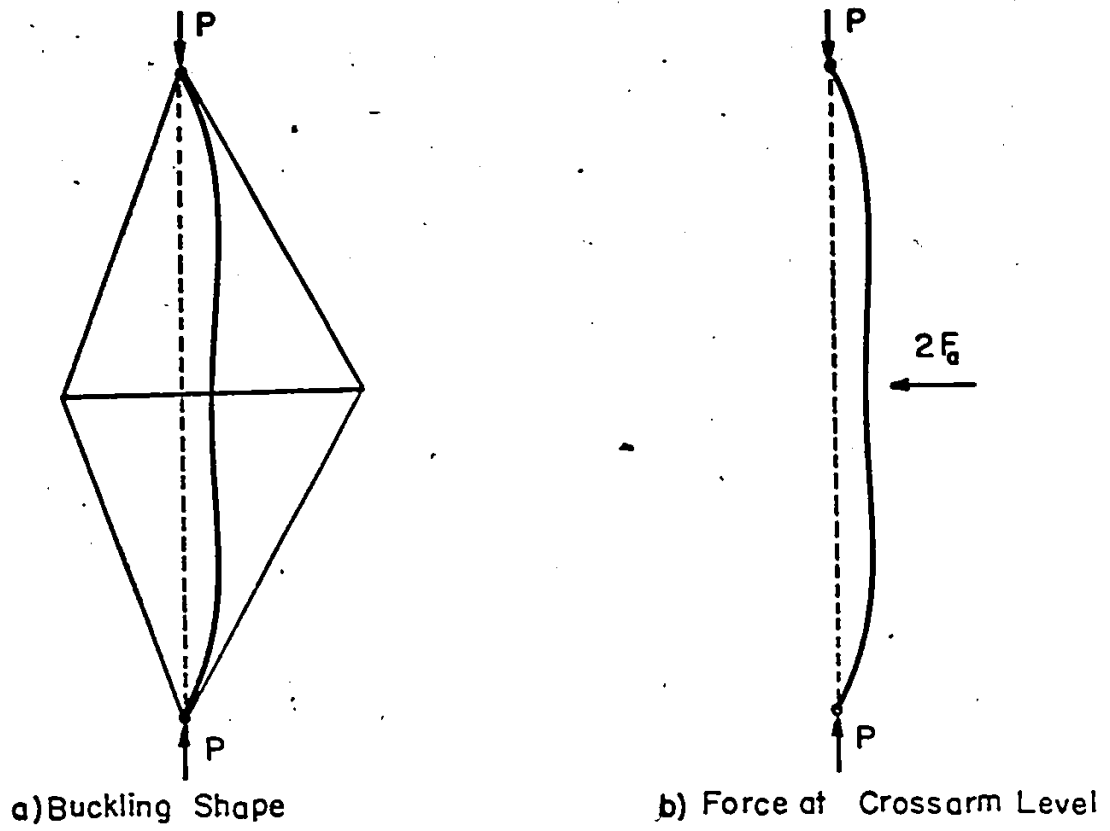


Fig.4-1

Influence of Crossarm Member Length on the Buckling Behavior ($\phi_{stay}=3/16"$)



c) Change in Length of Stays

Fig.4-2 The Additional Horizontal Force
at the Crossarm Level

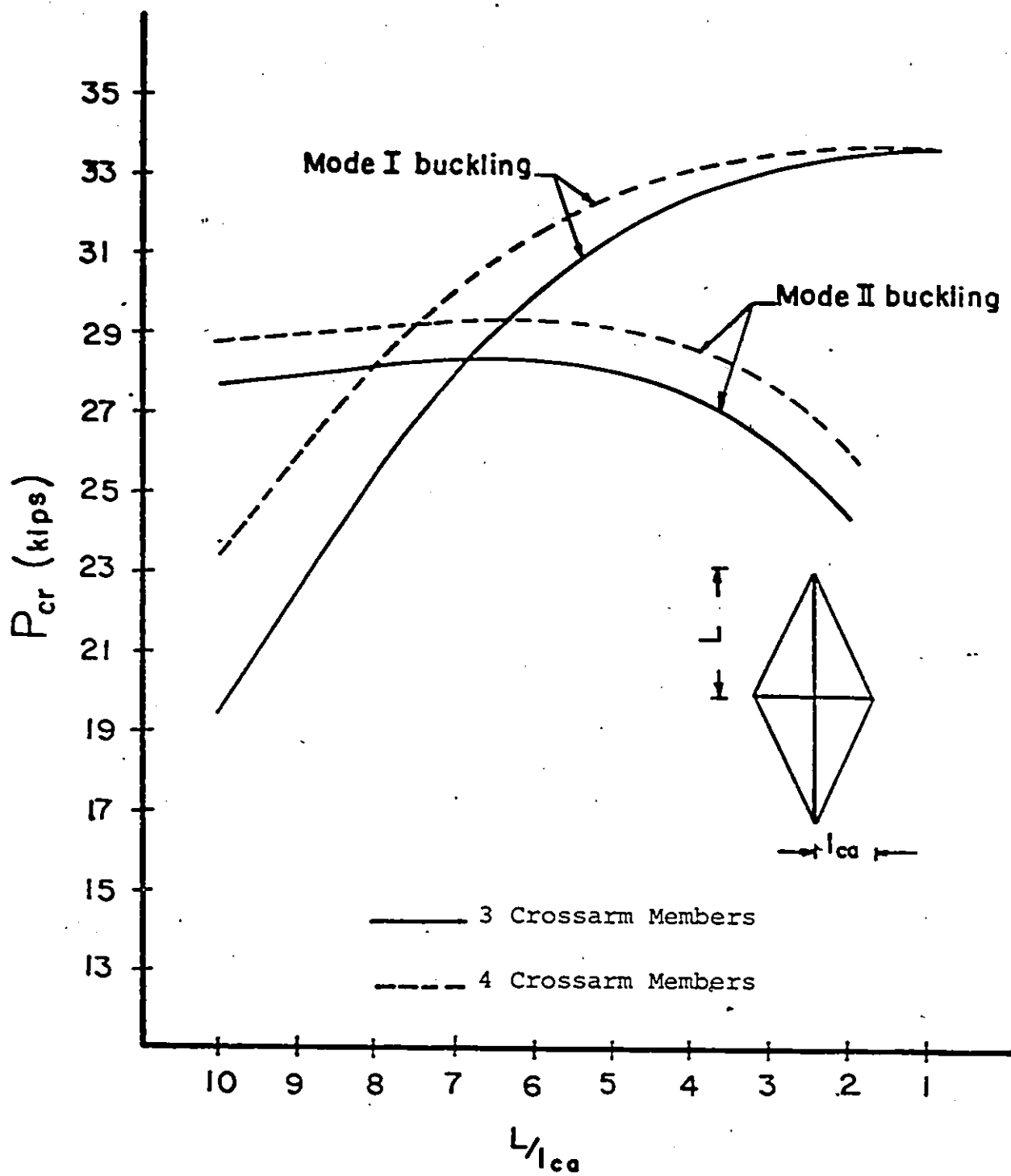


Fig. 4-3 Influence of Crossarm Member Length on the Buckling Behavior
 ($\phi_{stay} = 4/16$ in.)

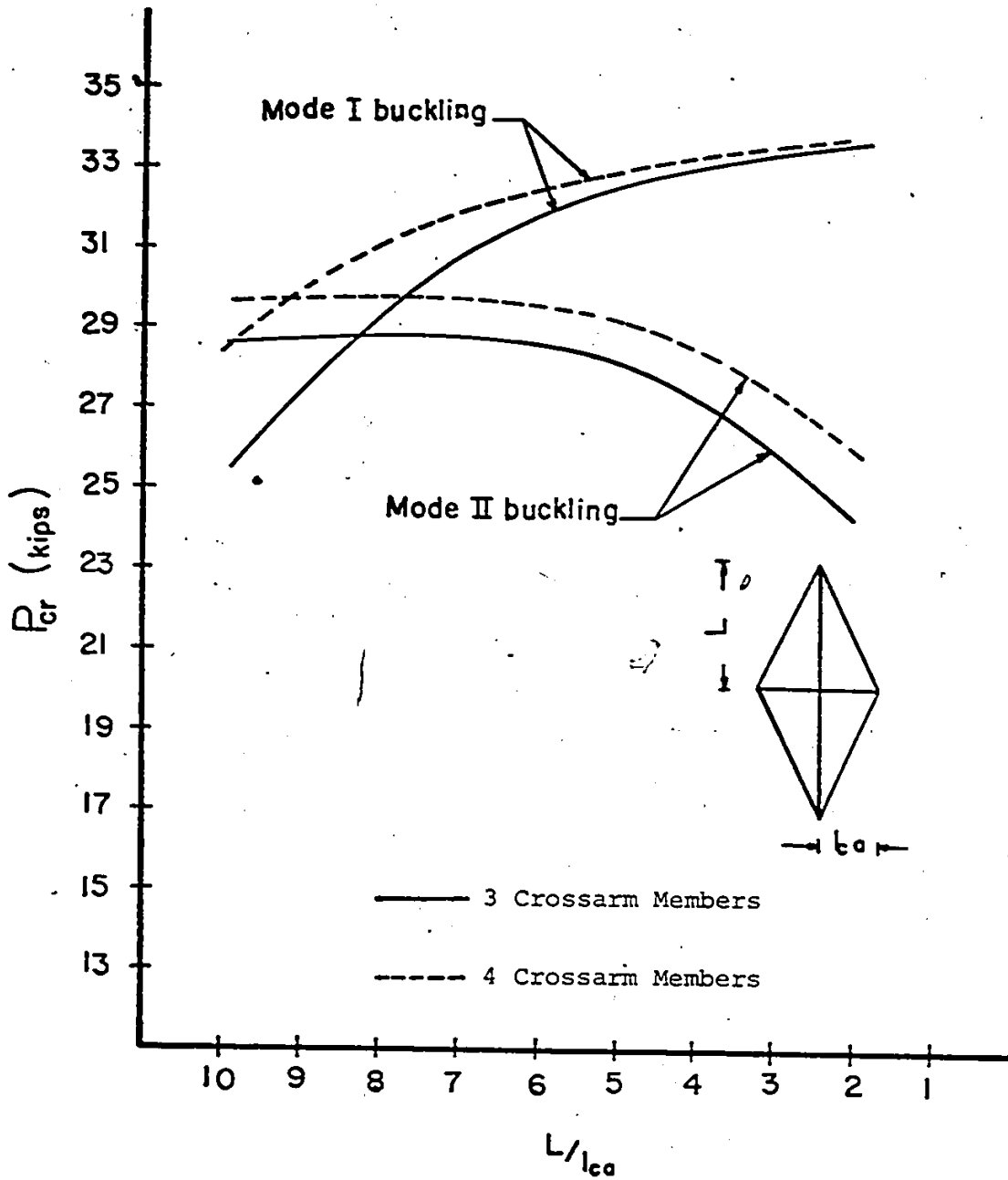


Fig. 4-4 Influence of Crossarm Member Length on the Buckling Behavior
 ($\phi_{stay} = 5/16$ in.)

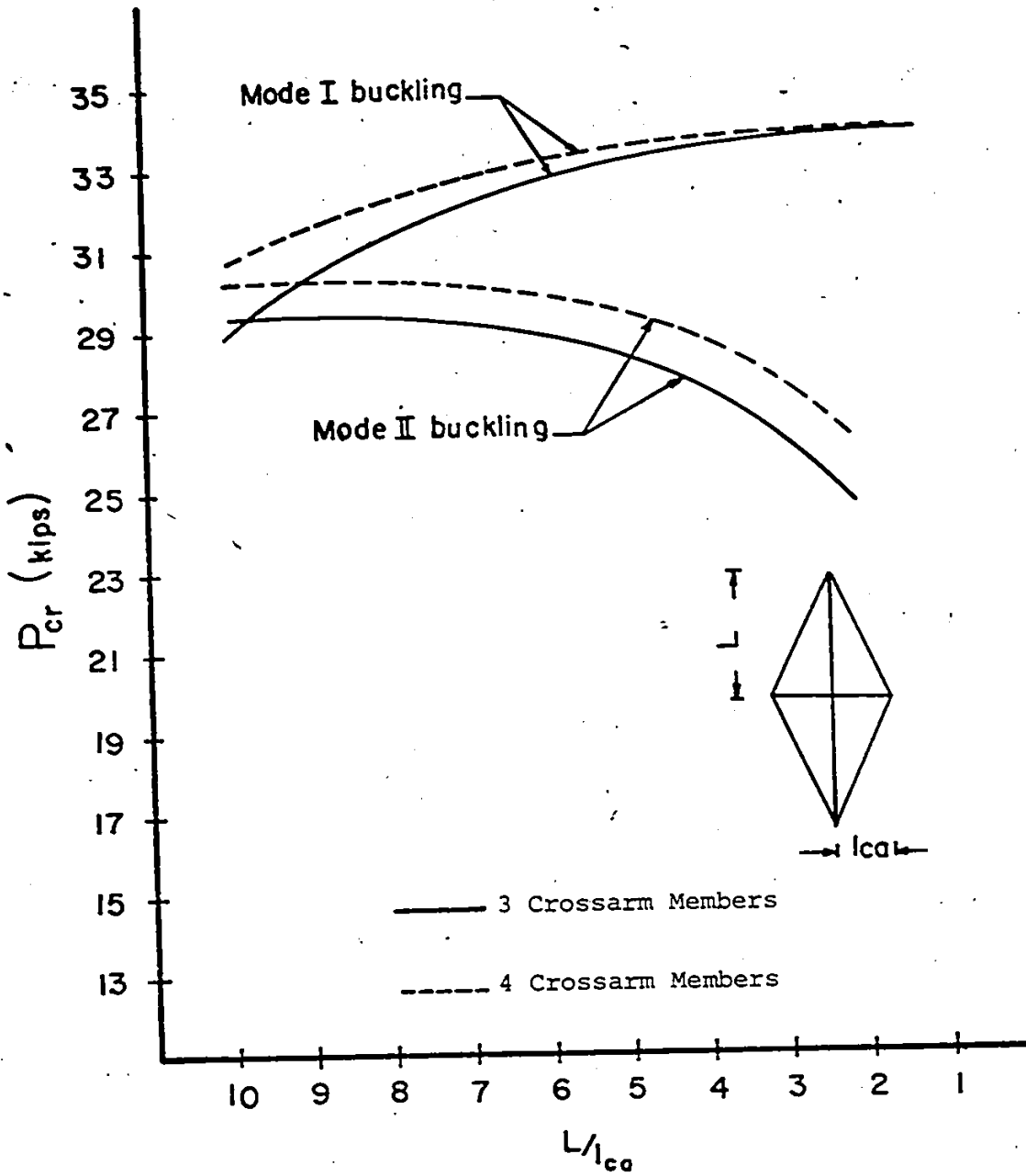


Fig. 4-5 Influence of Crossarm Member Length on the Buckling Behavior
 ($\phi_{stay} = 6/16$ in.)

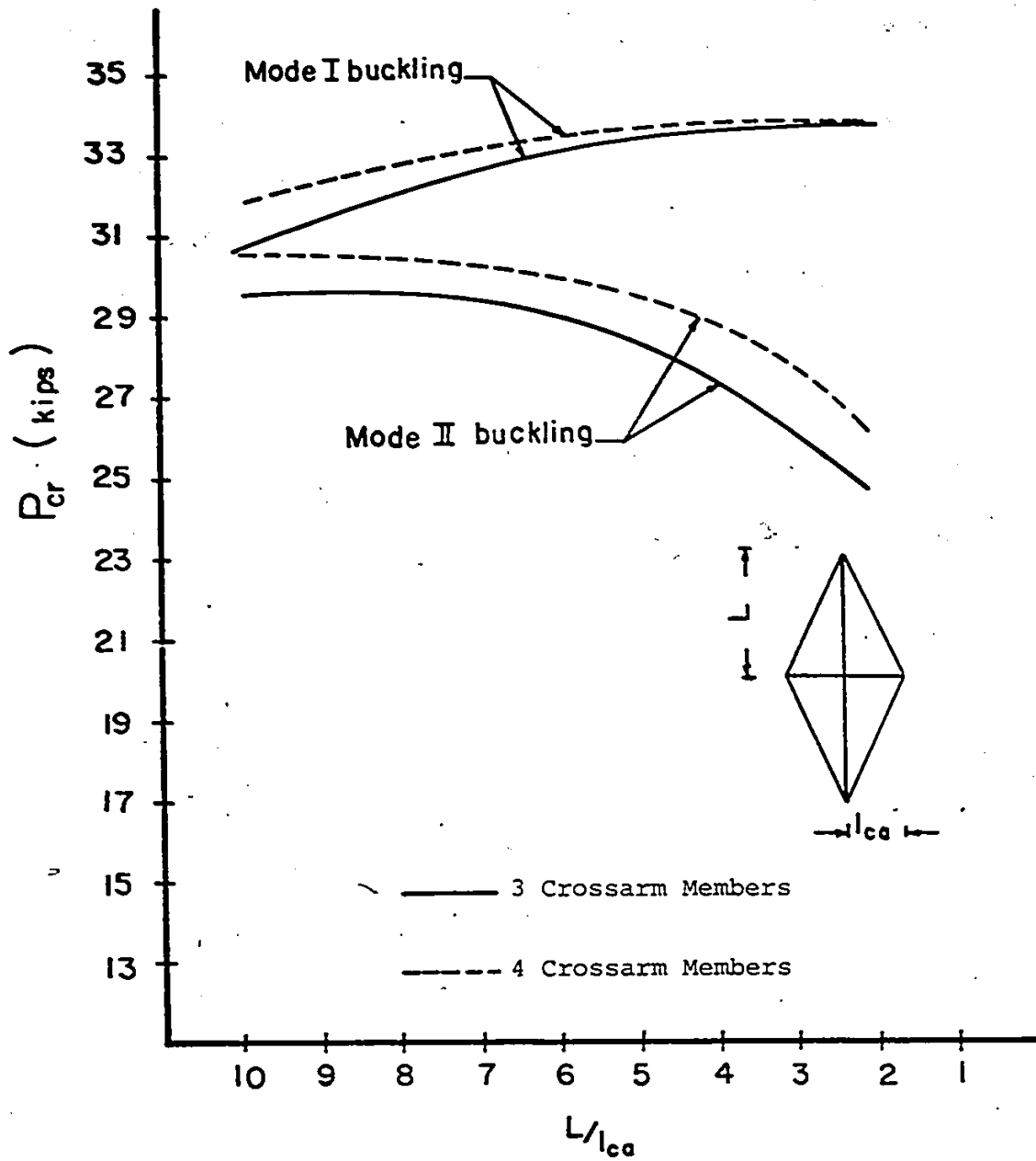


Fig. 4-6 Influence of Crossarm Member Length on the Buckling Behavior
 ($\phi_{stay} = 7/16$ in.)

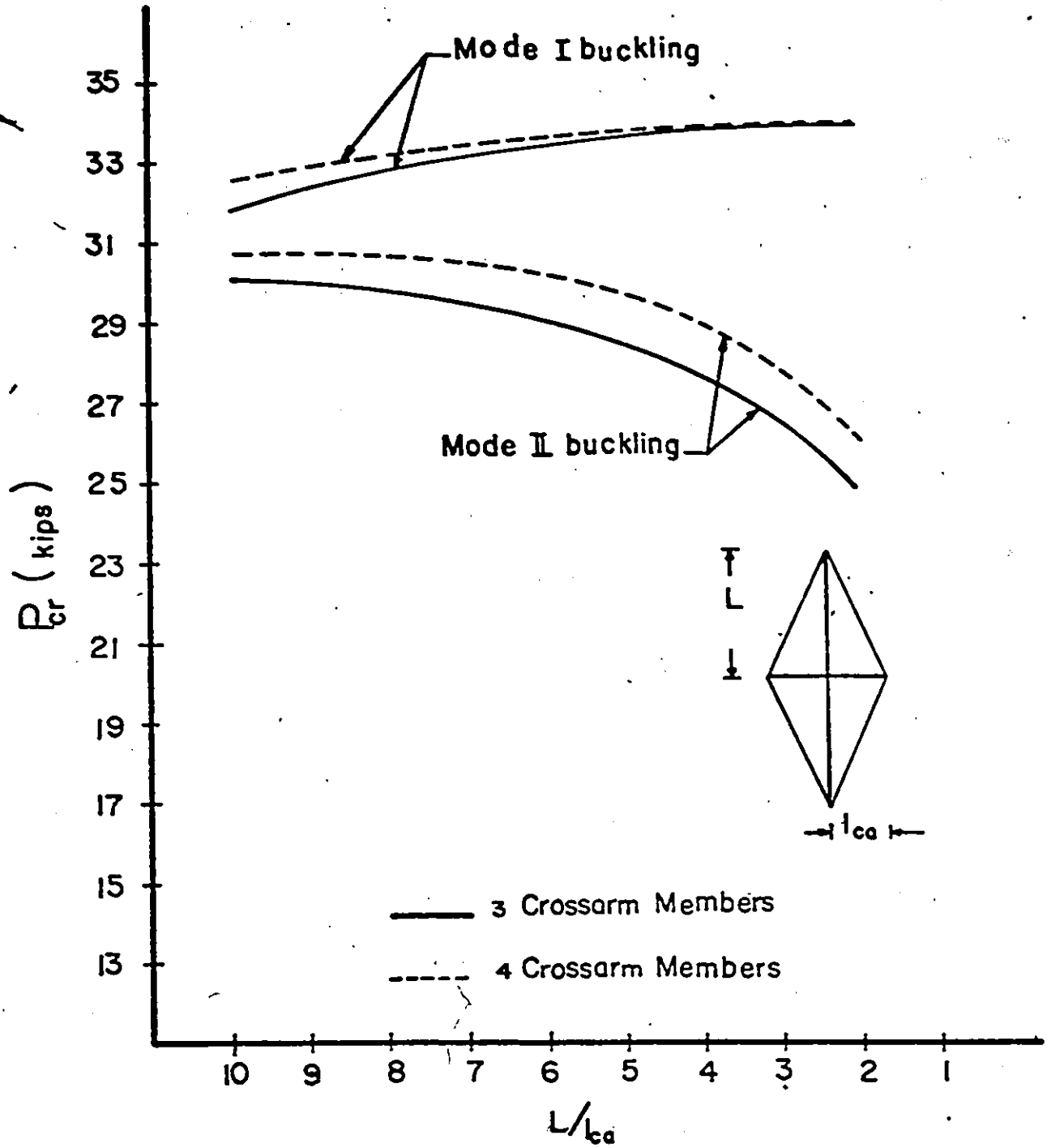


Fig. 4-7 Influence of Crossarm Member Length on the Buckling Behavior
 ($\phi_{stay} = 8/16 \text{ in.}$)

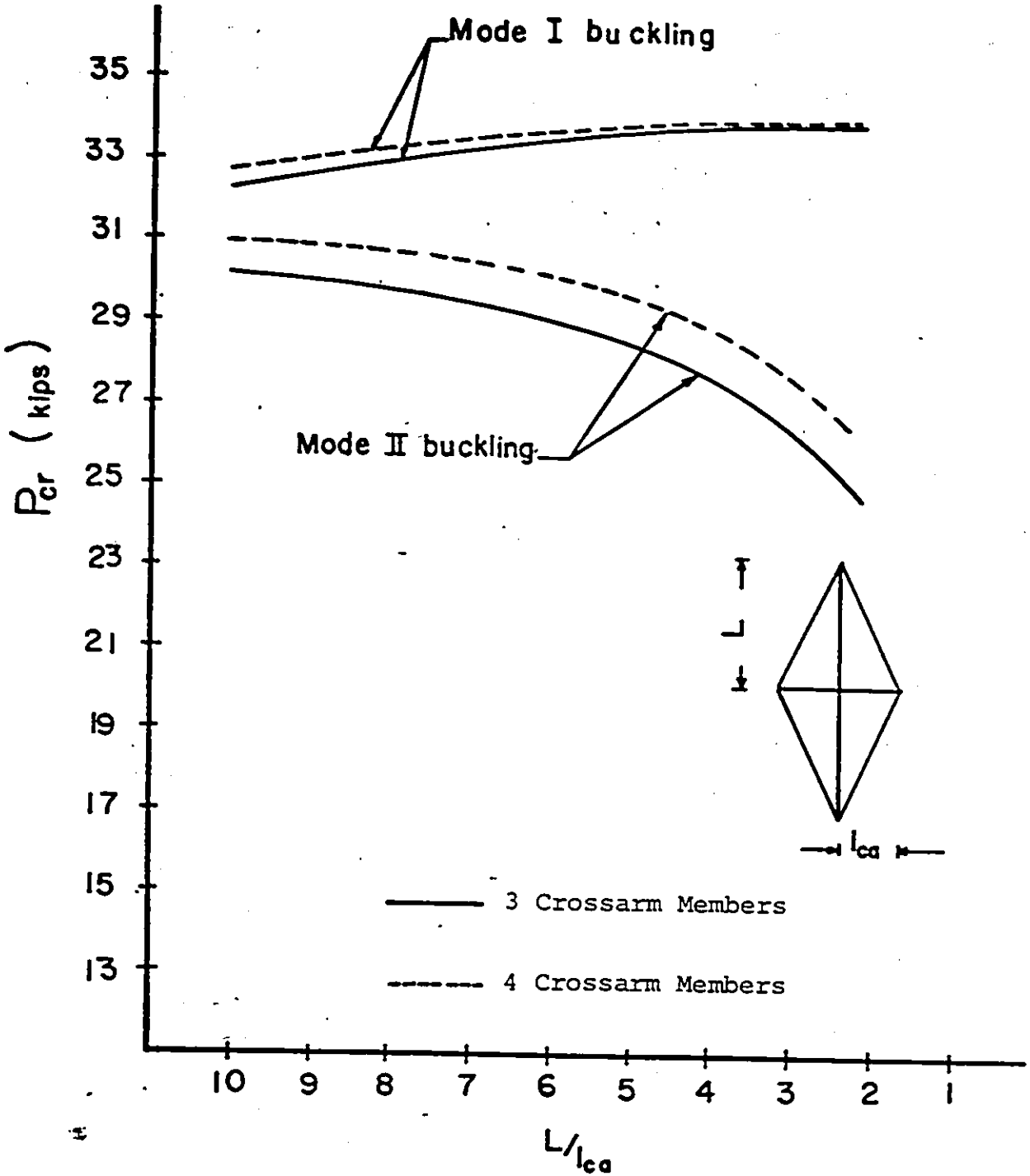


Fig. 4-8 Influence of Crossarm Member Length on the Buckling Behavior
 ($\phi_{stay} = 9/16$ in.)

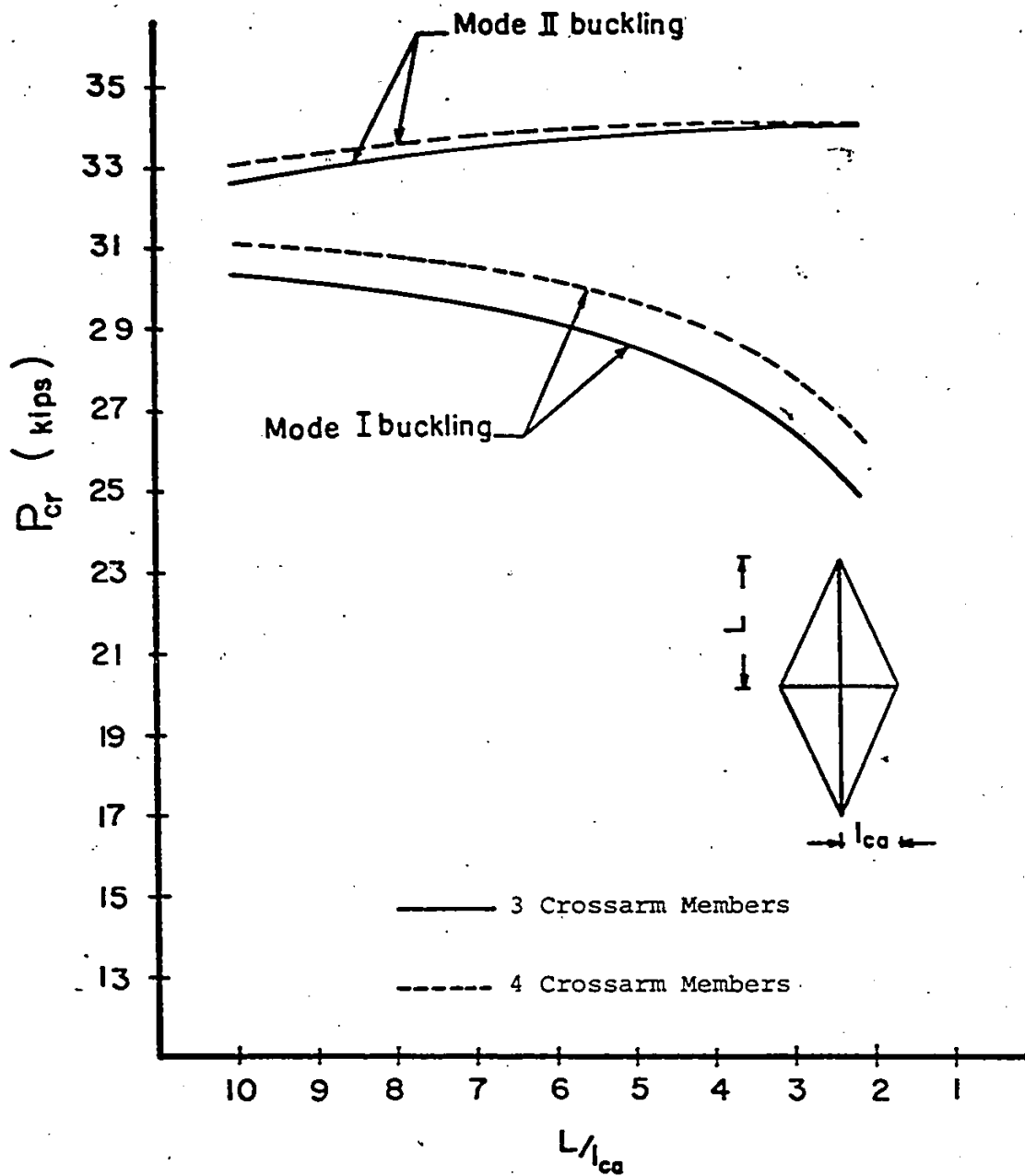


Fig. 4-9 Influence of Crossarm Member Length on the Buckling Behavior ($\phi_{stay} = 10/16$ in.)

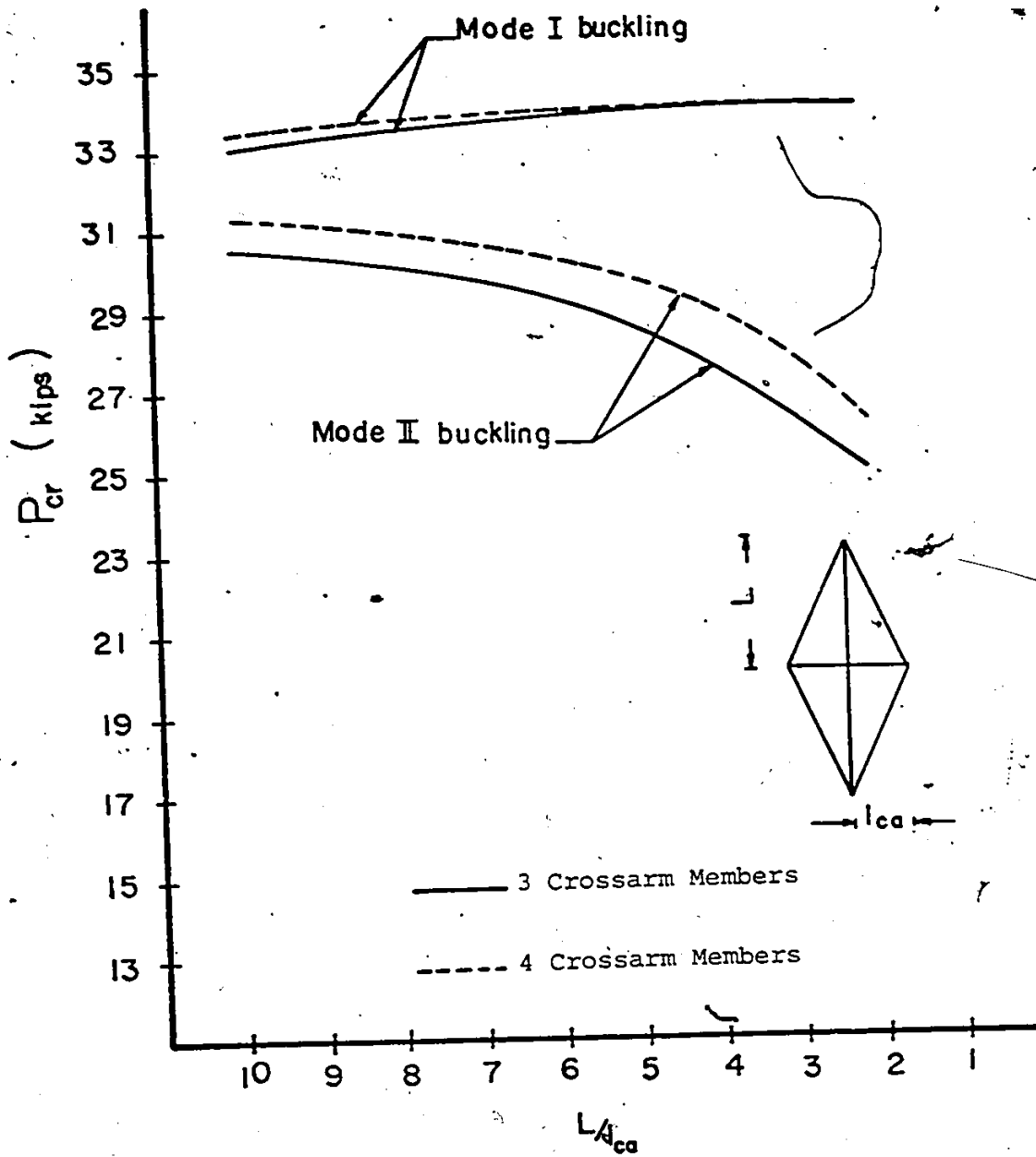
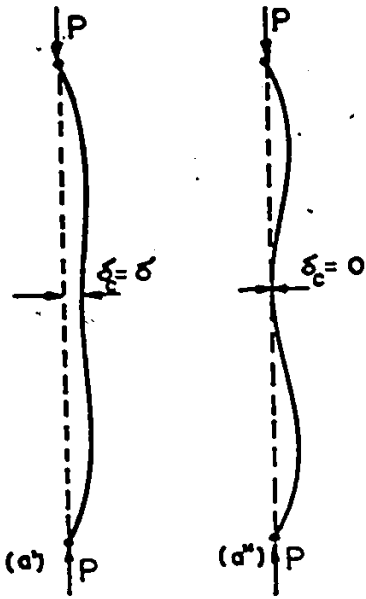
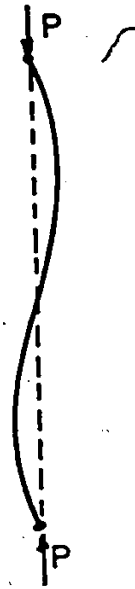


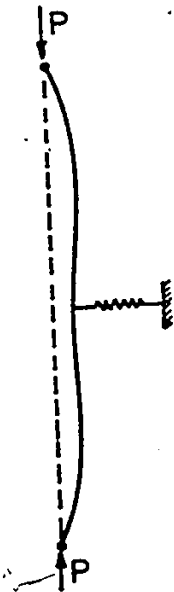
Fig. 4-10 Influence of Crossarm Member Length on the Buckling Behavior
 ($\phi_{stay} = 12/16$ in.)



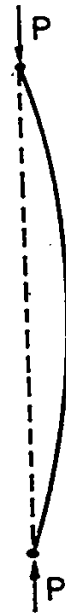
a) Mode I buckling



b) Mode II buckling



c) Model of buckling



d) Single Curvature b.

Fig. 4-11 Modes and Model of Buckling

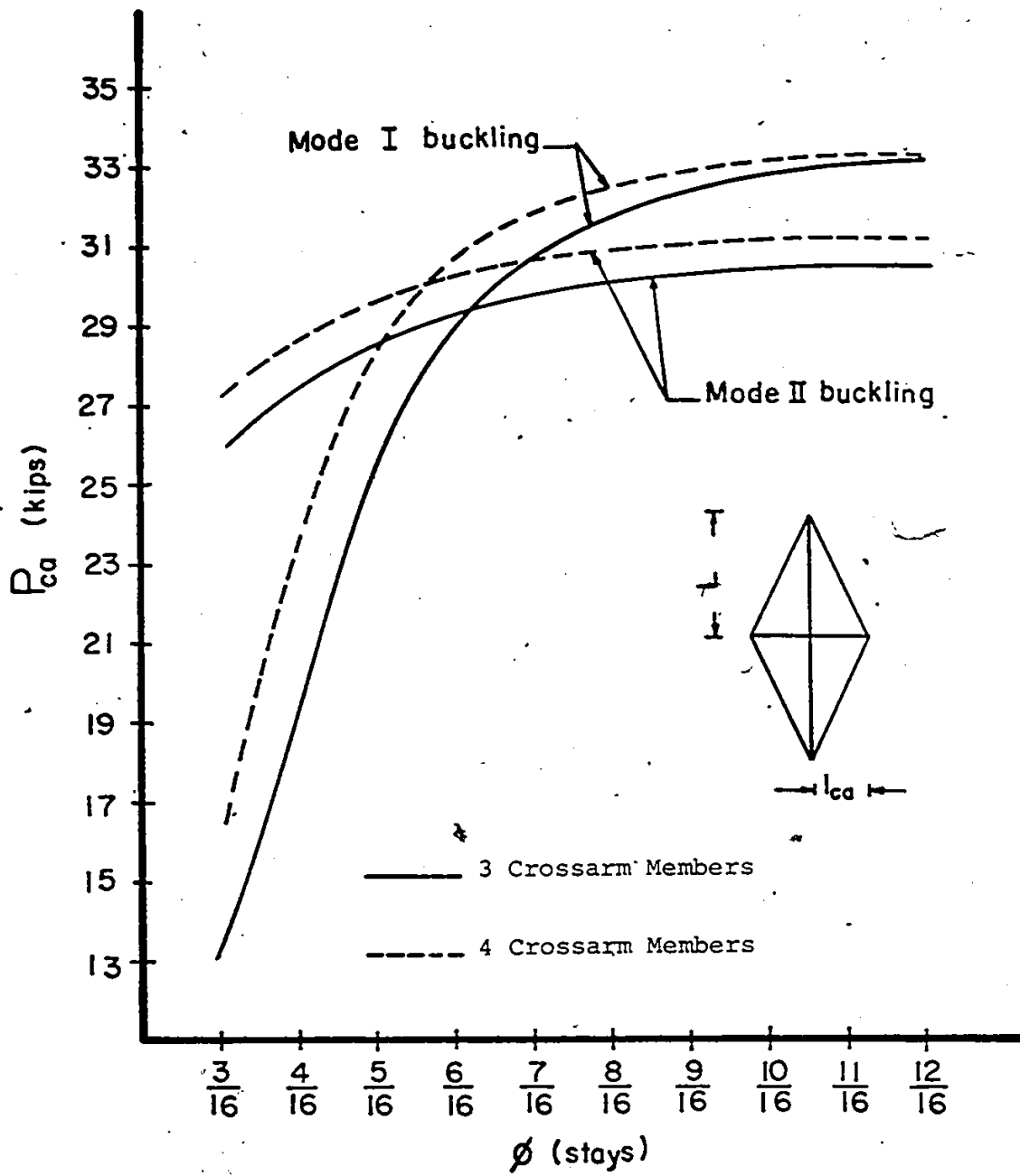
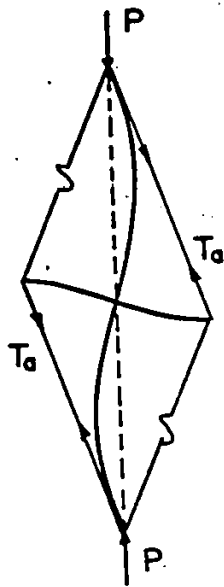
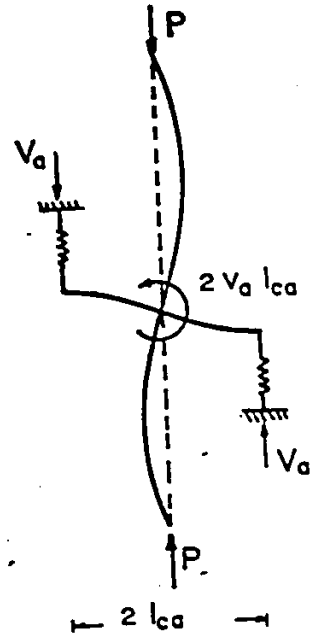


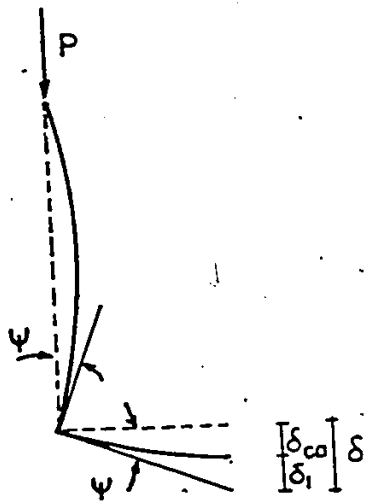
Fig.5-1 Influence of Stay Diameter on the Buckling Behavior
 ($L/l_{ca} = 10$)



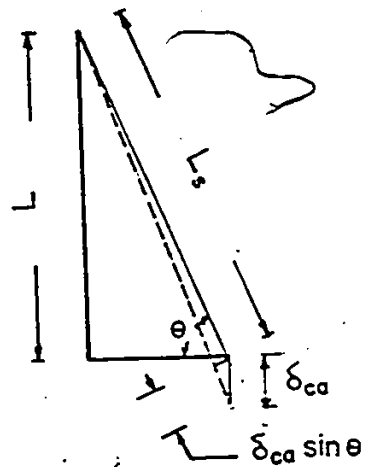
a) Buckling Mode



b) Model of Buckling



c) Rotation of the Column at the Crossarm



d) Elongation of the Stay

Fig.5-2 Model of Buckling and the Restraining Couple at the Crossarm Level

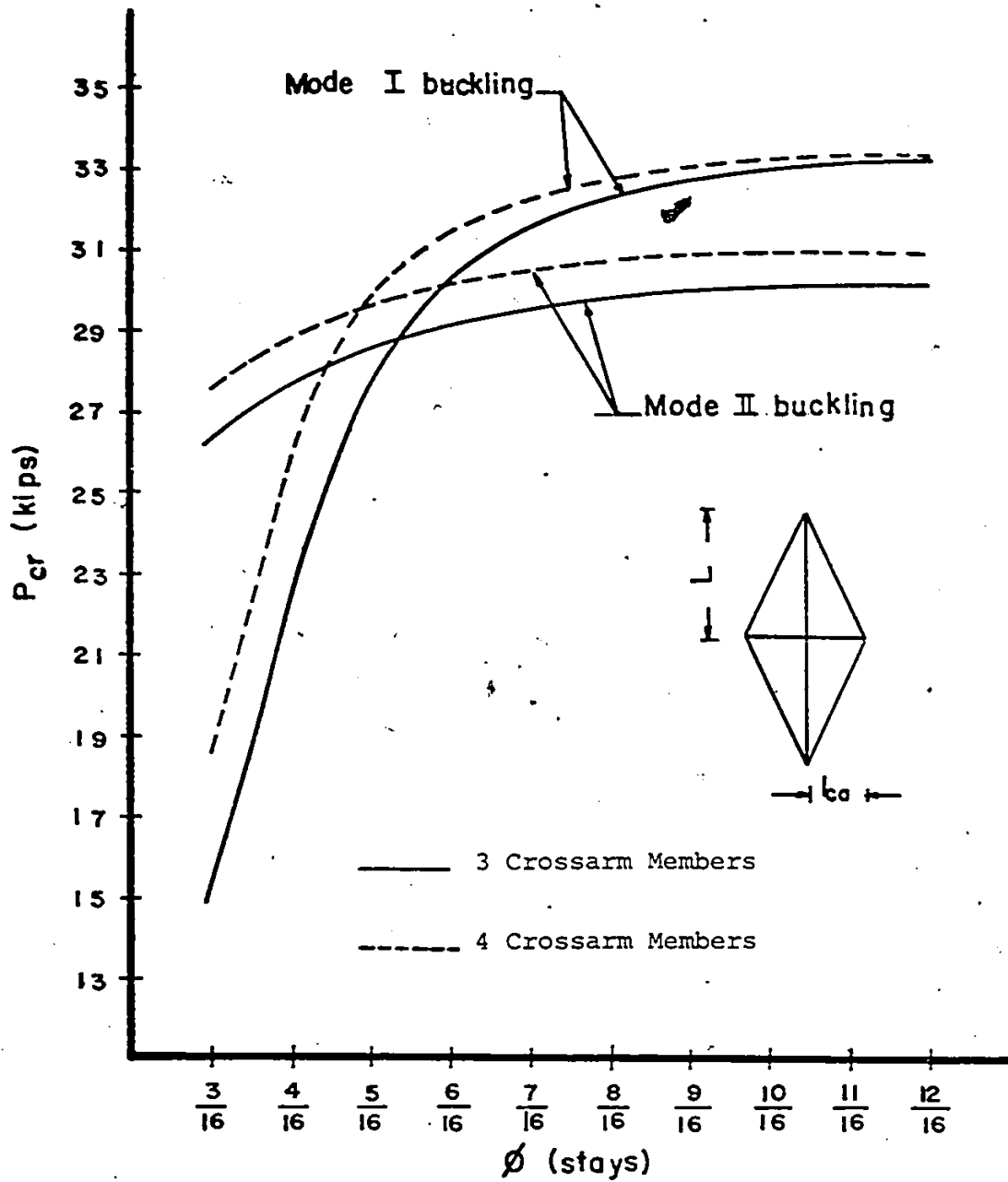


Fig.5-3 Influence of Stay Diameter
on the Buckling Behavior
 ($L/l_{ca} = 9$)

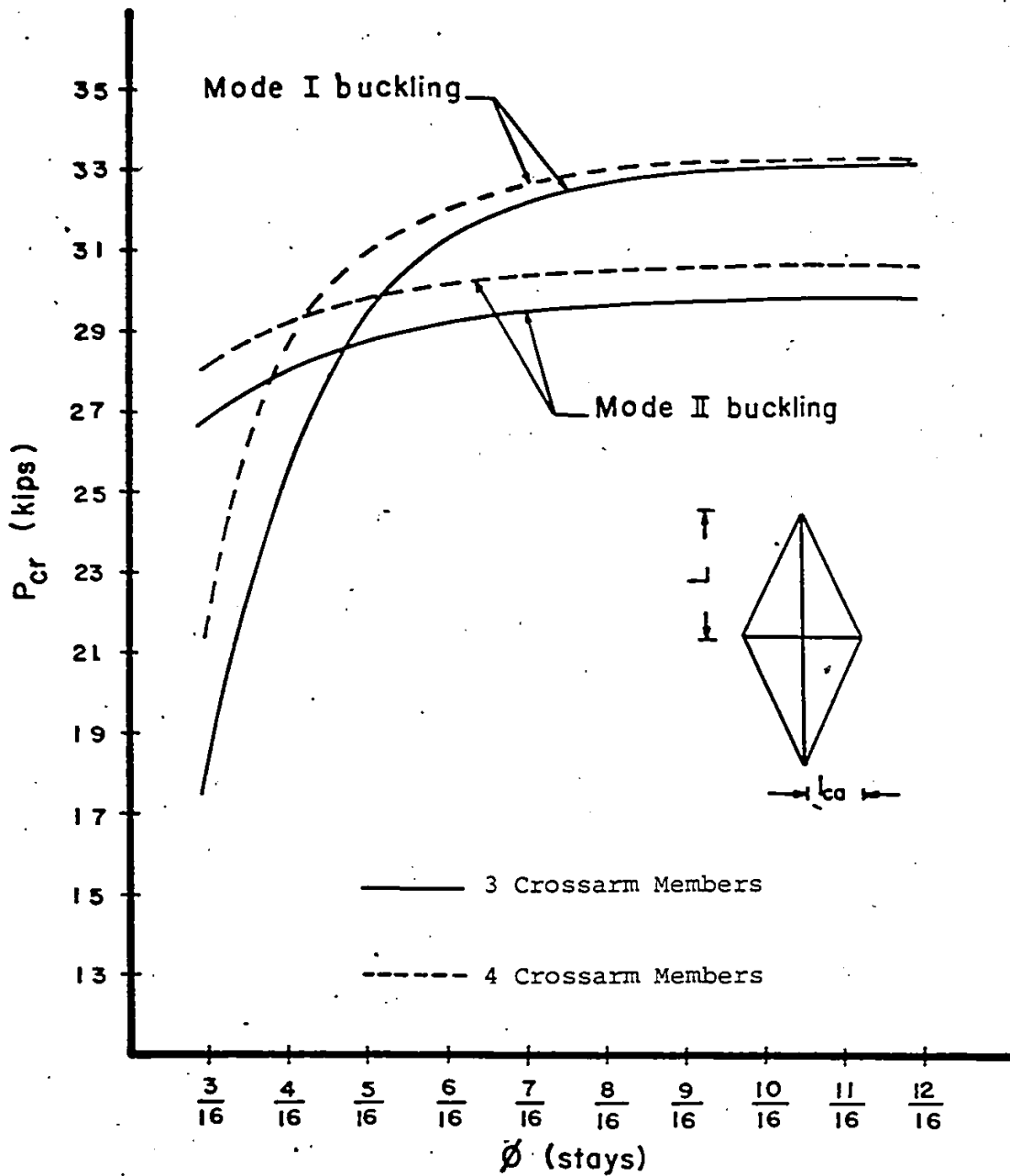


Fig.5-4 Influence of Stay Diameter
on the Buckling Behavior
 ($L/l_{ca} = 8$)

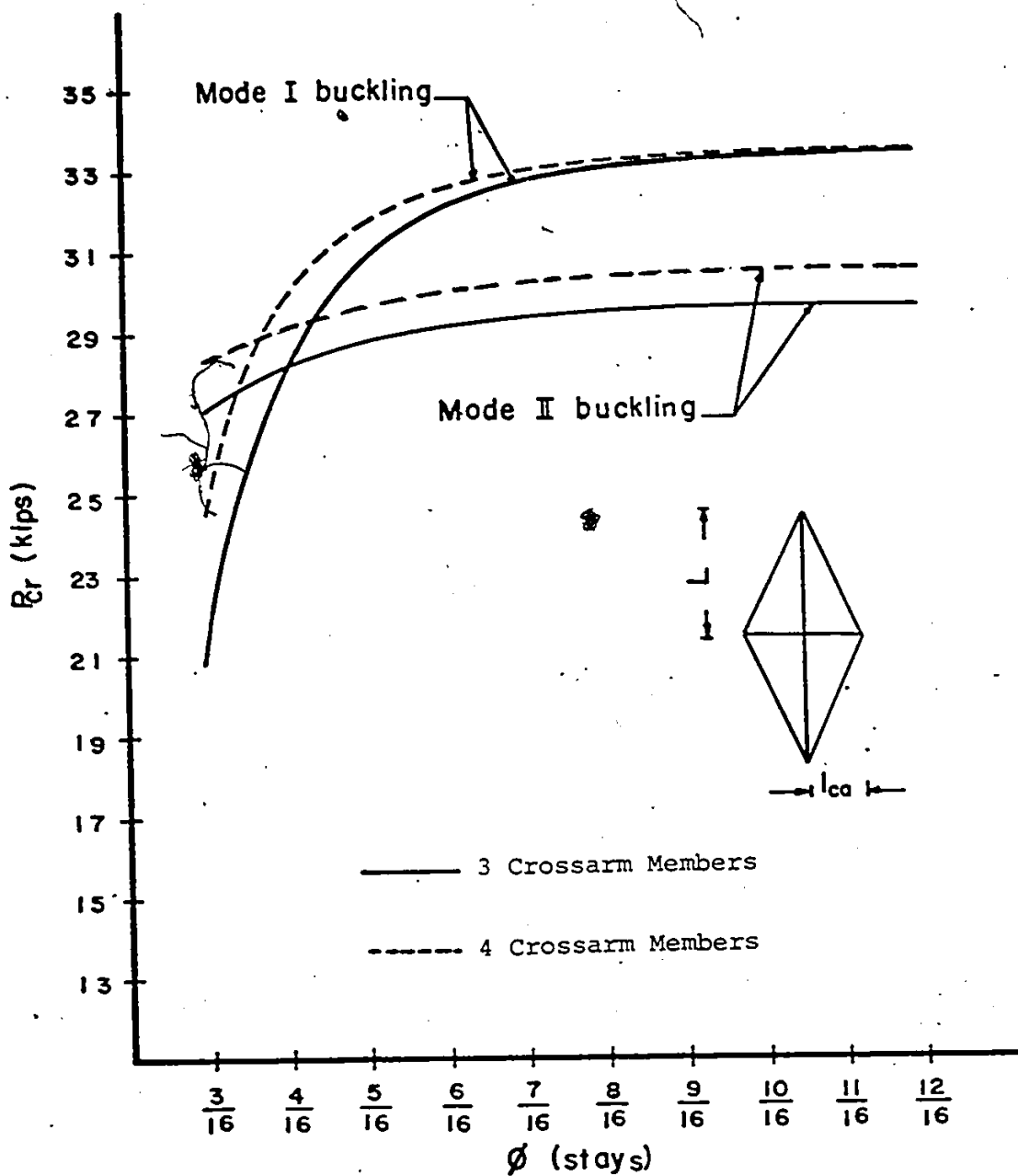


Fig. 5-5 Influence of Stay Diameter
on the Buckling Behavior
 ($L/l_{ca} = 7$)

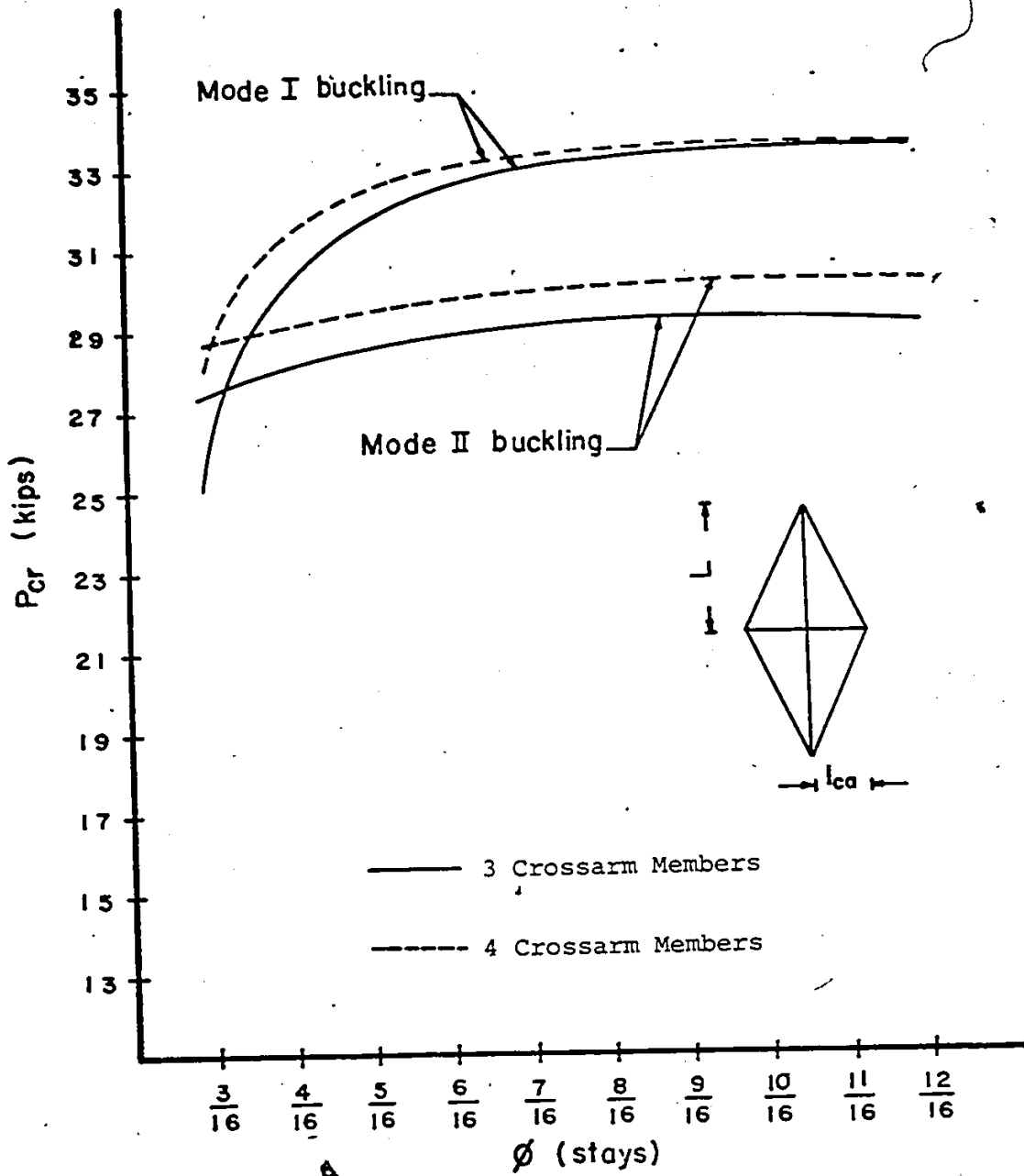


Fig. 5-6 Influence of Stay Diameter
on the Buckling Behavior
 ($L/l_{ca} = 6$)

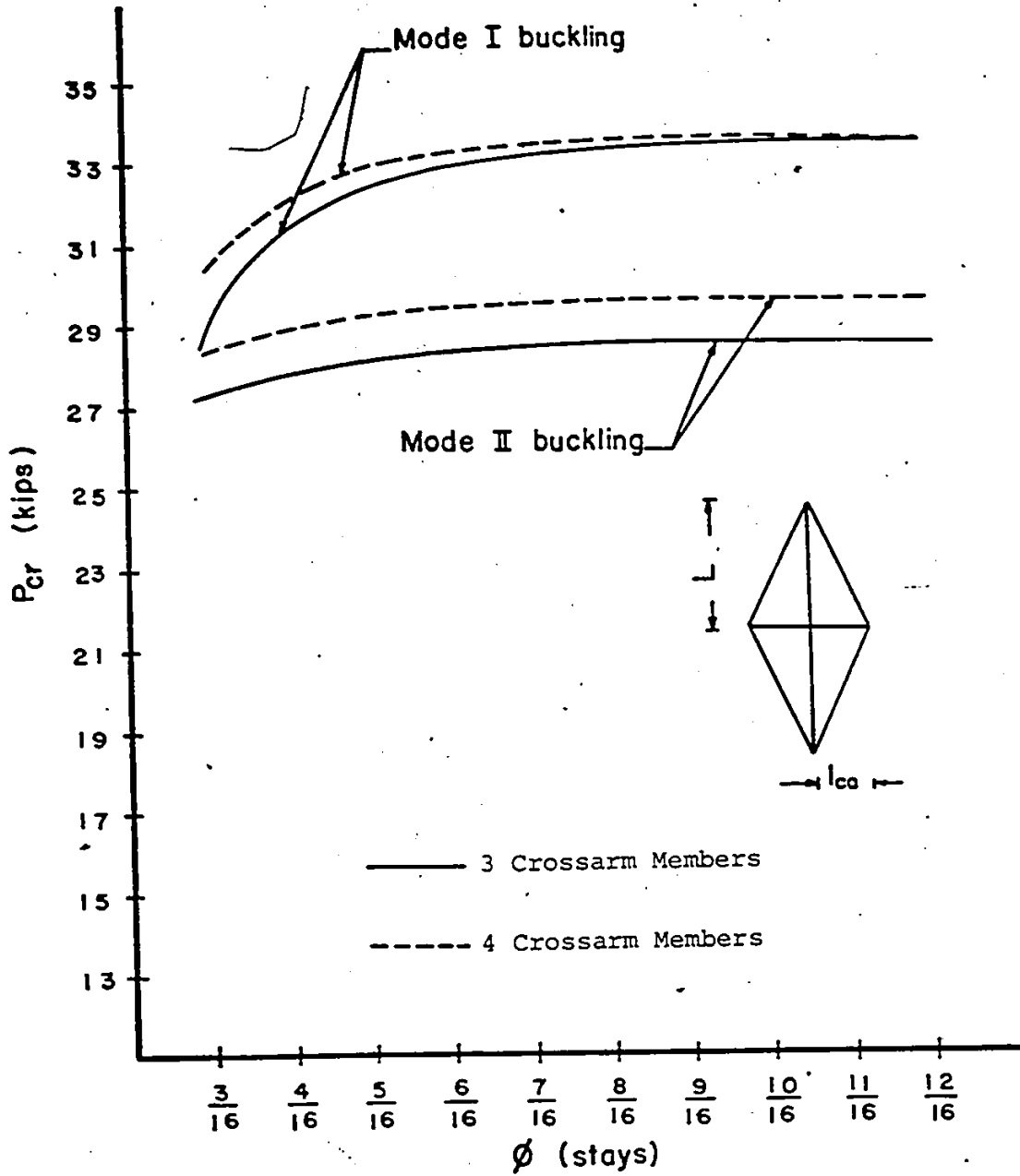


Fig. 5-7 Influence of Stay Diameter
on the Buckling Behavior
 ($L/l_{ca} = 5$)

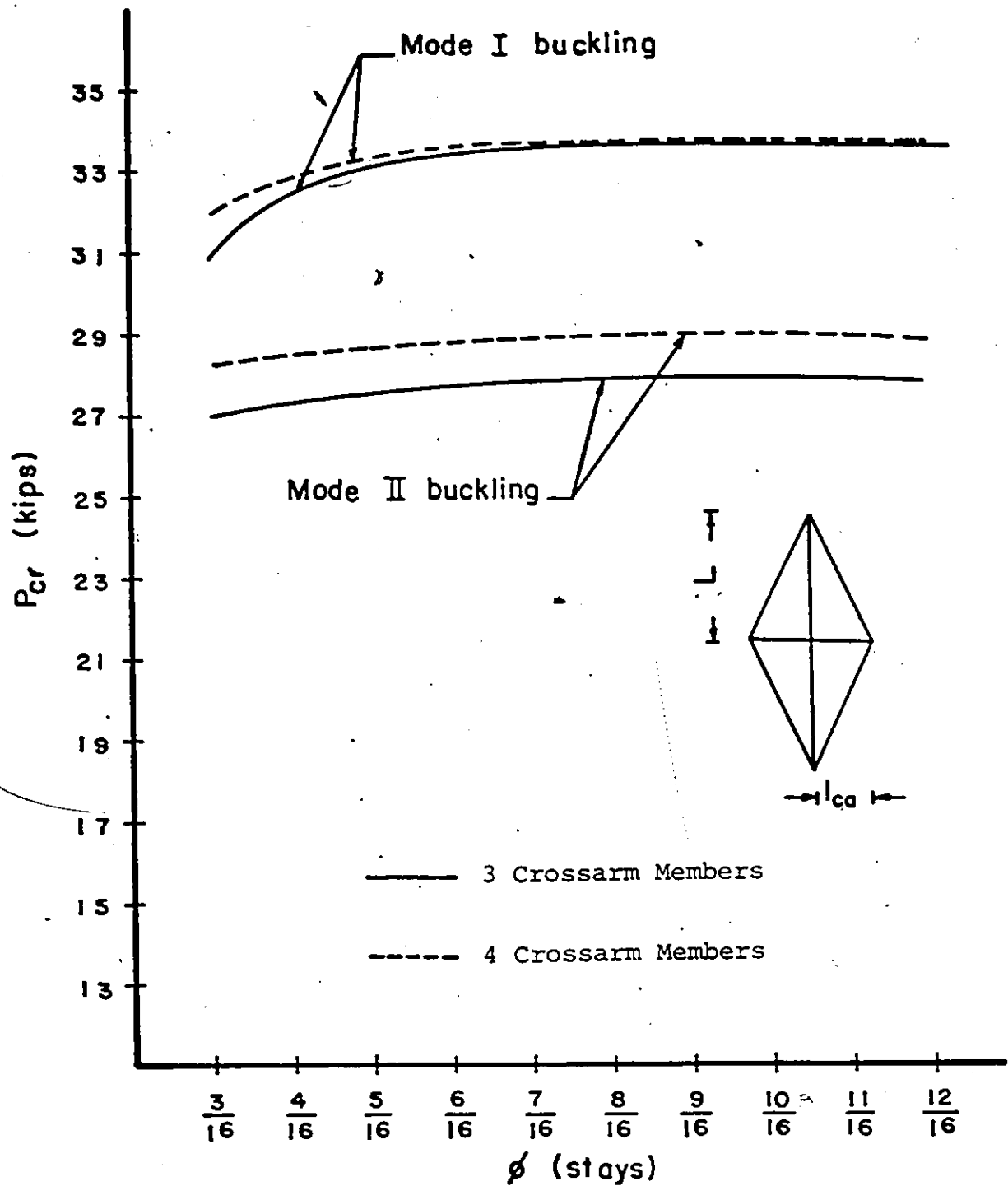


Fig.5-8 Influence of Stay Diameter
on the Buckling Behavior
 ($L/l_{ca} = 4$)

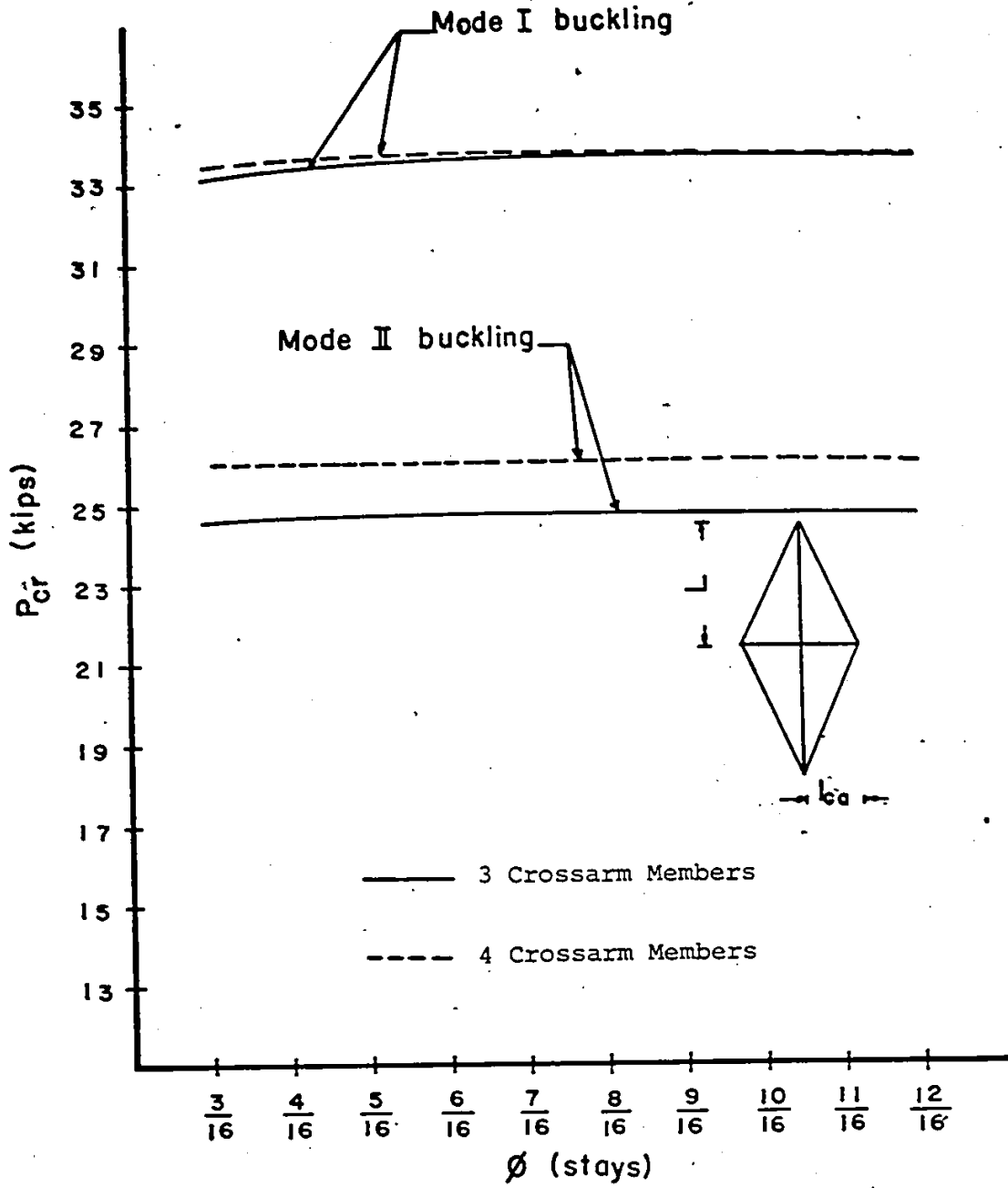


Fig.5-9 Influence of Stay Diameter on the Buckling Behavior
 $(L/l_{ca} = 2)$

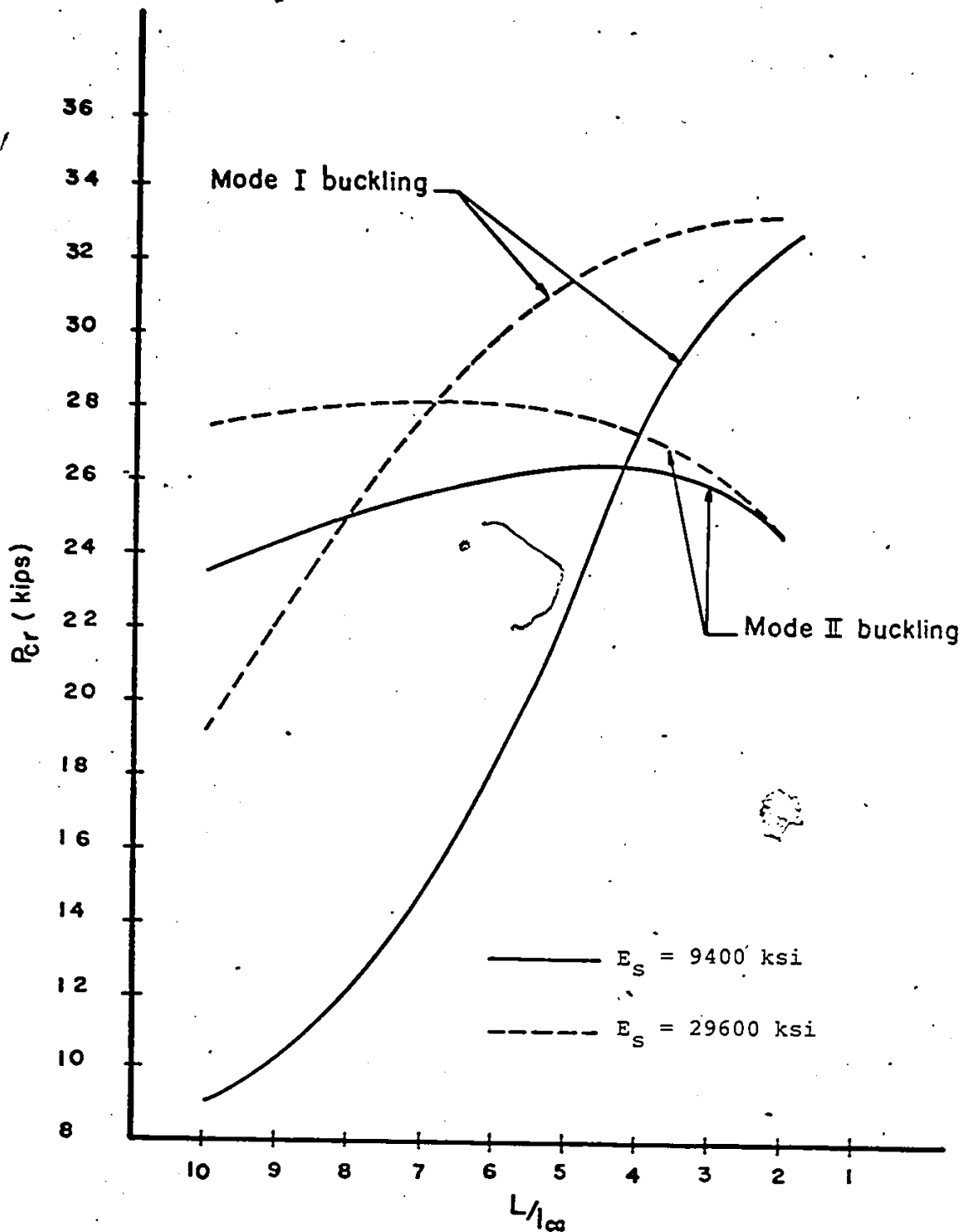


Fig5-10 Influence of Stay Modulus of Elasticity and Crossarm Member Length ($\phi = 0.25$ in.)

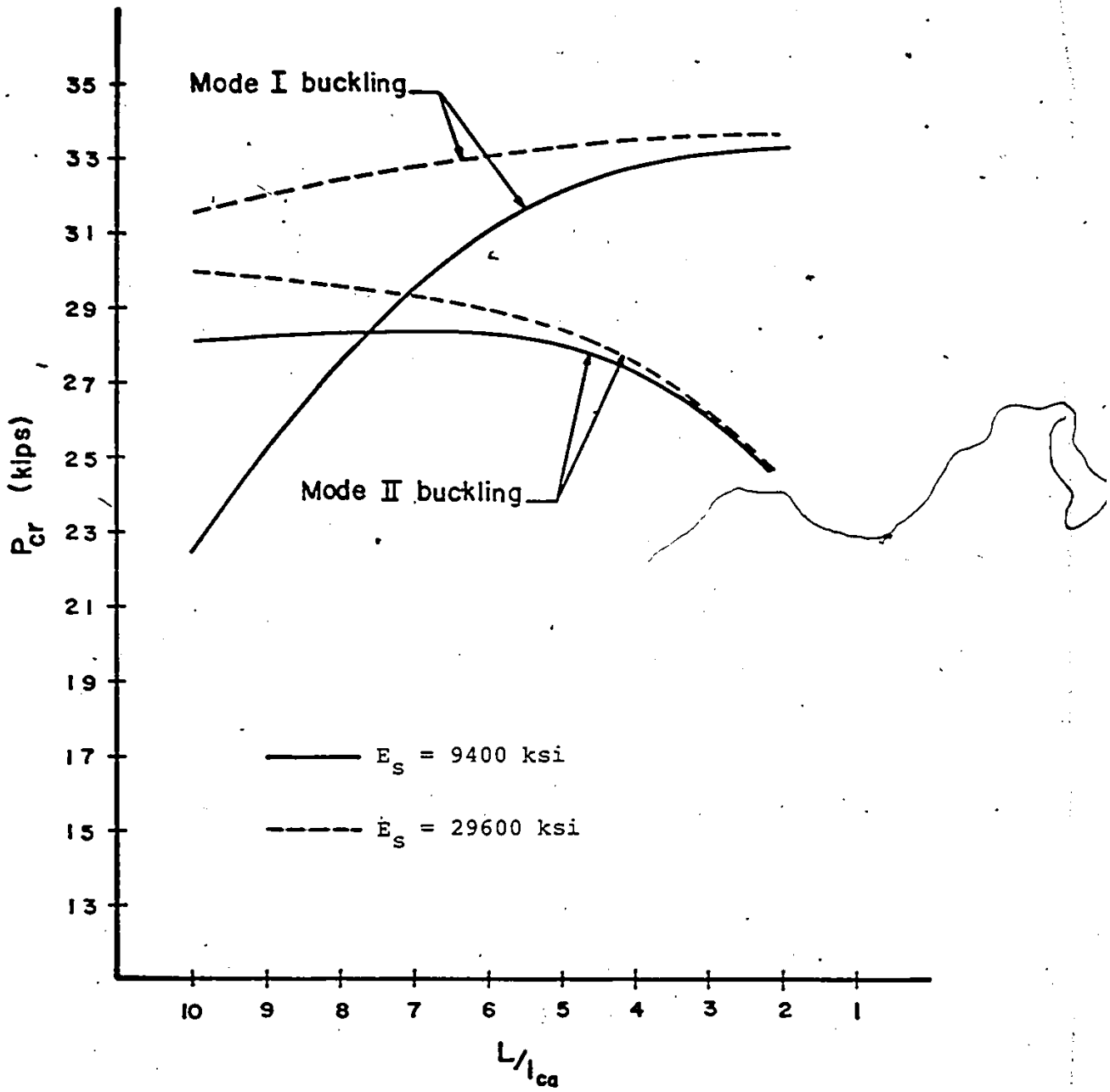


Fig 5-II Influence of Stay Modulus of Elasticity and Crossarm Member Length ($\phi = 0.5$ in.)

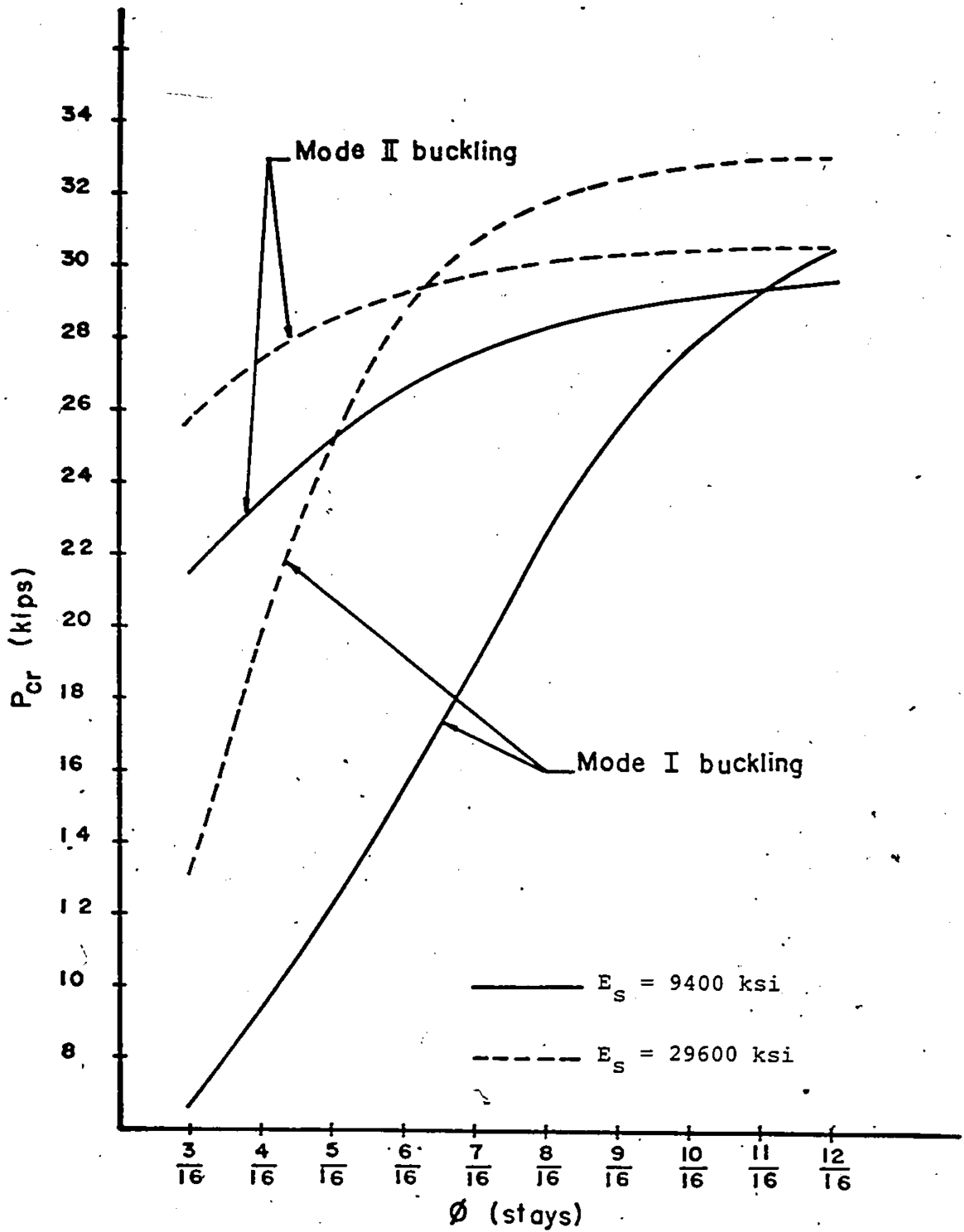


Fig 5-12 Influence of Stay Modulus of Elasticity and Stay Size
 ($L/l_{ca} = 10$)

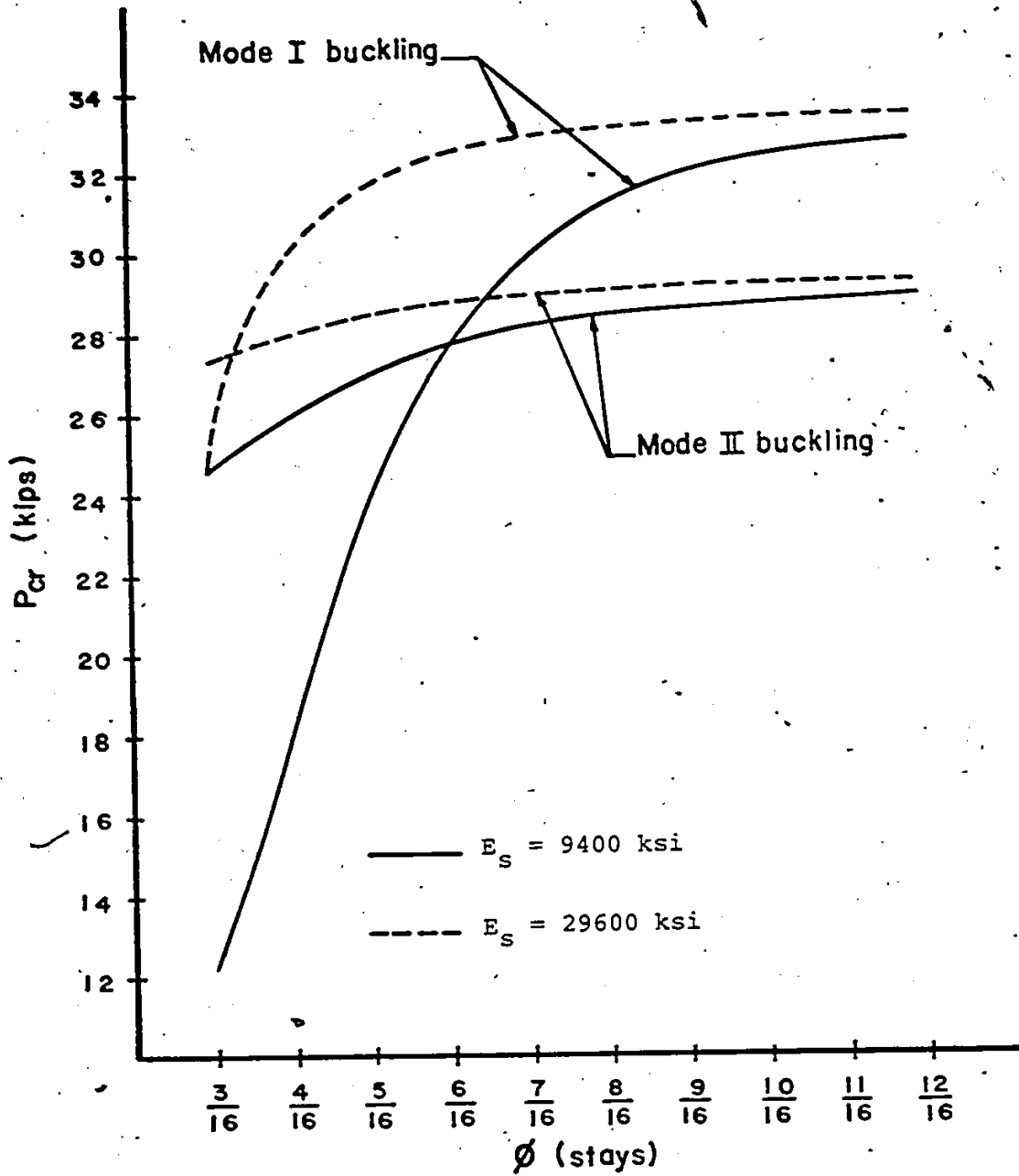


Fig. 5-13 Influence of Stay Modulus of Elasticity and Stay Size
 $(L/l_{ca} = 6)$

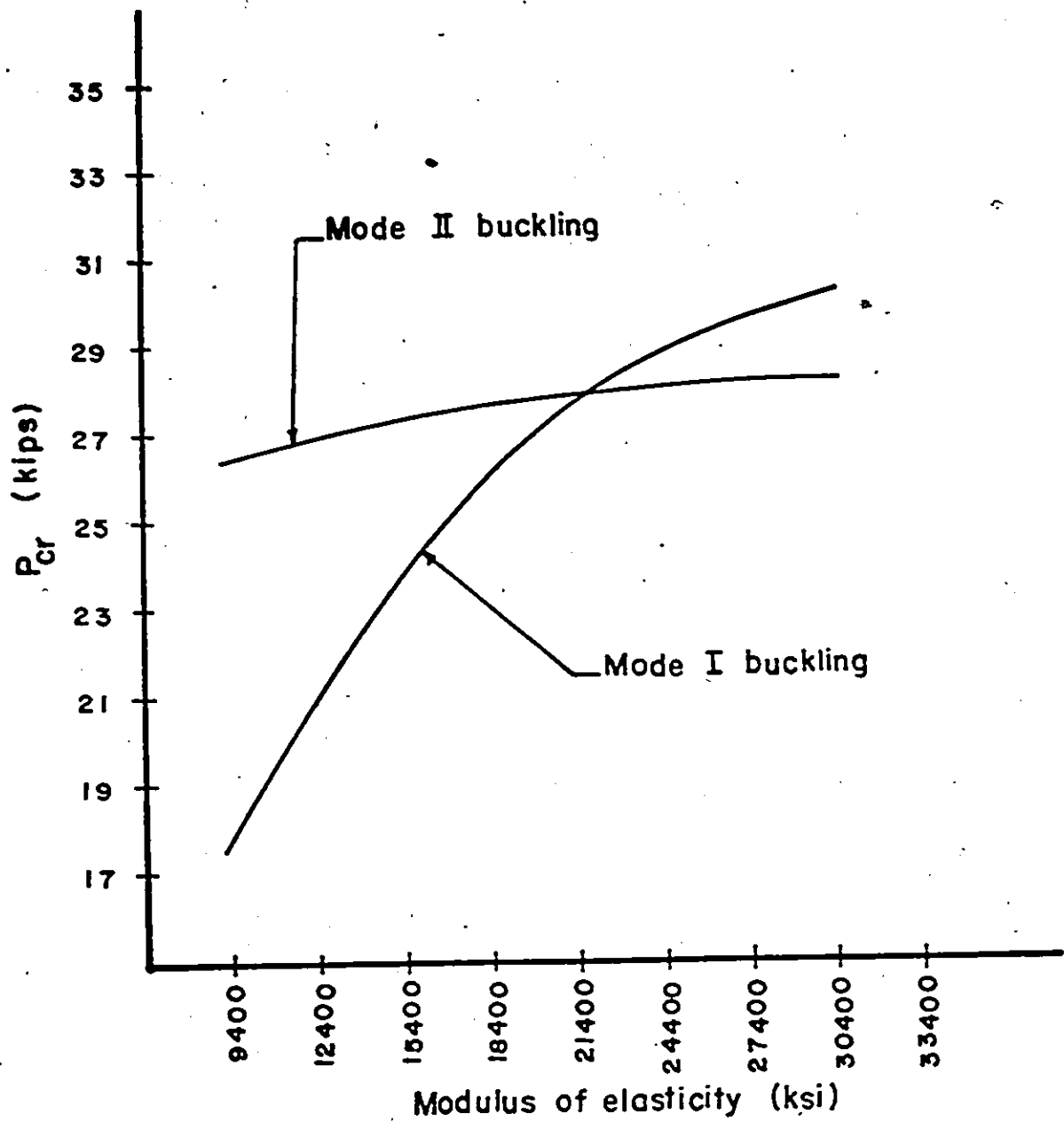


Fig.5-14 Influence of varying the Stay Modulus of Elasticity on Buckling Behavior

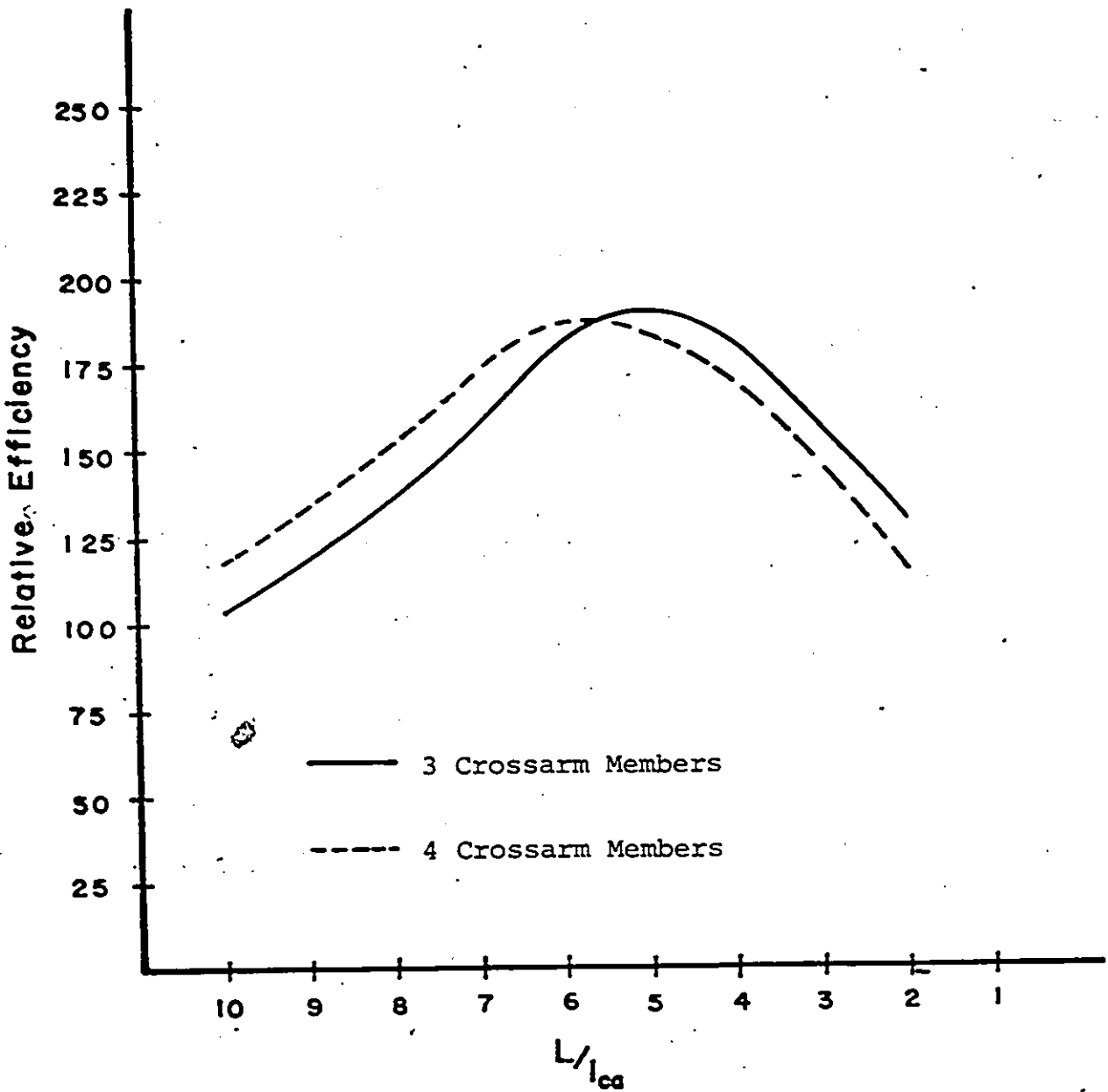


Fig.6-1 Influence of Crossarm Member
Length on the Relative Efficiency
($\phi = 3/16$ in.)

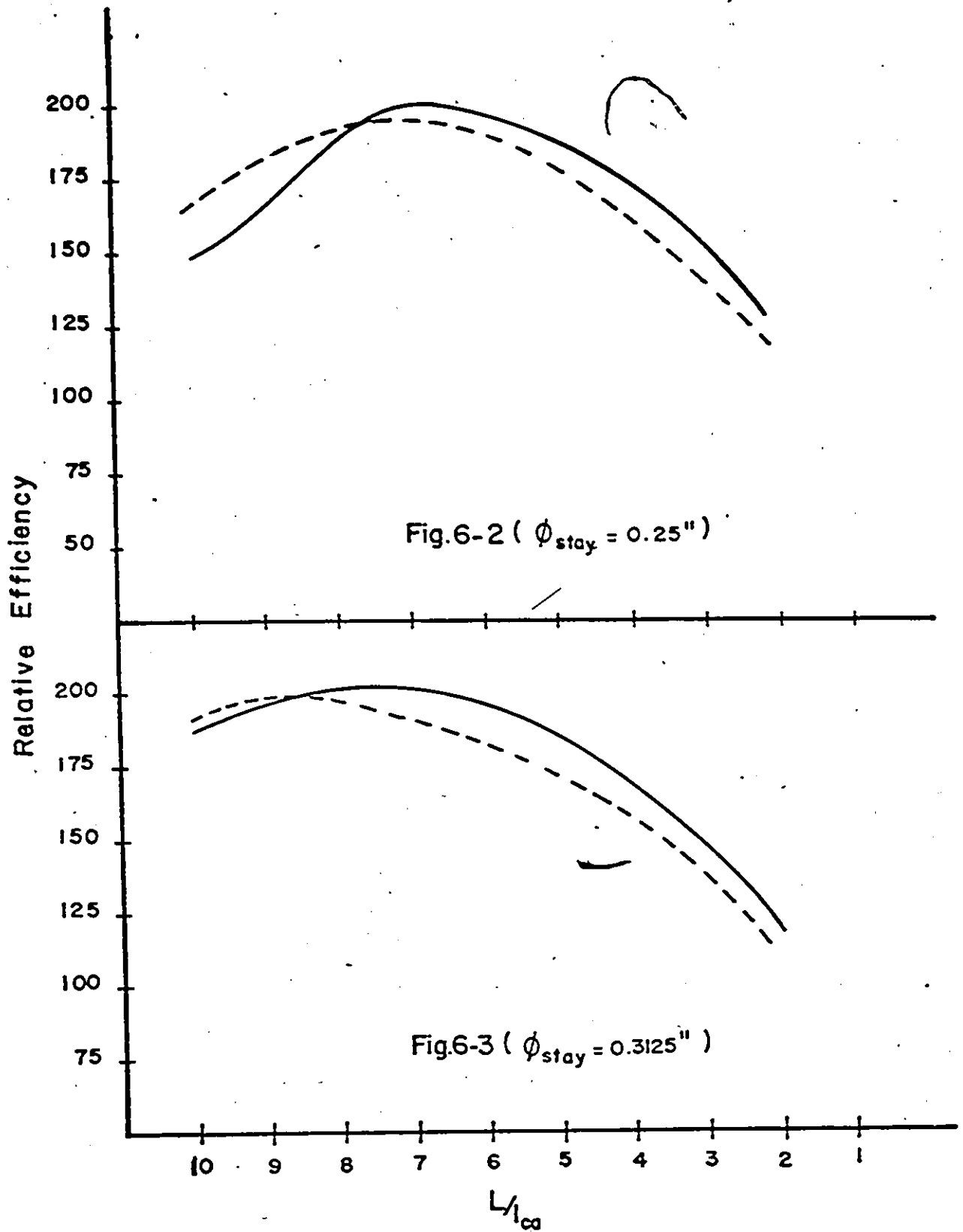
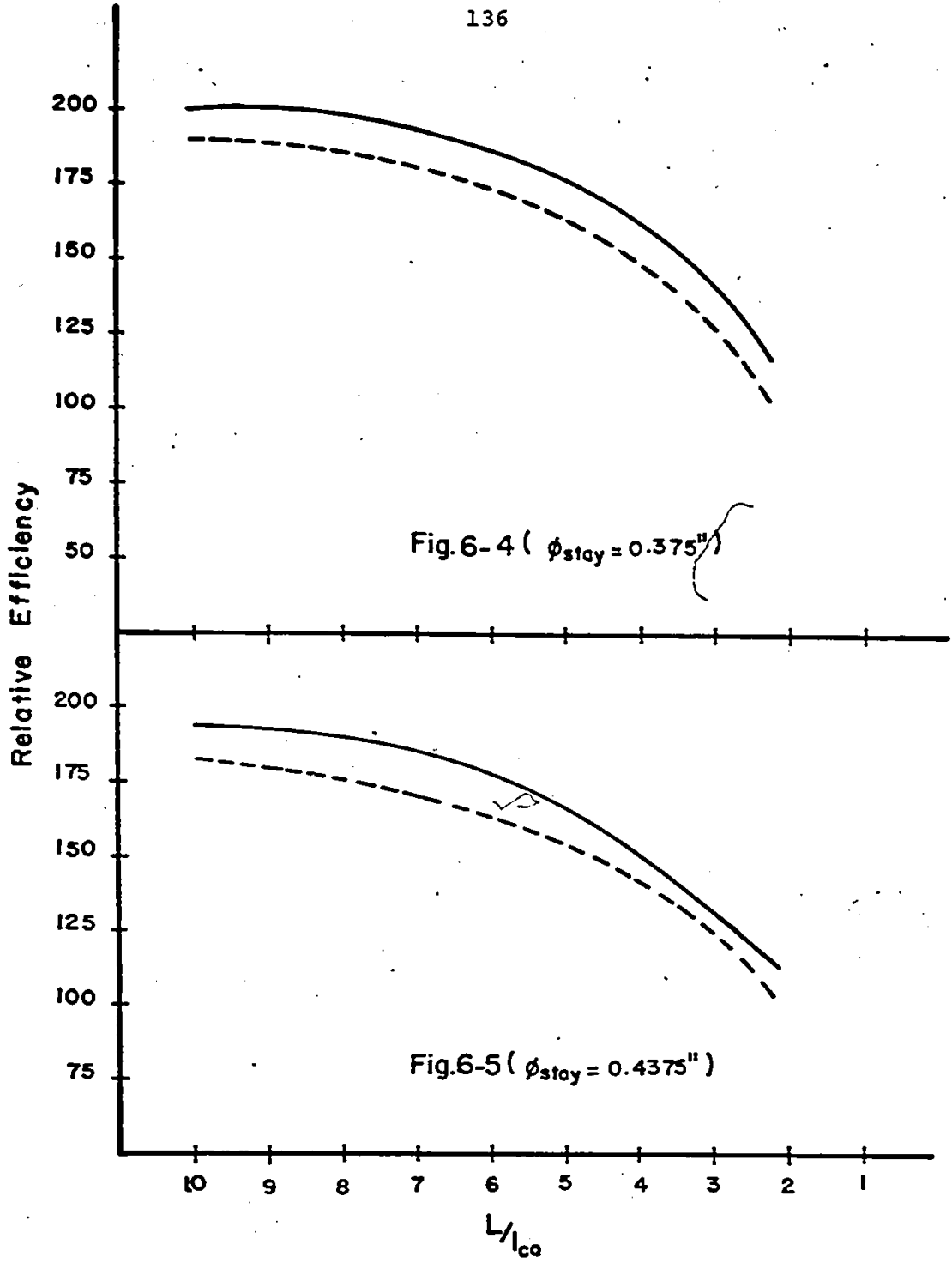


Fig. 6-2 ($\phi_{stay} = 0.25''$)

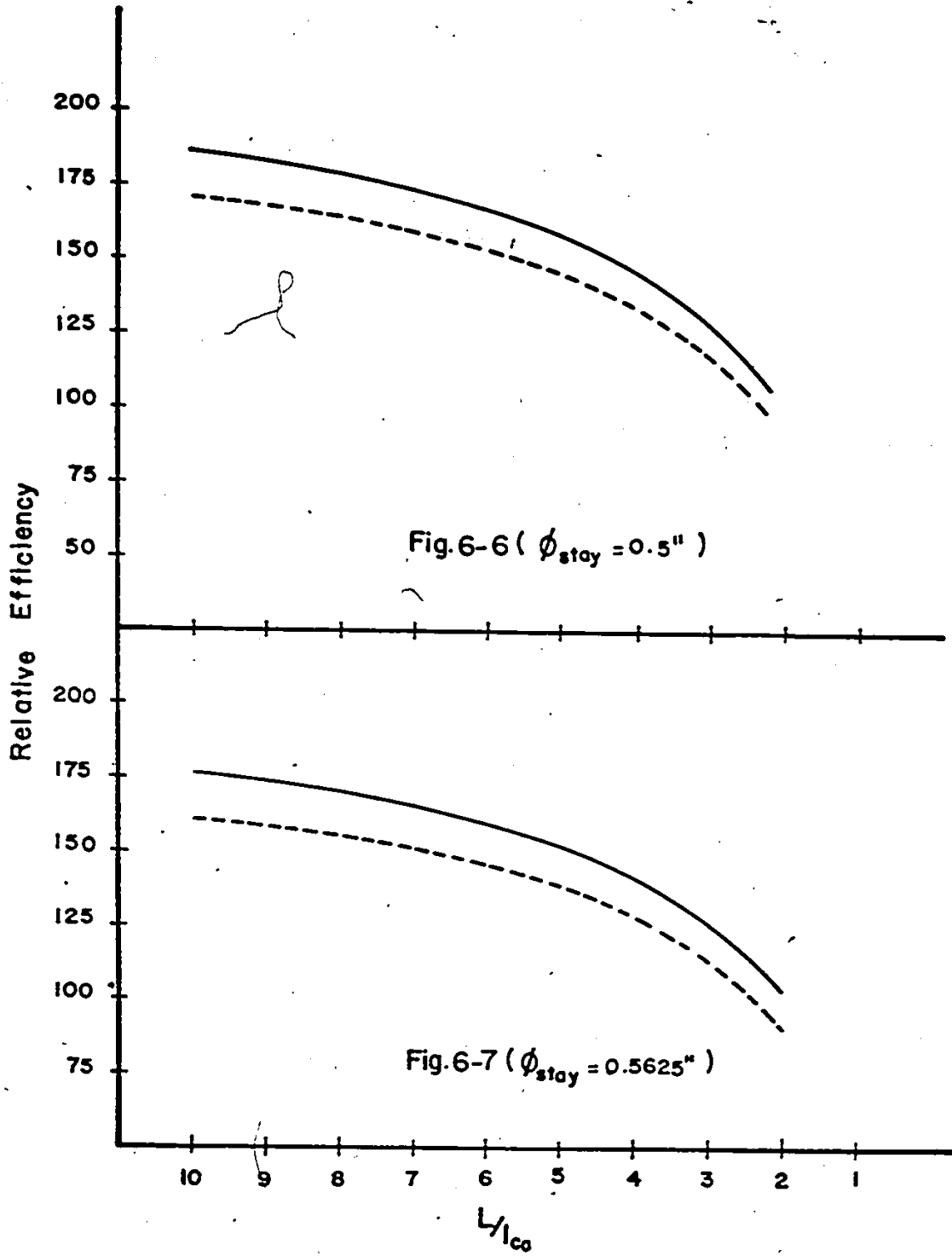
Fig. 6-3 ($\phi_{stay} = 0.3125''$)

3 Crossarm Members
 4 Crossarm Members



— 3 Crossarm Members
- - - 4 Crossarm Members

Relative Efficiency



Relative Efficiency

— 3 Crossarm Members

- - - 4 Crossarm Members

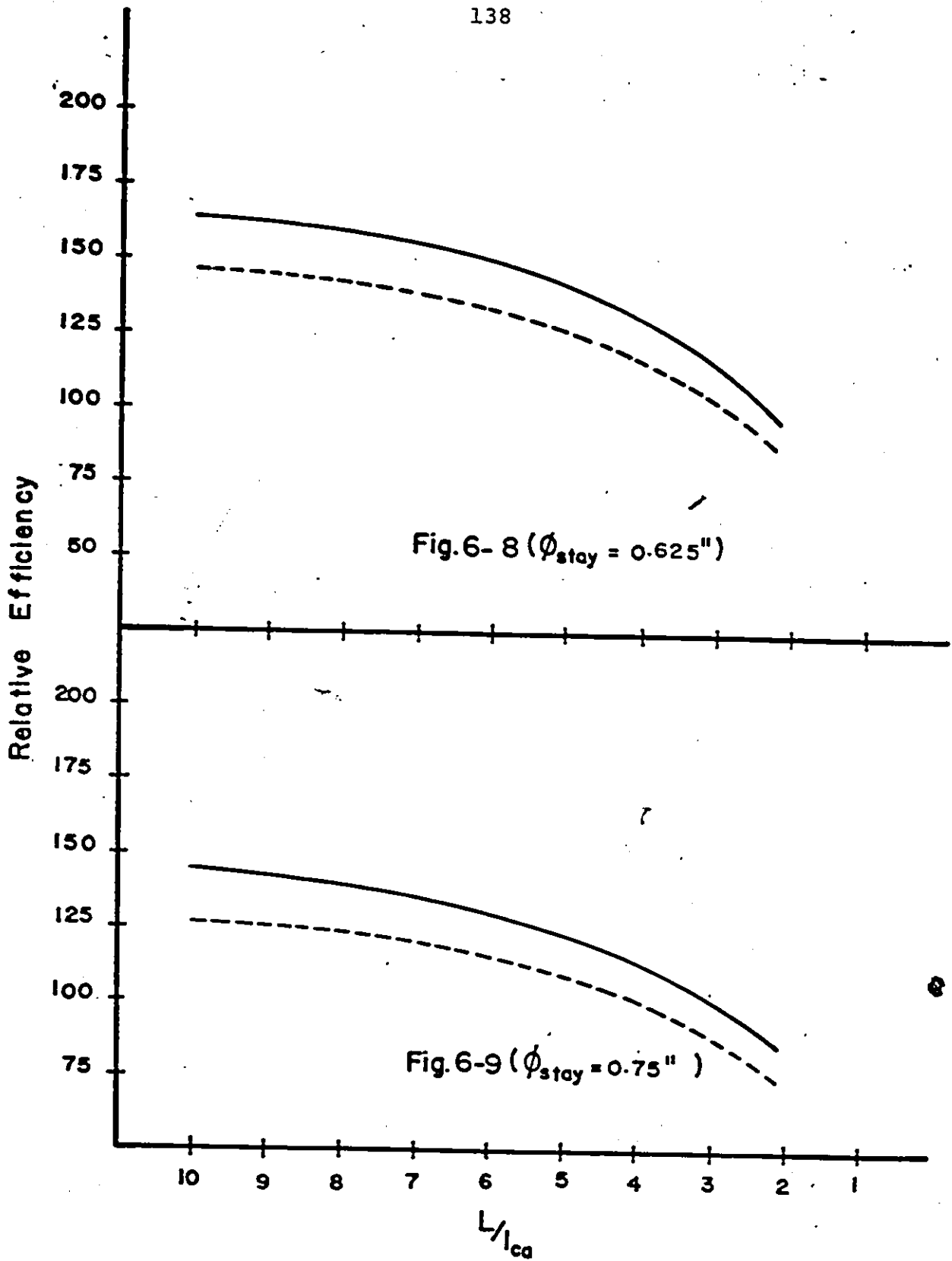


Fig. 6-8 ($\phi_{stay} = 0.625''$)

Fig. 6-9 ($\phi_{stay} = 0.75''$)

Relative Efficiency

— 3 Crossarm Members

- - - 4 Crossarm Members

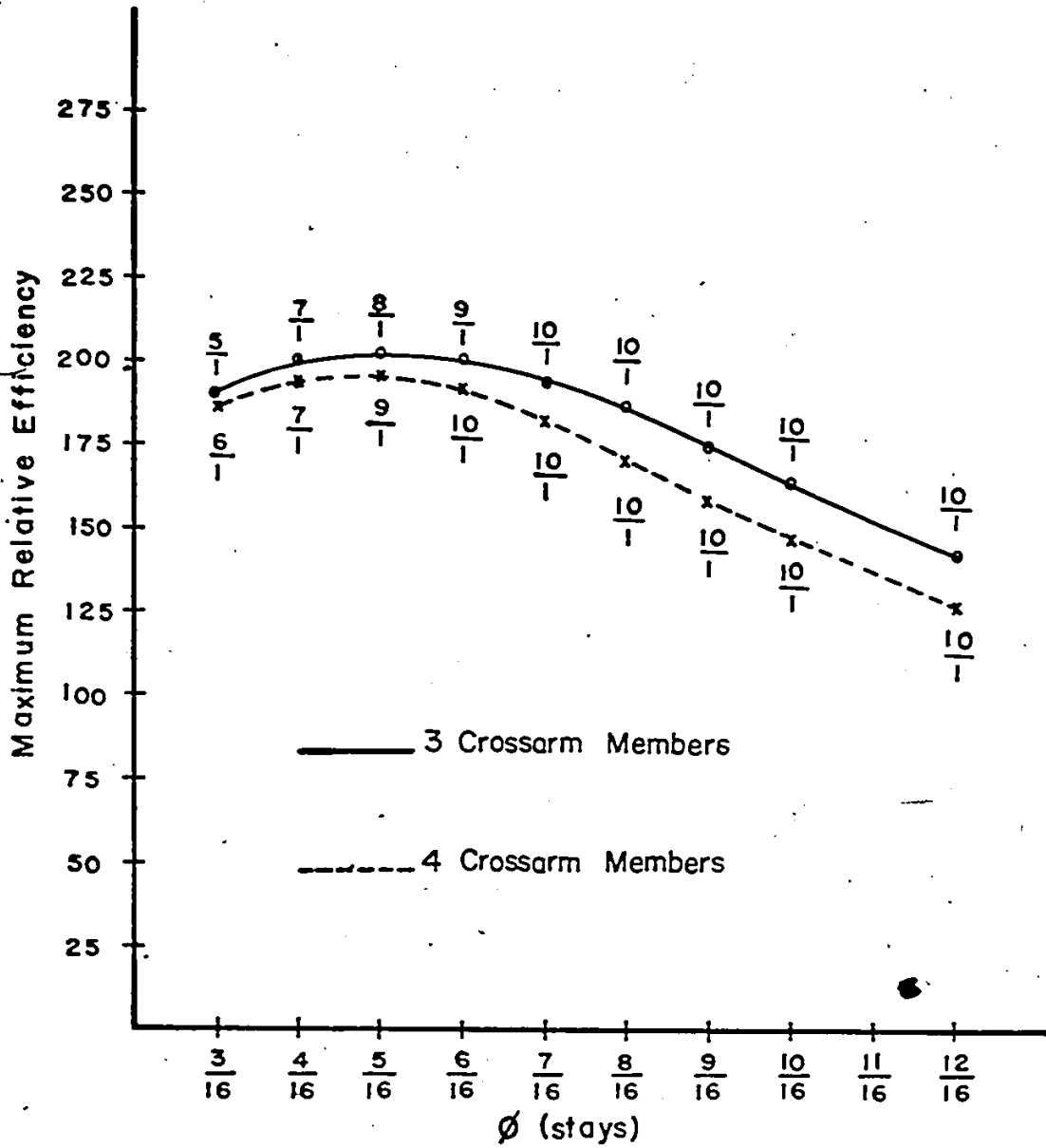
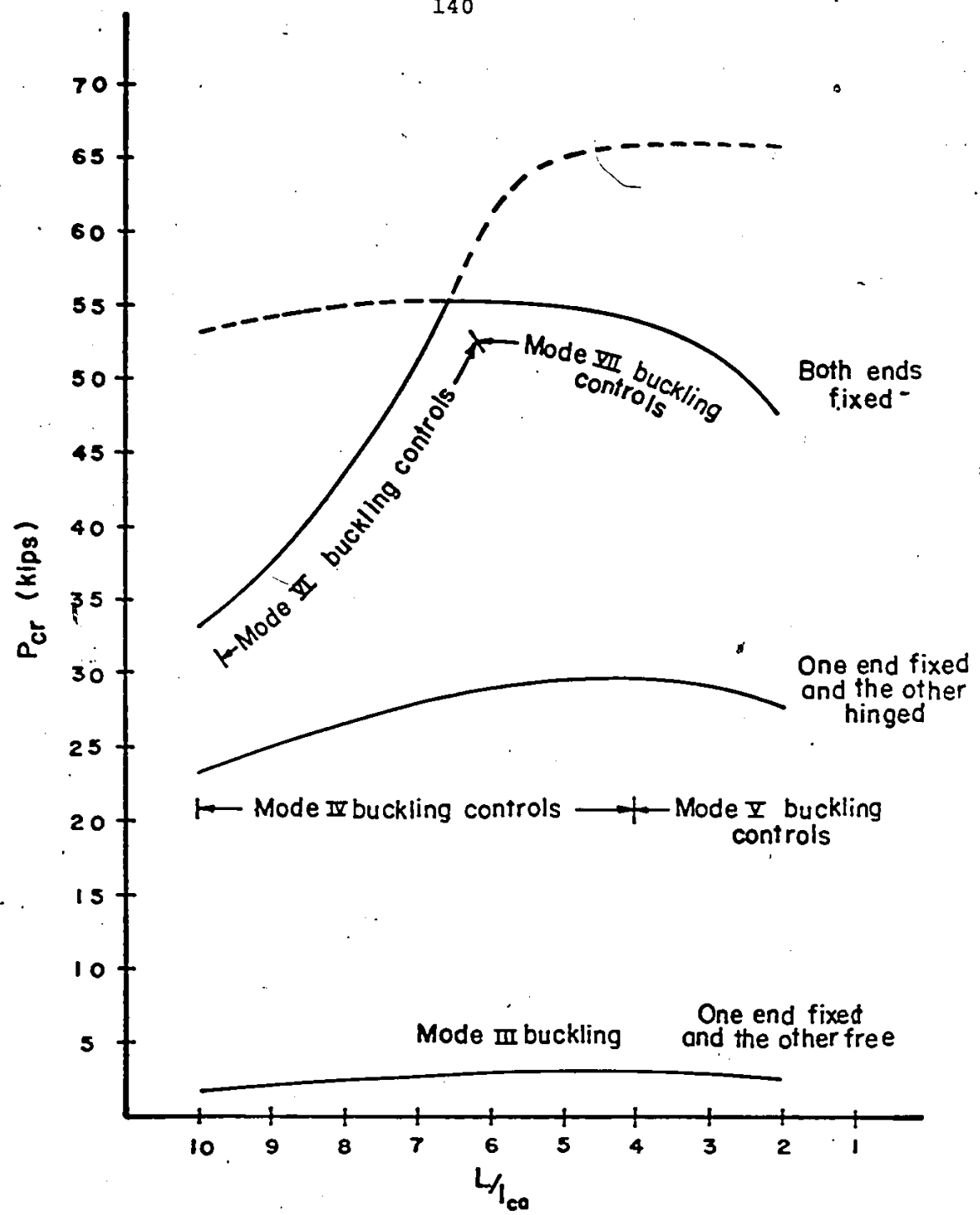
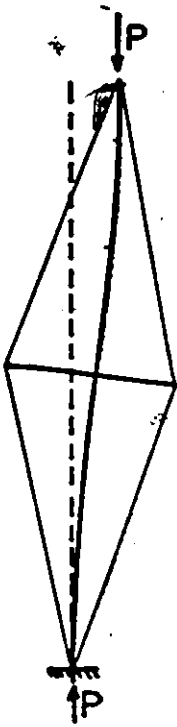


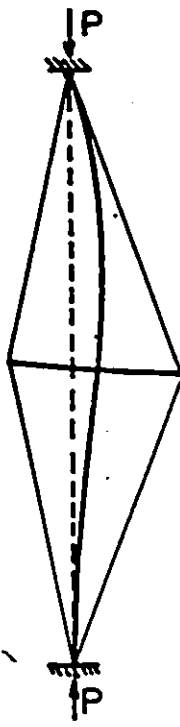
Fig.6-10 Influence of Stay Size on the Maximum Value of the Relative Efficiency



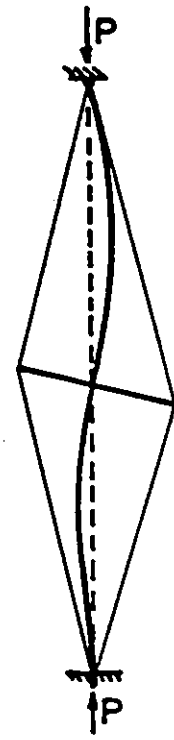
Influence of Crossarm Member Length and End Conditions on the Buckling Behavior
Fig.7-1



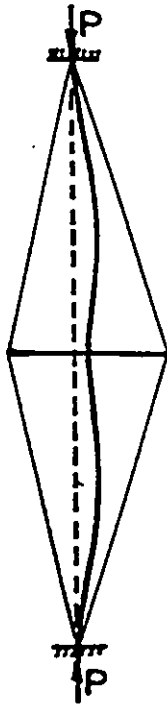
a) Mode III buckling



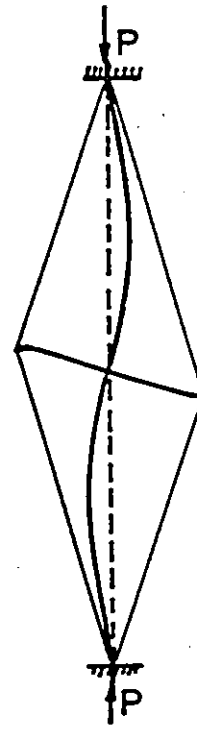
b) Mode IV buckling



c) Mode V buckling



d) Mode VI buckling



e) Mode VII buckling

Fig. 7-2

Modes of Buckling
For three cases of
End Conditions

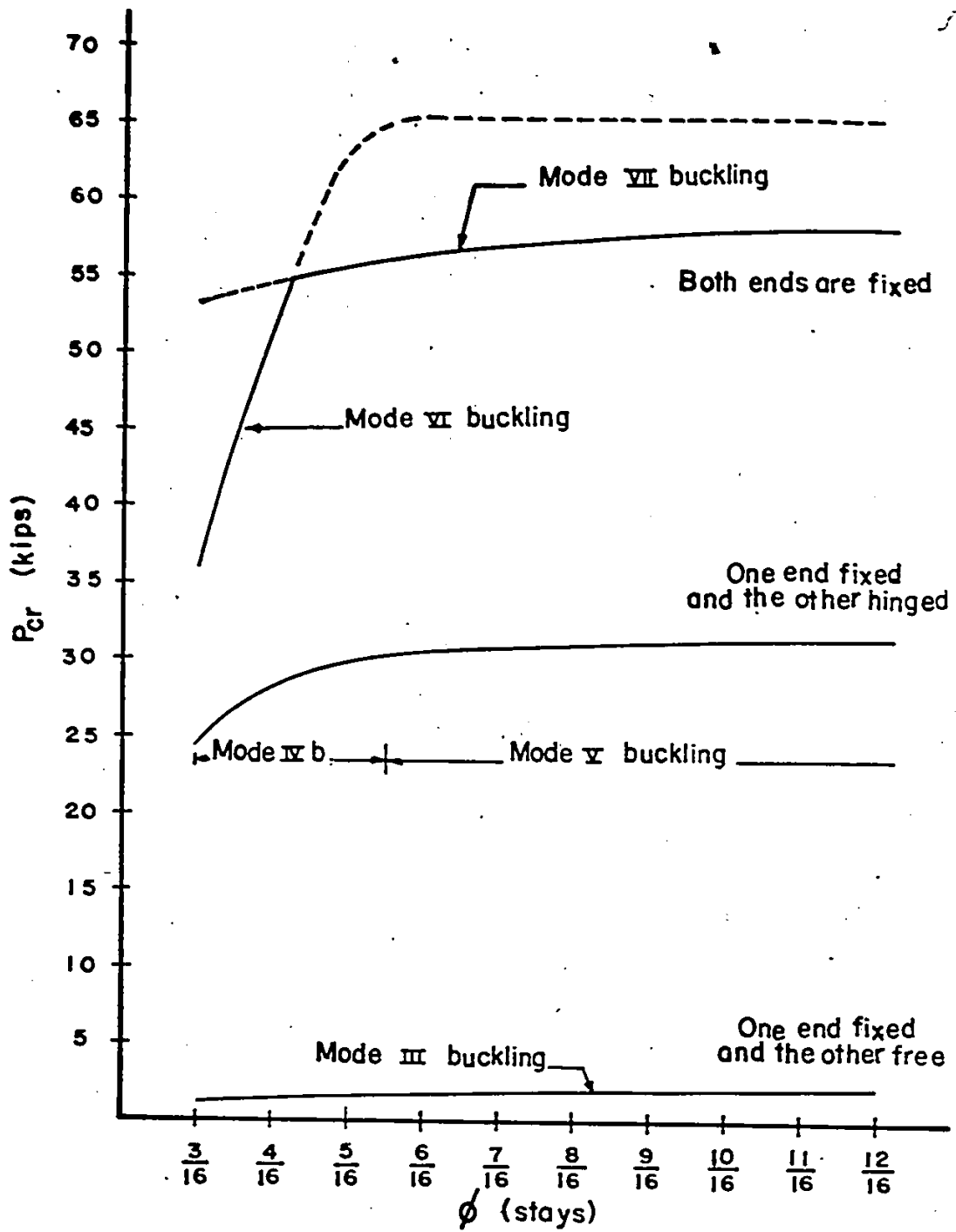


Fig. 7-3 Influence of Stay Size and End conditions on the Buckling Behavior

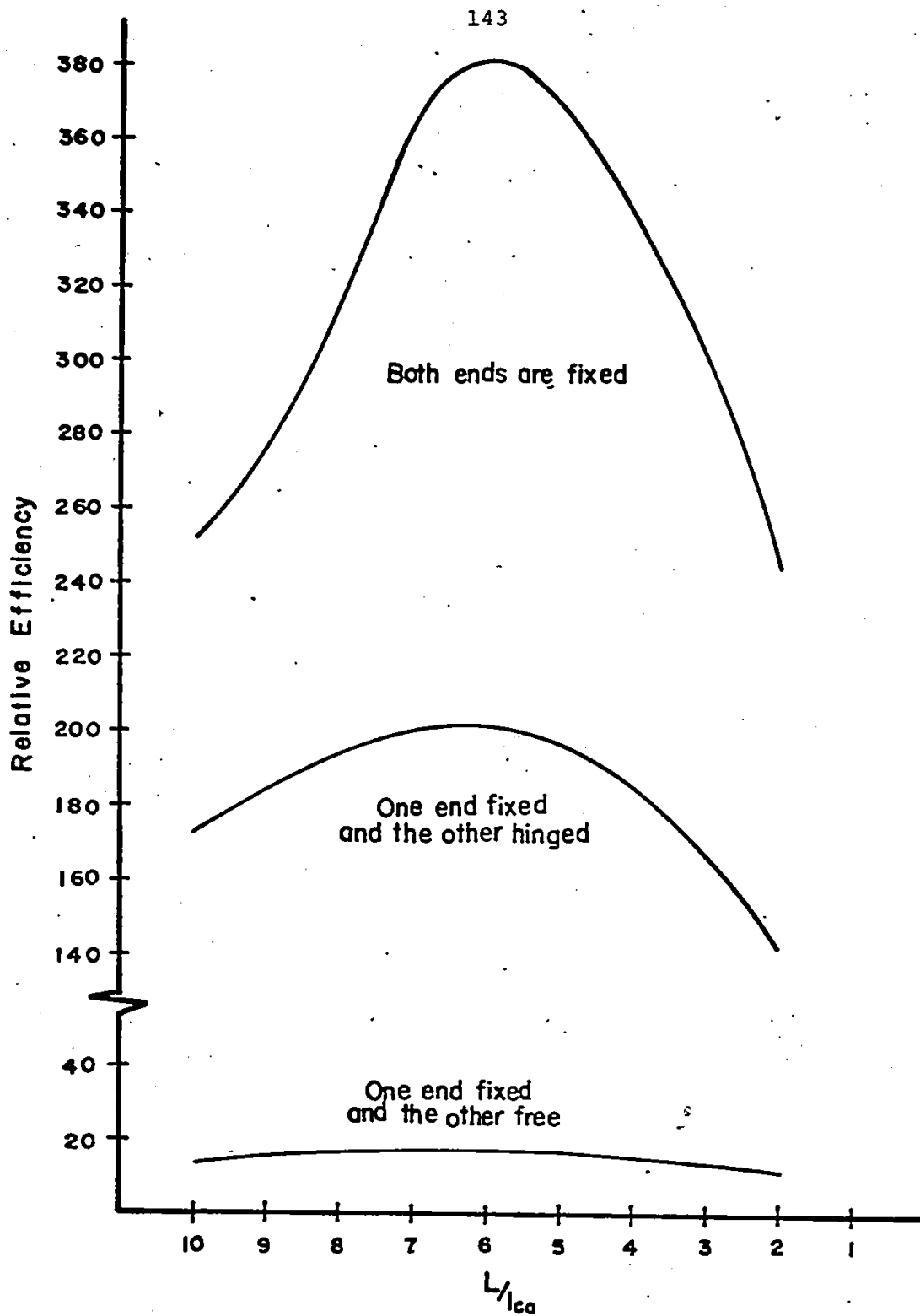


Fig. 7-4

Influence of Crossarm Member Length and End Conditions on the Relative Efficiency

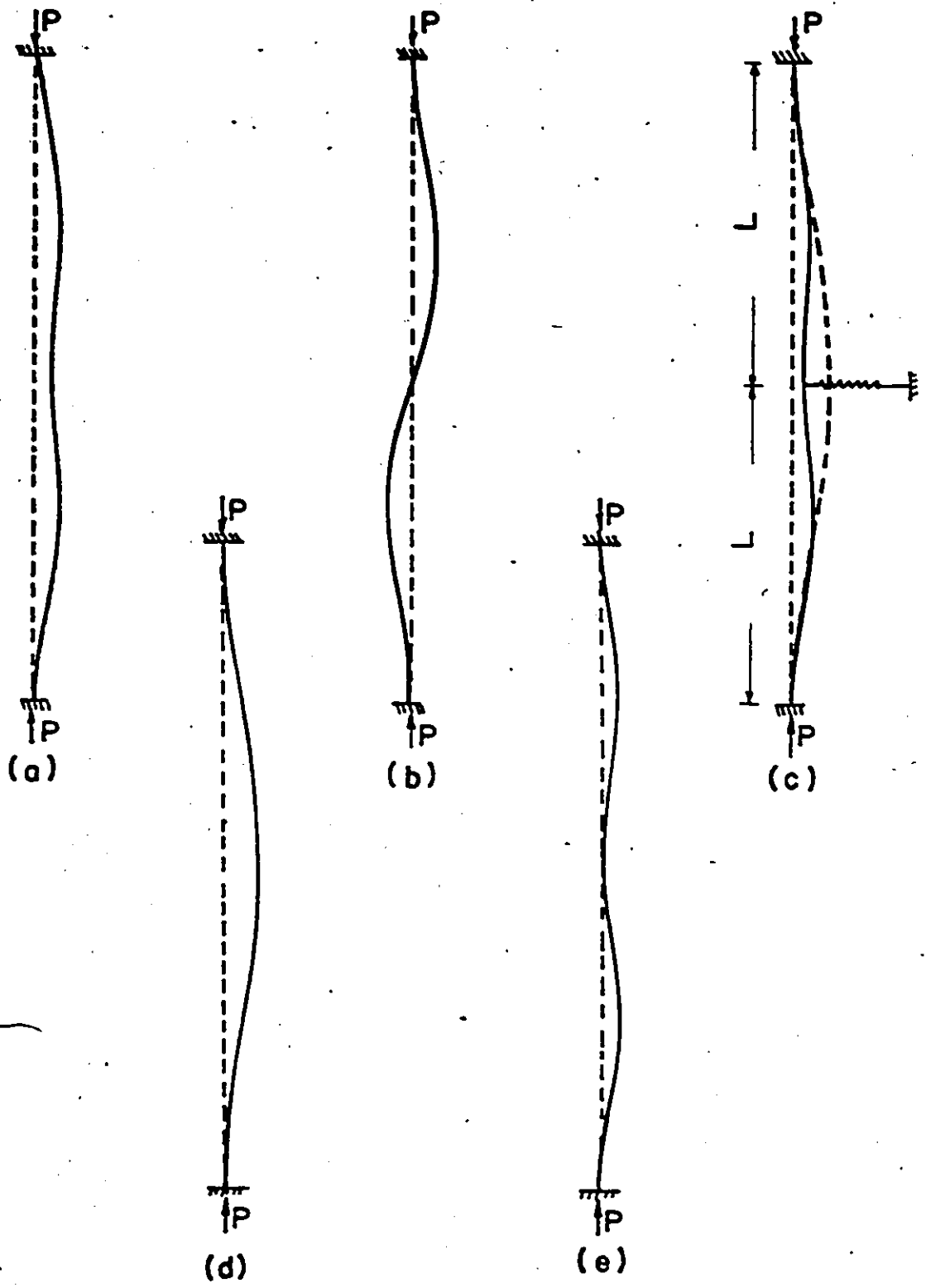


Fig. 7-5

Model and possible Modes
of Buckling for the case
of two Fixed Ends

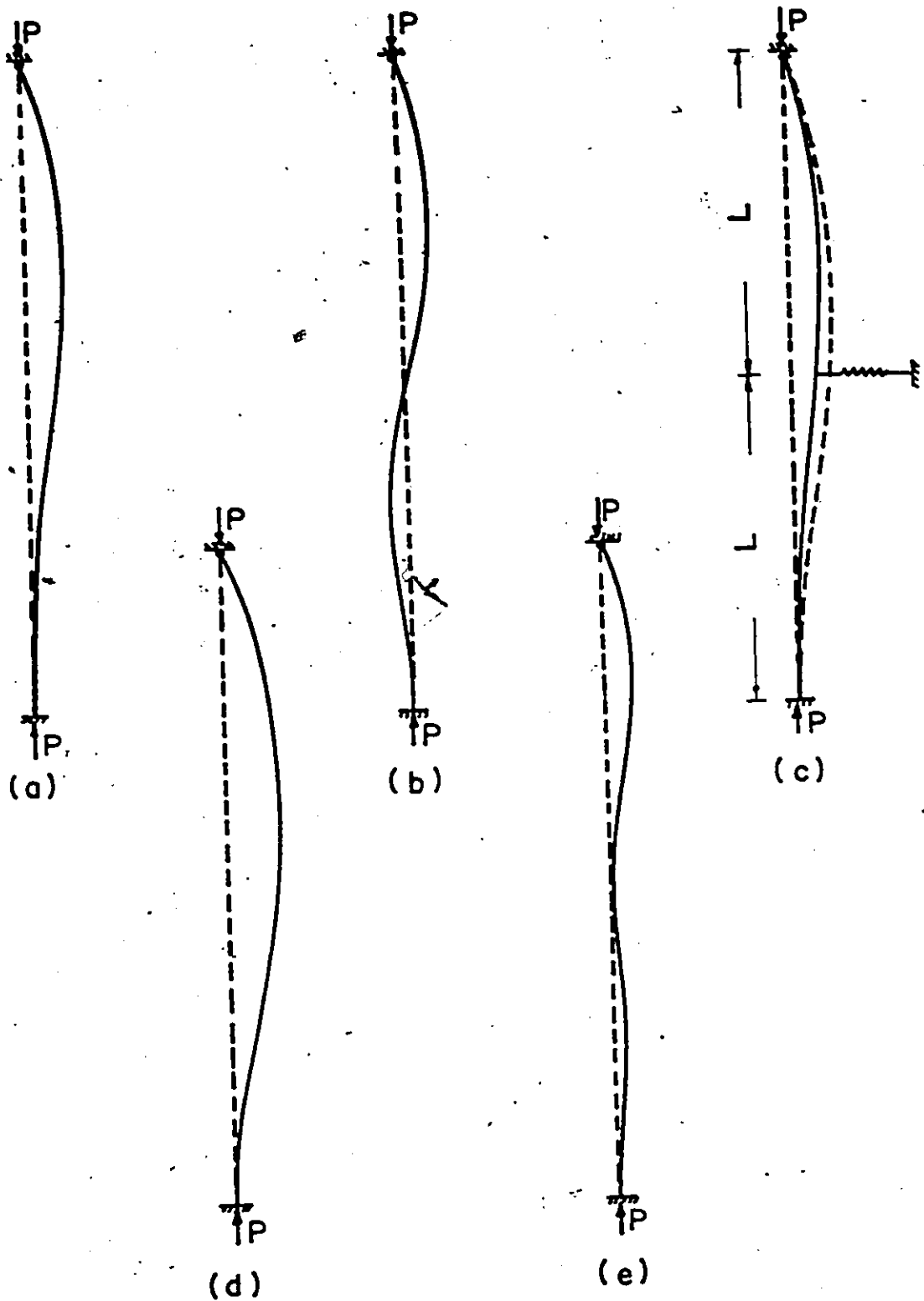


Fig. 7-6 Model and possible Modes of Buckling for the case of one End Fixed and the other Hinged.

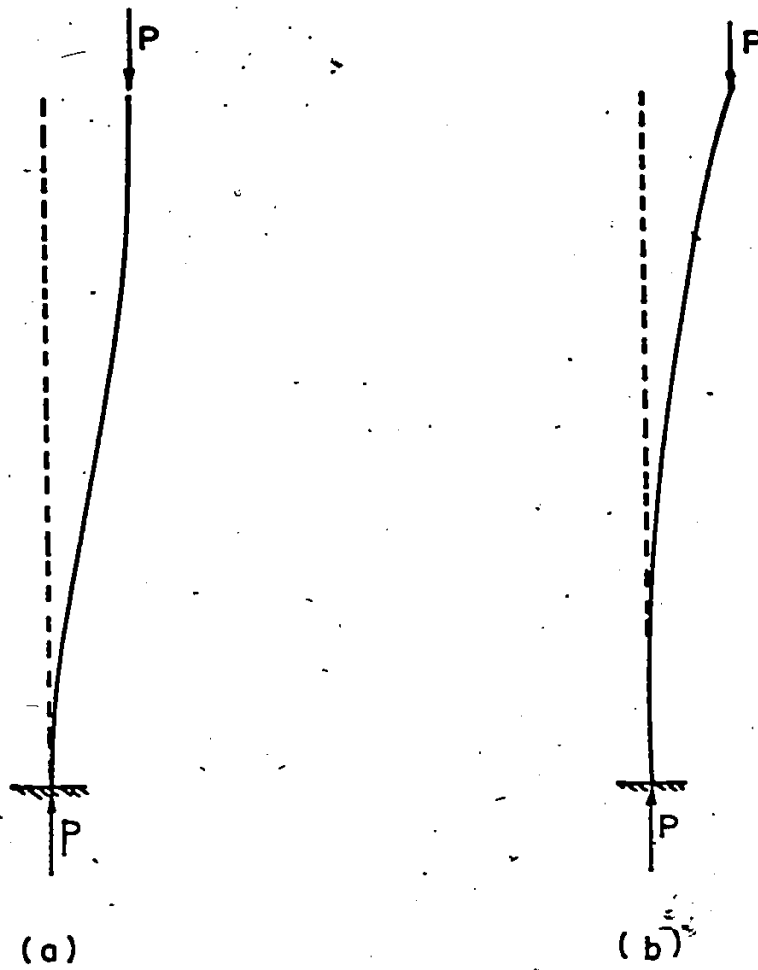
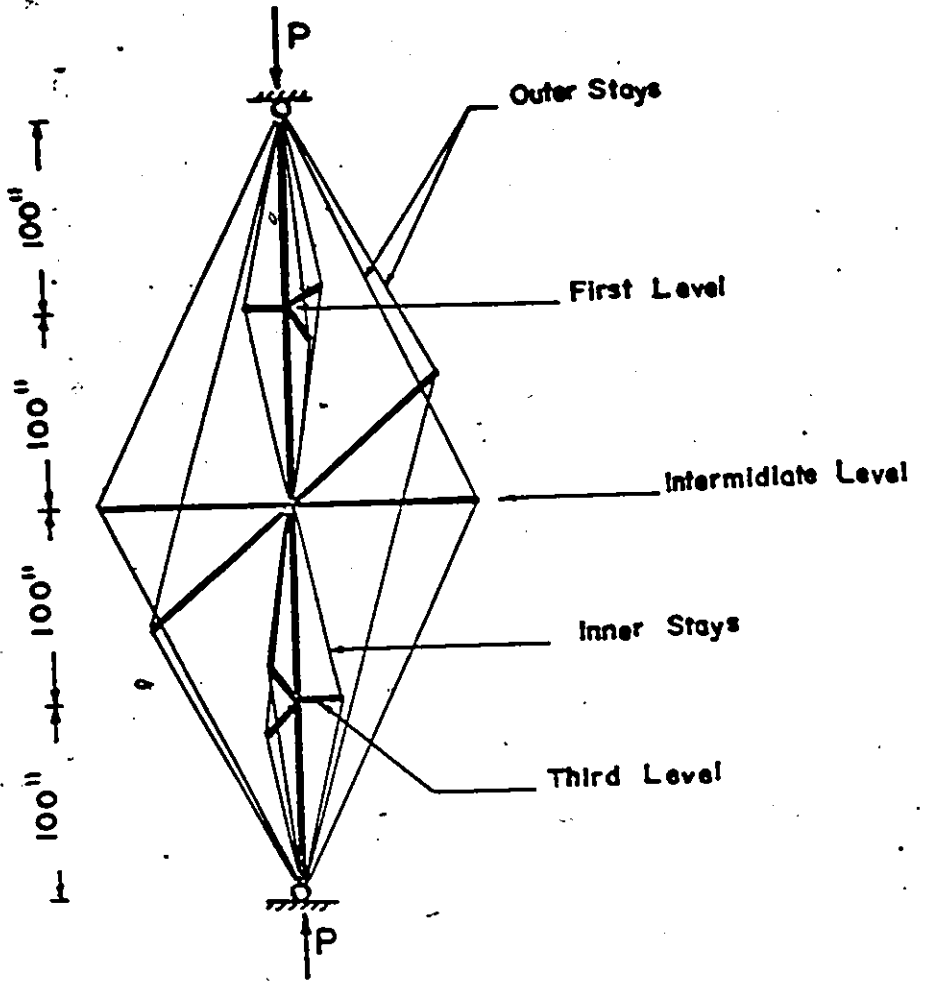
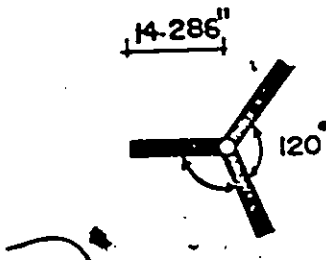


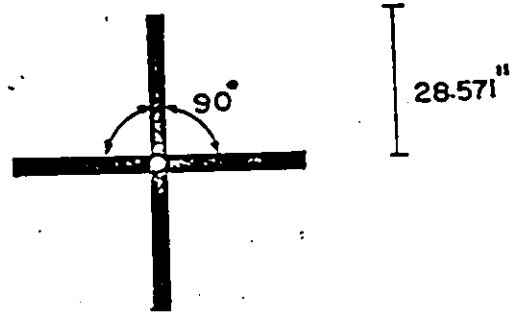
Fig. 7-7 Modes of Buckling for the case of one End Fixed and the other Free



a) Stayed Column



b) Crossarm Members (First Level)



c) Crossarm Members (Intermediate Level)

Fig. 7-8 Triple Crossarm Space Stayed Column
(Numerical Example)

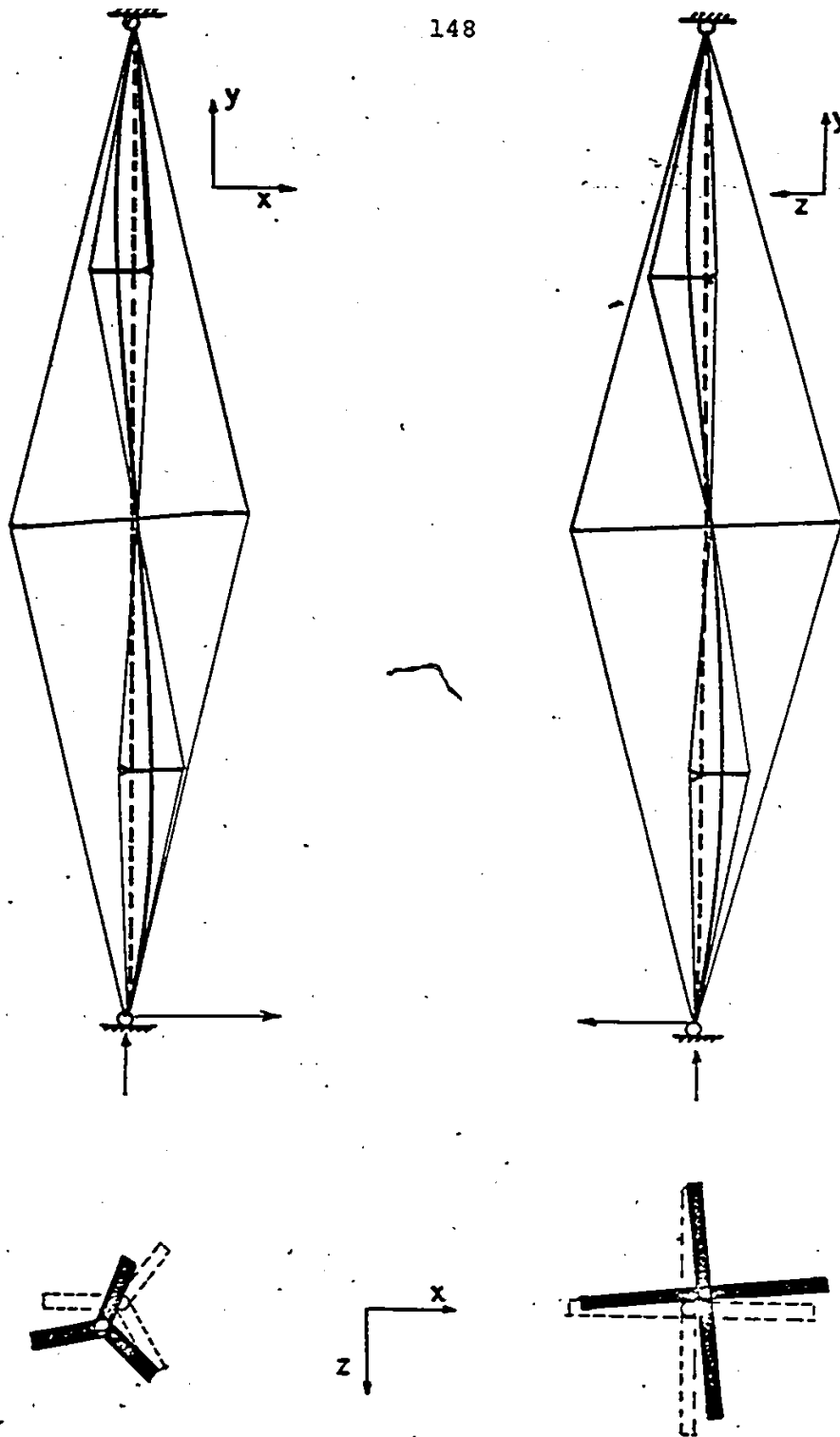


Fig.79 Mode of Buckling for
the Triple Crossarm
Stayed Column

APPENDIX A

Large Deflection Strain Displacement Equation
in Three-Dimension Analysis

Assumptions:

- 1) plane section before deformation remains plane after deformation
- 2) plane perpendicular to neutral axis before deformation remains perpendicular to it after deformation
- 3) section is incompressible in the transverse direction
- 4) displacements and rotations are relatively small.

Consider the section of the beam before and after deformation. Fig. (A.I)

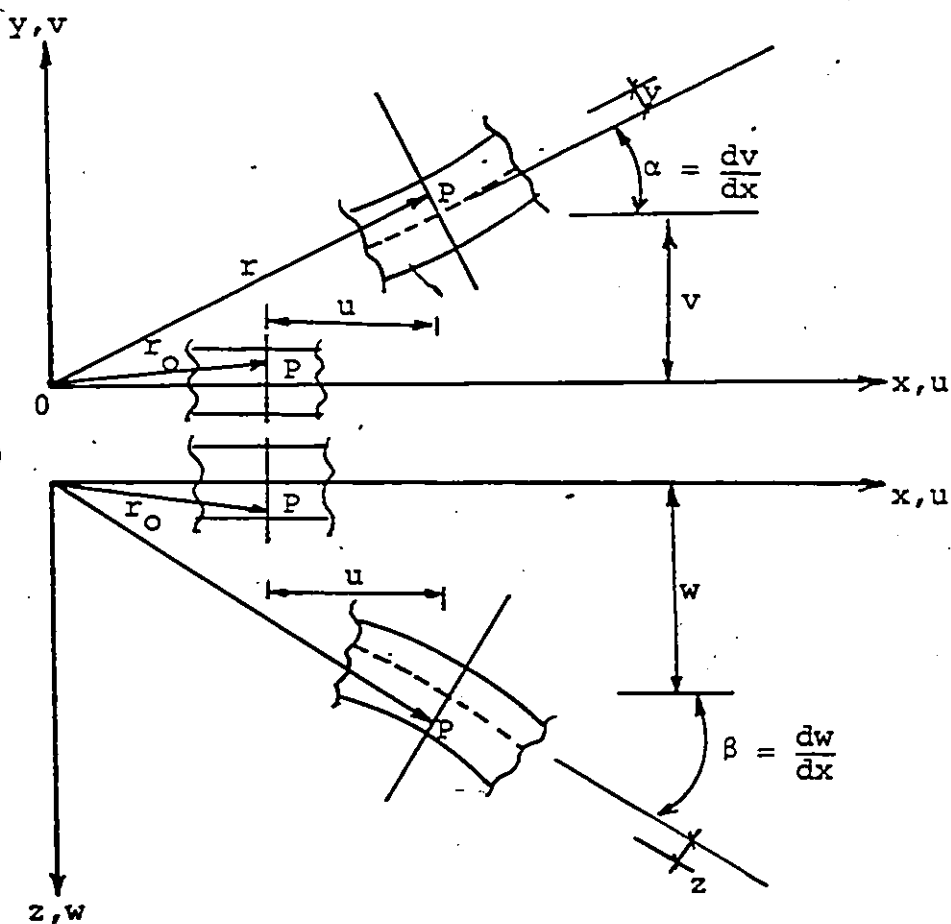


Fig. (A.I)

Let u , v and w be the displacement components in the x , y and z directions respectively of a point on the neutral surfaces.

The position vector of the point P a distance y and z from the neutral surfaces before deformation is

$$\underline{r}_0 = x \underline{i} + y \underline{j} + z \underline{k} \quad (\text{A.1})$$

The position vector of the same point after deformation is

$$\begin{aligned} \underline{r} = & (x + u - y \sin\alpha - z \sin\beta) \underline{i} + (v + y \cos\alpha) \underline{j} \\ & + (w + z \cos\beta) \underline{k} \end{aligned} \quad (\text{A.2})$$

Since rotations are assumed to be relatively small,

$$\text{then } \sin\alpha \approx \alpha \approx \frac{dv}{dx}$$

$$\sin\beta \approx \beta \approx \frac{dw}{dx}$$

$$\text{and, } \cos\alpha \approx \cos\beta = 1.0 \quad (\text{A.3})$$

Therefore,

$$\begin{aligned} \underline{r} = & (x + u - y \frac{dv}{dx} - z \frac{dw}{dx}) \underline{i} + (v + y) \underline{j} \\ & + (w + z) \underline{k} \end{aligned} \quad (\text{A.4})$$

Since the beam is assumed to be incompressible in the y and z directions, y and z are constants and from equation (A.1)

$$\underline{dr}_0 = dx \underline{i} \quad (\text{A.5})$$

and,

$$\underline{dr} = (1 + \frac{du}{dx} - y \frac{d^2v}{dx^2} - z \frac{d^2w}{dx^2}) dx \underline{i} + (\frac{dv}{dx}) dx \underline{j} + (\frac{dw}{dx}) dx \underline{k} \quad (\text{A.6})$$

Now,

$$|\underline{dr}_0|^2 = \underline{dr}_0 \cdot \underline{dr}_0 = dx^2 \quad (\text{A.7})$$

and,

$$|\underline{dr}|^2 = \underline{dr} \cdot \underline{dr} = \left(1 + \frac{du}{dx} - y \frac{d^2v}{dx^2} - z \frac{d^2w}{dx^2}\right) dx^2 \\ + \left(\frac{dv}{dx}\right)^2 dx^2 + \left(\frac{dw}{dx}\right)^2 dx^2$$

$$|\underline{dr}|^2 = \left[1 + \left(\frac{du}{dx}\right)^2 + y^2 \left(\frac{d^2v}{dx^2}\right)^2 + z^2 \left(\frac{d^2w}{dx^2}\right)^2 + 2 \frac{du}{dx} \right. \\ - 2y \frac{d^2v}{dx^2} - 2z \frac{d^2w}{dx^2} - 2y \frac{du}{dx} \frac{d^2v}{dx^2} - 2z \frac{du}{dx} \frac{d^2w}{dx^2} \\ \left. - 2yz \frac{d^2v}{dx^2} \frac{d^2w}{dx^2} + \left(\frac{dv}{dx}\right)^2 + \left(\frac{dw}{dx}\right)^2\right] dx^2 \quad (\text{A.8})$$

By the definition of strain

$$\epsilon_{xx} = \frac{|\underline{dr}| - |\underline{dr}_0|}{|\underline{dr}_0|} = \frac{|\underline{dr}|}{|\underline{dr}_0|} - 1$$

$$(\epsilon_{xx} + 1) = \frac{|\underline{dr}|}{|\underline{dr}_0|} \quad (\text{A.9})$$

$$(\epsilon_{xx} + 1)^2 = \frac{|\underline{dr}|^2}{|\underline{dr}_0|^2}$$

$$\epsilon_{xx}^2 + 2\epsilon_{xx} + 1 = 1 + \left(\frac{du}{dx}\right)^2 + y^2 \left(\frac{d^2v}{dx^2}\right)^2 + z^2 \left(\frac{d^2w}{dx^2}\right)^2 \\ + 2 \frac{du}{dx} - 2y \frac{d^2v}{dx^2} - 2z \frac{d^2w}{dx^2} - 2y \frac{du}{dx} \frac{d^2v}{dx^2} \\ - 2z \frac{du}{dx} \frac{d^2w}{dx^2} - 2yz \frac{d^2v}{dx^2} \frac{d^2w}{dx^2} + \left(\frac{dv}{dx}\right)^2 + \left(\frac{dw}{dx}\right)^2 \quad (\text{A.10})$$

Now assuming that

1. ϵ_{xx} is small i.e. $\epsilon_{xx}^2 = 0$
2. $\frac{du}{dx}$ is small i.e. $(\frac{du}{dx})^2 = 0$
3. Strain due to bending ($y\frac{d^2v}{dx^2}$ and $z\frac{d^2w}{dx^2}$) are small

$$\text{i.e. } y^2 \left(\frac{d^2v}{dx^2}\right)^2 = z^2 \left(\frac{d^2w}{dx^2}\right)^2 = yz \left(\frac{d^2v}{dx^2}\right) \left(\frac{d^2w}{dx^2}\right) = 0$$

However, the terms $(\frac{dv}{dx})^2$ and $(\frac{dw}{dx})^2$ cannot be similarly discarded. Discarding such terms will result in omitting the contribution of rotation to ϵ_{xx} and these are precisely the terms which must be retained. It can be observed from Eq. (A.10) that the lowest order rotational terms appear as a nonlinear contribution to the strain-displacement equation. Therefore discarding these terms $(\frac{dv}{dx})^2$ and $(\frac{dw}{dx})^2$ leads to a linear strain-displacement equation. Consequently the equation will not account for the nonlinearity in the problem and the method fails.

In view of these considerations Eq. (A.10) will be retained in the simplified form

$$\epsilon_{xx} = \frac{du}{dx} - y\frac{d^2v}{dx^2} - z\frac{d^2w}{dx^2} + \frac{1}{2} \left(\frac{dv}{dx}\right)^2 + \frac{1}{2} \left(\frac{dw}{dx}\right)^2 \quad (\text{A.11})$$

Eq. (A.11) represents the large deflection strain displacement in three-dimensions.

APPENDIX B

Generation of Displacement Functions for a Space
Frame Element by the Use of Interpolation Formulas

The one dimensional Hermite interpolation polynomials are used to generate the displacement functions Eq. 2.19, for the general space frame element shown in Fig. 2.V Chapter (2). These polynomials, $H_{\eta_i}^{(N)}(S)$, have the properties:

$$(1): H_{oi}^{(N)}(S_j) = \delta_{ij}$$

$$\frac{d}{ds} H_{oi}^{(N)}(S_j) = 0$$

.

.

.

$$\frac{d^N}{ds^N} H_{oi}^{(N)}(S_j) = 0$$

$$(2): H_{li}^{(N)}(S_j) = 0$$

$$\frac{d}{ds} H_{li}^{(N)}(S_j) = \delta_{ij}$$

.

.

.

$$\frac{d^N}{ds^N} H_{li}^{(N)}(S_j) = 0$$

.

.

.

$$(N+1): H_{Ni}^{(N)}(S_j) = 0$$

.

.

$$\frac{d^N}{ds^N} H_{Ni}^{(N)}(S_j) = \delta_{ij}$$

where,

N = Number of derivatives that the set can interpolate

S_j = Specific values of the argument, S , of the polynomial ($j = 1, 2$)

i = station or end point number ($i = 1, 2$)

n = index, ranging over the number of derivatives to be interpolated ($k = 0 \rightarrow N$)

In the following two such polynomials* will be dealt with. For convenience the following values will be considered: $i, j = 1, 2$ and $S_1 = 0$ and $S_2 = b$.

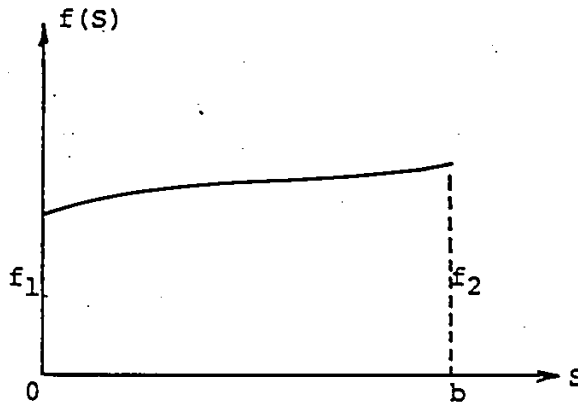
A) LAGRANGE (zeroth order Hermite) INTERPOLATION

FORMULA:

In this case $N = 0$, $i = 1, 2$, $j = 1, 2$ and $S_1 = 0$, $S_2 = b$. The idea is to interpolate the function between the two points ($S_1 = 0$ and $S_2 = b$) shown in the Fig. below when the function values are known at the two end points.

$$\begin{aligned} \therefore f_1 &= f(S = S_1 = 0), \\ f_2 &= f(S = S_2 = b) \end{aligned} \tag{B.1}$$

*detailed formulations can be found in F. K. Bagner, R. L. Fox and L. A. Schmit, Jr. ⁽²¹⁾ and G. Monforton ⁽²²⁾.



In this case ($N = 0$) the requirements become:

$$H_{01}^{(0)}(S = S_1 = 0) = 1$$

$$H_{01}^{(0)}(S = S_2 = b) = 0$$

$$H_{02}^{(0)}(S = S_1 = 0) = 0$$

$$H_{02}^{(0)}(S = S_2 = b) = 1 \quad (\text{B.2})$$

A pair of polynomials, $H_{01}^{(0)}(S)$ and $H_{02}^{(0)}(S)$, having these properties is

$$H_{01}^{(0)}(S) = \frac{S - S_2}{S_1 - S_2} = \frac{S - b}{b}$$

$$H_{02}^{(0)}(S) = \frac{S - S_1}{S_2 - S_1} = \frac{S}{b} \quad (\text{B.3})$$

These are known as Lagrange interpolation formulas.

Formulas B.3 can be used to interpolate a function, $f(S)$, at the two points $S = 0$ and $S = b$ as

$$f(S) = H_{o1}^{(o)}(S) f_1 + H_{o2}^{(o)}(S) f_2 \quad \text{or}$$

$$f(S) = (1 - S/b) f_1 + S/b f_2 \quad (\text{B.4})$$

given the values f_1 and f_2 .

Using Eq. B.4 the variation of axial displacement $\tilde{u}(S)$ and the variation of the rotation of the cross-section about the longitudinal axis $\tilde{\beta}(S)$ can be obtained as follows:

a) For the variation of $\tilde{u}(S)$, the displacements at both ends \tilde{u}_p and \tilde{u}_q are known. If

$$f_1 = \tilde{u}_1 = \tilde{u}_p$$

$$f_2 = \tilde{u}_2 = \tilde{u}_q$$

$$\text{and } b = L$$

are substituted into Eq. B.4 leads to

$$\tilde{u}(S) = (1 - S/L)\tilde{u}_p + (S/L)\tilde{u}_q$$

$$\text{or } \tilde{u}(S) = \tilde{u}_p + (\tilde{u}_p - \tilde{u}_q) S/L \quad (\text{B.5})$$

b) For the variation of $\tilde{\beta}(S)$, the end rotations $\tilde{\beta}_p$ and $\tilde{\beta}_q$ at p and q respectively are known. Then by the same manner if

$$f_1 = \tilde{\beta}_1 = \tilde{\beta}_p$$

$$f_2 = \tilde{\beta}_2 = \tilde{\beta}_q$$

$$\text{and } b = L$$

are substituted into Eq. B.4 leads to

$$\tilde{\beta}(S) = (1 - S/L)\tilde{\beta}_p + (S/L)\tilde{\beta}_q$$

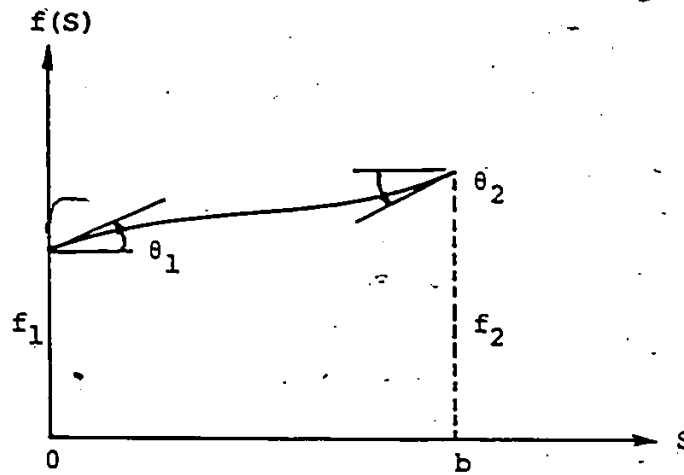
$$\text{or } \tilde{\beta}(S) = \tilde{\beta}_p + (\tilde{\beta}_q - \tilde{\beta}_p)S/L \quad (\text{B.6})$$

However, the Lagrange interpolation formula cannot be used to generate the expressions for the lateral displacement distributions $\tilde{v}(S)$ and $\tilde{w}(S)$ in planes S_1S_2 and S_1S_3 respectively. That is because at $S = S_1 = 0$ and $S = S_2 = L$ the values of the function and its first derivatives are known and Lagrange interpolation formulas interpolate only the function between two points when the function values are known at these two points. This means that Lagrange interpolation formulas do not account for the effect of the end rotation on the lateral displacements. Therefore the first order Hermite will be used to generate the expressions for the lateral displacement distributions $\tilde{v}(S)$ and $\tilde{w}(S)$.

B) OSCILLATORY (first order Hermite) INTERPOLATION

FORMULA:

In this case $N = 1$, $i = 1, 2$, $J = 1, 2$ and $S_1 = 0$, $S_2 = b$. The idea is to interpolate a function between the two points ($S_1 = 0$ and $S_2 = b$) when the function values and its first derivatives are known at the two end points as shown below.



where,

$$\theta_1 = f_{s1} = \frac{df}{ds}(s = s_1 = 0)$$

$$\theta_2 = f_{s2} = \frac{df}{ds}(s = s_2 = b)$$

$$f_1 = f(s = s_1 = 0)$$

$$f_2 = f(s = s_2 = b)$$

(B.7)

In this case ($N = 1$) the requirements are

$$H_{01}^{(1)}(s = s_1 = 0) = 1 \quad \frac{d}{ds} H_{01}^{(1)}(s = s_1 = 0) = 0$$

$$H_{01}^{(1)}(s = s_2 = b) = 0 \quad \frac{d}{ds} H_{01}^{(1)}(s = s_2 = b) = 0$$

$$H_{02}^{(1)}(s = s_1 = 0) = 0 \quad \frac{d}{ds} H_{02}^{(1)}(s = s_1 = 0) = 0$$

$$H_{02}^{(1)}(s = s_2 = b) = 1 \quad \frac{d}{ds} H_{02}^{(1)}(s = s_2 = b) = 0$$

$$H_{11}^{(1)}(s = s_1 = 0) = 0 \quad \frac{d}{ds} H_{11}^{(1)}(s = s_1 = 0) = 1$$

$$H_{11}^{(1)}(s = s_2 = b) = 0 \quad \frac{d}{ds} H_{11}^{(1)}(s = s_2 = b) = 0$$

$$\begin{aligned} H_{12}^{(1)}(S = S_1 = 0) &= 0 & \frac{d}{ds} H_{12}^{(1)}(S = S_1 = 0) &= 0 \\ H_{12}^{(1)}(S = S_2 = b) &= 0 & \frac{d}{ds} H_{12}^{(1)}(S = S_2 = b) &= 1 \end{aligned}$$

(B.8)

A set polynomials which satisfies these are

$$\begin{aligned} H_{01}^{(1)}(S) &= \left[1 - 2 \left(\frac{S - S_1}{S_1 - S_2} \right) \right] \left[\frac{S - S_2}{S_1 - S_2} \right]^2 \\ &= \frac{1}{b^3} (2S^3 - 3bS^2 + b^3) \end{aligned}$$

$$\begin{aligned} H_{02}^{(1)}(S) &= \left[1 - 2 \left(\frac{S - S_2}{S_2 - S_1} \right) \right] \left[\frac{S - S_1}{S_2 - S_1} \right]^2 \\ &= \frac{-1}{b^3} (2S^3 - 3bS^2) \end{aligned}$$

$$\begin{aligned} H_{11}^{(1)}(S) &= (S - S_1) \left[\frac{S - S_2}{S_1 - S_2} \right]^2 \\ &= \frac{1}{b^2} (S^3 - 2bS^2 + b^2S) \end{aligned}$$

$$\begin{aligned} H_{12}^{(1)}(S) &= (S - S_2) \left[\frac{S - S_1}{S_2 - S_1} \right]^2 \\ &= \frac{1}{b^2} (S^3 - bS^2) \end{aligned} \tag{B.9}$$

Eqs. B.9 can now be used to interpolate a function, $f(S)$, and its derivative at the two points 0 and b , given the values f_1, f_{S1}, f_2 and f_{S2} as

$$f(S) = H_{01}^{(1)}(S) f_1 + H_{11}^{(1)}(S) f_{S1} + H_{02}^{(1)}(S) f_2 + H_{12}^{(1)}(S) f_{S2} \tag{B.10}$$

Substituting Eqs. B.9 into B.10 leads to

$$f(s) = \frac{1}{b^3} (2s^3 - 3bs^2 + b^3) f_1 + \frac{1}{b^2} (s^3 - 2bs^2 + b^2s) f_{s1} \\ - \frac{1}{b^3} (2s^3 - 3bs^2) f_2 + \frac{1}{b^2} (s^3 - bs^2) f_{s2} \quad (B.11)$$

Using Eq. B.11 the lateral displacement distribution $\tilde{v}(s)$ can be obtained as follows:

Let,

$$f_1 = \tilde{v}_1 = \tilde{v}_p$$

$$f_{s1} = \frac{d\tilde{v}(s)}{ds} (s = s_1 = 0) = \tilde{\lambda}_p$$

$$f_2 = \tilde{v}_2 = \tilde{v}_q$$

$$f_{s2} = \frac{d\tilde{v}(s)}{ds} (s = s_2 = b) = \tilde{\lambda}_q$$

$$\text{and } b = L$$

Eq. B.11 reduces to

$$\tilde{v}(s) = \left[1 - 3\left(\frac{s}{L}\right)^2 + 2\left(\frac{s}{L}\right)^3 \right] \tilde{v}_p + \left[\left(\frac{s}{L}\right) - 2\left(\frac{s}{L}\right)^2 + \left(\frac{s}{L}\right)^3 \right] L \tilde{\lambda}_p \\ + \left[3\left(\frac{s}{L}\right)^2 - 2\left(\frac{s}{L}\right)^3 \right] \tilde{v}_q + \left[2\left(\frac{s}{L}\right)^2 + \left(\frac{s}{L}\right)^3 \right] L \tilde{\lambda}_q \quad (B.12)$$

Also the lateral displacement distribution $\tilde{w}(s)$ can be obtained as follows:

Let,

$$f_1 = \tilde{w}_1 = \tilde{w}_p$$

$$f_{s1} = \frac{d\tilde{w}(s)}{ds} (s = s_1 = 0) = -\tilde{\theta}_q$$

$$f_2 = \tilde{w}_2 = \tilde{w}_q$$

$$f_{s_2} = \frac{d\tilde{w}(s)}{ds} \quad (s = s_2 = b) = -\tilde{\theta}_q$$

and

$$\begin{aligned} \tilde{w}(s) = & \left[1 - 3\left(\frac{s}{L}\right)^2 + 2\left(\frac{s}{L}\right)^3 \right] \tilde{w}_p - \left[\left(\frac{s}{L}\right) - 2\left(\frac{s}{L}\right)^2 + \left(\frac{s}{L}\right)^3 \right] L \tilde{\theta}_p \\ & + \left[3\left(\frac{s}{L}\right)^2 - 2\left(\frac{s}{L}\right)^3 \right] \tilde{w}_q - \left[-\left(\frac{s}{L}\right)^2 + \left(\frac{s}{L}\right)^3 \right] L \tilde{\theta}_q \end{aligned}$$

(B.13)

APPENDIX C

LISTING OF COMPUTER PROGRAMS

d

IBFAHIM ABDEL SALAM HATHOJT
 TO CALCULATE THE BUCKLING LOAD OF STAYED COLUMNS IN 3 DIMENSION
 BY STABILITY FUNCTIONS

NOTATIONS

- * M = NUMBER OF ELEMENTS
- * N = NUMBER OF NODES
- * NDF = NUMBER DEGREE OF FREEDOM
- * NDS = NUMBER OF ELEMENTS WITH BENDING STIFFNESS
- * NKG = NUMBER OF ELEMENTS WITH SIGNIFICANT AXIAL LOAD
- * NM = NUMBER OF BUCKLING LOADS REQUIRED
- * NN = DIMENSION OF THE PROBLEM
- * IVC = VARIABLE CORRELATION TABLE
- * CN = CO ORDINATE OF NODAL POINTS
- * D22 = OUTER DIAMETER
- * D11 = INNER DIAMETER
- * E = MODULUS OF ELASTICITY
- * G = MODULUS OF RIGIDITY
- * AA = CROSS SECTIONAL AREA
- * MI = MOMENT OF INERTIA
- * DC = DIRECTION COSINES
- * PF = EULER LOAD
- * P1 = INTIAL LOAD
- * DP = INCREMENTAL LOAD
- * SF = STIFFNESS STABILITY FUNCTION
- * CF = CARRY OVER STABILITY FUNCTION
- * MFF = SWAY STABILITY FUNCTION
- * T = TRANSFORMATION MATRIX
- * EKL = ELEMENT STIFFNESS MATRIX LOCAL COORDINATE
- * EKG = ELEMENT STIFFNESS MATRIX GLOBAL COORDINATE
- * SMK = MASTER STABILITY STIFFNESS MATRIX
- * LMDA = EIGEN VALUE
- * EIGV = EIGEN VECTOR
- * LGTH = LENGTH OF ELEMENT
- * ALPHA(FOR GENERAL MEMBER) = ANGLE BETWEEN HORIZONTAL AND PRINCIPAL CROSS SECTION AXES
- * ALPHA(FOR VERTICAL MEMBER) = ANGLE FROM GLOBAL Z TO LOCAL X3. POSITIVE IF TOWARD GLOBAL X AXIS

0001
 0002
 0003
 0004
 0005
 0006
 0007
 0008
 0009
 0010

 0011
 0012
 0013
 0014

 0015
 0016

 0017
 0018

 0019
 0020

 0021
 0022
 0023
 0024
 0025
 0026
 0027
 0028

```

DIMENSION CN(20,4),EKL(12,2),EKG(12,12),T(12,12),SMK(40,40)
DIMENSION DC(40,4),PE(20),G(40),MI(40),MN(40,2),LGTH(40),E(40)
DIMENSION IVC(40,12),D22(10),D11(40),AA(40),EIGV(1600),LMDA(6,100)
DIMENSION SF(40),CF(40),MFF(40)
DIMENSION ALPHA(40)
DIMENSION SMKV(1600)
REAL MFF,MI,LGTH,LMDA
REAL MI
PI=3.14159265
NPROB=0
C1****INPUT DATA*****
    READ(5,10) M,N,NDF,NN,NKG,NBS,NM
    10 FORMAT(7I3)
    READ(5,12) P1,DP
    12 FORMAT(2F10.5)
    C    READ MEMBER END NODES (IN NUMERICAL ORDER BY MEMBER)
    READ(5,20) ((MN(I,J),J=1,2),I=1,M)
    20 FORMAT(2I3)
    C    READ VC TABLE (BY MEMBER, IN SAME ORDER AS MEMBER END NODES)
    READ(5,30)((IVC(I,J),J=1,12),I=1,M)
    30 FORMAT(12I4)
    C    READ COORDINATES (IN NUMERICAL ORDER BY NODE, X THEN Y THEN Z COORD.)
    READ(5,40) ((CN(I,J),J=1,NN),I=1,N)
    40 FORMAT(3F10.4)
    C    READ OUTER AND INNER DIAMETERS (IN NUMERICAL ORDER BY MEMBER)
    49 READ (5,50) NUM,MS,MF,DO
    50 FORMAT (3I3,F10.0)
    IF (NUM.EQ. 0) GO TO 55
    DO 51 I=MS,MF
    51 D22(I)=DO
    GO TO 49
    55 READ (5,50) NUM,MS,MF,DI
    IF (NUM.EQ. 0) GO TO 60
    
```


FORTRAN IV G LEVEL 21

MAIN

DATE = 76346

05/35/17

```

0064      707 CONTINUE
0065      WRITE(6,220)
0066      220 FORMAT(///.30X,6HM=MBR,AX,7H-ALPHA1,/)
0067      DO 747 I=1,M
0068      WRITE(6,230) I,ALPHA1(I)
0069      230 FORMAT(31X,13.7X,F0.3)
0100      747 CONTINUE
0101      WRITE(6,234)
0102      234 FORMAT(///.10X,30HINITIAL LOAD AND DLTA LOAD ARE,/)
0103      WRITE(6,235)PI,DP
0104      235 FORMAT(12X,F10.5,10X,F10.5,/)
C      CALCULATE EULER LOAD FOR EACH COLUMN ELEMENT
0105      DO 501 I=1,NKG
0106      PE(I)=PI*PI*E(I)*MI(I)/LGTH(I)**2
0107      WRITE(6,236)
0108      236 FORMAT(///.20X,25HEULER LOAD FOR ELEMENT1,2,/)
0109      WRITE(6,237)(J,PE(J),J=1,NKG)
0110      237 FORMAT(15X,15.10X,F10.5)
C      CALCULATE RMC AND STABILITY FUNCTIONS
0111      MSIZE=NCF+1
0112      DO 121 K=1,NM
0113      MSIZE=MSIZE-1
0114      KK=MSIZE+(MSIZE*MSIZE-MSIZE)/2
0115      P=PI
0116      DP1=DP
0117      DO 131 I=1,100
0118      P=P+DP1
0119      DO 502 J=1,NKG
0120      RHO=P/PE(J)
0121      CALL STAFUN (RHO,C1,S1,M1)
0122      CF(J)=C1
0123      SF(J)=S1
0124      MFF(J)=M1
0125      502 CONTINUE
0126      NKG1=NKG+1
0127      DO 800 J=NKG1,M
0128      CF(J)=0.5
0129      SF(J)=4.0
0130      MFF(J)=1.0
0131      800 CONTINUE
C      SET UP MASTER STIFFNESS MATRIX
0132      CALL STASM (M,MI,AA,E,G,LGTH,DC,NDF,IVC,SF,CF,MFF,SMK,ALPHA1)
0133      CALL BAKY (NDF,SMK,SMKV)
0134      CALL EIGEN (SMKV,EIGV,NDF,0)
0135      LMDA(K,1)=SMKV(KK)
0136      IF(1.E0.) GO TO 131
0137      MM=I-1
0138      X=LMDA(K,MM)
0139      Y=LMDA(K,1)
0140      IF(X*Y) 901,902,133
0141      901 DP1=-DP1/4.0
0142      IF(ABS(DP1).LE.0.005) GO TO 902
0143      133 WRITE(6,301)
0144      WRITE(6,302) K,LMDA(K,1),P,I
0145      131 CONTINUE
0146      902 WRITE(6,301)
0147      301 FORMAT(10X,13HNO. OF C.LOAD,13X,10HEIGN VALUE,10X,3H P,10X,
116HNO. OF ITERATION,/)
0148      WRITE(6,302) K,LMDA(K,1),P,I
0149      302 FORMAT(14X,14.16X,F13.7X,F9.6X,18,/)
0150      WRITE(6,903)
0151      903 FORMAT(25X,12HEIGEN VECTOR)
0152      DO 141 J=1,NDF
0153      WRITE(6,904)EIGV(NDF*NDF,NDF*K+J)
0154      904 FORMAT(25X,F15.12)
0155      141 CONTINUE
0156      WRITE(6,151)
0157      151 FORMAT(///.25X,35HTHE MASTER ELASTIC STIFFNESS MATRIX,/)
0158      CALL PMOUT (SMK,29,29,40,40)
0159      WRITE(6,152)
0160      152 FORMAT(///.25X,35HTRANSFORM OF S.S.MATRIX INTO VECTOR)
0161      CALL PMOUT (SMKV,435,1,1,700,1)
0162      121 CONTINUE
0163      STOP
0164      END

```

FORTRAN IV G LEVEL 21

STAFUN

DATE = 76J46

05/35/17

```

0001 SUBROUTINE STAFUN (RH),C,S,Z)
C*****
C TO CALCULATE THE STABILITY FUNCTIONS
C*****
0002 REAL M1,MFF
0003 PI=3.14159265
0004 A=(PI/2.0)*(SQRT(RHO))
0005 A2=2.0*A
0006 A2S=SIN(A2)
0007 A2C=COS(A2)
0008 COT=A2C/A2S
0009 XTAN=SIN(A)/COS(A)
0010 C=(A2 A2S)/(A2S A2+A2C)
0011 S=((1.0 A2*COT)*A)/(XTAN A)
0012 Z=(2.0*S*(1.0+C))/(2.0*S*(1.0+C) PI**2*RHO)
0013 RETURN
0014 END

```

FORTRAN IV G LEVEL 21

STASH

DATE = 76346

05/35/17

```

0001 SUBROUTINE STASH(M,MI,AA,E,G,EL,DC,NDF,IVC,SF,CF,MFF,SMK,ALPHA)
C *****
C THIS SUBROUTINE WILL TRY TO CALCULATE THE MASTER ELASTIC STIFFNESS M.C
C *****
0002 DIMENSION AA(40),E(40),G(40),FL(10),DC(40,4),IVC(40,12)
0003 DIMENSION FKL(12,12),EKG(12,12),T(12,12),SMK(40,40)
0004 DIMENSION MI(40),MFF(40),SF(40),ALPHA(40),J(12,12),V(12,12)
0005 DIMENSION CF(40)
0006 FCAL MI,MFF
0007 DO 104 I=1,40
0008 DO 104 J=1,40
0009 104 SMK(I,J)=0.0
0010 DO 100 K=1,M
0011 FA=SF(K)*(1.0+CF(K))
0012 FB=2.0*FA/MFF(K)
0013 FC=SF(K)
0014 PI=3.14159265
0015 ALPHA=ALPHA(K)*PI/180.
0016 CX=DC(K,1)
0017 CY=DC(K,2)
0018 CZ=DC(K,3)
0019 DO 1 I=1,12
0020 DO 1 J=1,12
0021 1 T(I,J)=0.0
0022 T(1,1)=CX
0023 T(1,2)=CY
0024 T(1,3)=CZ
0025 IF(CX+CZ)8,9,8
0026 8 ELONE=SQRT(CX**2+CZ**2)
0027 T(2,1)=(CX*CY*COS(ALPHA)+CZ*SIN(ALPHA))/ELONE
0028 T(2,2)=SQRT(CX**2+CZ**2)*COS(ALPHA)
0029 T(2,3)=(-CY*CZ*COS(ALPHA)+CX*SIN(ALPHA))/ELONE
0030 T(3,1)=(CX*CY*SIN(ALPHA)+CZ*COS(ALPHA))/ELONE
0031 T(3,2)=-SQRT(CX**2+CZ**2)*SIN(ALPHA)
0032 T(3,3)=(CY*CZ*SIN(ALPHA)+CX*COS(ALPHA))/ELONE
0033 GO TO 10
0034 9 T(2,1)=-CY*COS(ALPHA)
0035 T(2,3)=CY*SIN(ALPHA)
0036 T(3,1)=SIN(ALPHA)
0037 T(3,3)=COS(ALPHA)
0038 10 DO 2 I=4,6
0039 DO 2 J=4,6
0040 JJ=J-3
0041 II=I-3
0042 2 T(I,J)=T(II,JJ)
0043 DO 3 I=7,9
0044 DO 3 J=7,9
0045 II=I-3
0046 JJ=J-3
0047 3 T(I,J)=T(II,JJ)
0048 DO 4 I=10,12
0049 DO 4 J=10,12
0050 II=I-3
0051 JJ=J-3
0052 4 T(I,J)=T(II,JJ)
0053 DO 5 I=1,12
0054 DO 5 J=1,12
0055 5 EKL(I,J)=0.0
0056 EKL(1,1)=E(K)*AA(K)/EL(K)
0057 FKL(1,7)=EKL(1,1)
0058 EKL(2,2)=FB*E(K)*MI(K)/EL(K)**3
0059 EKL(2,6)=FA*E(K)*MI(K)/EL(K)**2
0060 EKL(2,8)=EKL(2,2)
0061 EKL(2,12)=EKL(2,6)
0062 EKL(3,3)=FB*E(K)*MI(K)/EL(K)**3
0063 EKL(3,5)=FA*E(K)*MI(K)/EL(K)**2
0064 EKL(3,9)=-EKL(3,3)
0065 EKL(3,11)=EKL(3,5)
0066 EKL(4,4)=2.0*G(K)*MI(K)/EL(K)
0067 EKL(4,10)=-EKL(4,4)
0068 EKL(5,5)=FC*E(K)*MI(K)/EL(K)
0069 EKL(5,9)=EKL(3,11)
0070 EKL(5,11)=CF(K)*FC*E(K)*MI(K)/FL(K)
0071 EKL(6,6)=FC*E(K)*MI(K)/EL(K)
0072 EKL(6,8)=EKL(2,6)
0073 EKL(6,12)=CF(K)*FC*E(K)*MI(K)/EL(K)
0074 EKL(7,7)=EKL(1,1)
0075 EKL(8,8)=EKL(2,8)

```

FORTRAN IV G LEVEL 21

STASH

DATE = 76346

05/35/17

```

0076      CKL(8,12)=EKL(2,12)
0077      EKL(9,5)=EKL(3,9)
0078      EKL(9,11)=EKL(3,11)
0079      EKL(10,10)=EKL(4,10)
0080      EKL(11,11)=EKL(5,5)
0081      EKL(12,12)=EKL(6,6)
0082      DO 6 I=2,12
0083      II=I-1
0084      DO 6 J=1,11
0085      6 EKL(I,J)=EKL(J,I)
0086      CALL TRANS (T,U,12,12)
0087      CALL MULT (U,EKL,V,12,12,12)
0088      CALL MULT (V,T,EKG,12,12,12)
0089      DO 101 I=1,12
0090      IL=IVC(K,I)
0091      IF(IL.EQ.0) GO TO 101
0092      DO 102 J=1,12
0093      IN=IVC(K,J)
0094      IF(IN.EQ.0) GO TO 102
0095      IL1=IABS(IL)
0096      IN1=IABS(IN)
0097      JJ=IL1/IL
0098      KK=IN1/IN
0099      SMK(IL1,IN1)=SMK(IL1,IN1)+JJ*KK*EKG(I,J)
0100      102 CONTINUE
0101      101 CONTINUE
0102      100 CONTINUE
0103      RETURN
0104      END

```

FORTRAN IV G LEVEL 21

STASH

DATE = 76346

05/35/17

```

*OPTIONS IN EFFECT* ID,ERCDIC,SOURCE,NOLIST,NODECK,LOAD,NOMAP
*OPTIONS IN EFFECT* NAME = STASH  LINCNT = 80
*STATISTICS* SOURCE STATEMENTS = 104, PROGRAM SIZE = 6582
*STATISTICS* NO DIAGNOSTICS GENERATED

```

FORTRAN IV G LEVEL 21

MULT

DATE = 76338

05/12/43

```

0001      SUBROUTINE MULT (A,B,C,M,K,N)
C*****
C      THIS WILL MULTIPLY TWO MATRICES
C*****
0002      DIMENSION A(M,K),B(K,N),C(M,N)
0003      DO 20 I=1,M
0004      DO 20 J=1,N
0005      C(I,J)=0.0
0006      DO 20 L=1,K
0007      C1=A(I,L)*B(L,J)
0008      20 C(I,J)=C(I,J)+C1
0009      RETURN
0010      END

```

X

FORTRAN IV G LEVEL 21

TRANS

DATE = 76338

05/12/43

```

0001      SUBROUTINE TRANS(U,V,K,L)
C*****
C      THIS SUBROUTINE WILL TRANSPOSE A MATRIX
C*****
0002      DIMENSION U(L,K),V(K,L)
0003      DO 10 I=1,K
0004      DO 10 J=1,L
0005      10 V(I,J)=U(J,I)
0006      RETURN
0007      END

```

FORTRAN IV G LEVEL 21

TRANS

DATE = 76346

05/35/17

```

*OPTIONS IN EFFECT* ID,EBCDIC,SOURCE,NOLIST,NODECK,LOAD,NOMAP
*OPTIONS IN EFFECT* NAME = TRANS * LINECNT = 80
*STATISTICS* SOURCE STATEMENTS = 7,PROGRAM SIZE = 554
*STATISTICS* NO DIAGNOSTICS GENERATED

```

FORTRAN IV G LEVEL 21

BAKY

DATE = 76346

05/35/17

```

0001 SUBROUTINE BAKY (NOF,SMK,SMKV)
      C *****
      C THIS SUBROUTINE WILL TRY TO TRANSFER THE UPPER TRIANGLE MATRIX TO VECTOR
      C *****
0002 DIMENSION SMK(40,40),SMKV(700)
0003 DO 109 I=1,700
0004 109 SMKV(I)=0.0
0005 N)NA=0
0006 DO 17 L=1,NOF
0007 DO 18 LL=1,L
0008 N)NA=N)NA+1
0009 SMKV(N)NA)=SMK(LL,L)
0010 18 CONTINUE
0011 17 CONTINUE
0012 RETURN
0013 END

```

FORTRAN IV G LEVEL 21

BAKY

DATE = 76346

05/35/17

```

*OPTIONS IN EFFECT* ID,EBCDIC,SOURCE,NOLIST,NODECK,LOAD,NJMAP
*OPTIONS IN EFFECT* NAME = BAKY * LINECNT = 80
*STATISTICS* SOURCE STATEMENTS = 13,PROGRAM SIZE = 518
*STATISTICS* NO DIAGNOSTICS GENERATED

```

FORTRAN IV G LEVEL 21

PMOUT

DATE = 76346

05/35/17

```

0001      SUBROUTINE PMOUT (A,NI,NJ,M,NDIM,NDIM)
C*****
C      THIS SUBROUTINE PRINTS CJT MATRIX A(ORDER NI,NJ),STORED IN DIMENSION
C      (MCI,M,NDIM) IN MAIN PROGRAM.
C*****
0002      DIMENSION A(MCI,M,NDIM)
0003      JC=0
0004      KEND=0
0005      10 JB=JE+1
0006      JC=JB+5
0007      IF(JE-NJ)25,20,20
0008      JE=NJ
0009      KEND=1
0010      25 IF(M)41,41,30
0011      30 WRITE(6,40)(J,J=JB,JE)
0012      40 FORMAT(11HROW/COLUMN,15,5I19)
0013      41 DO 50 I=1,NI
0014      50 WRITE(6,60)I,(A(I,J),J=JB,JE)
0015      60 FORMAT(14,6E19,5)
0016      IF(KEND)10,10,70
0017      70 RETURN
0018      END

```


C Ibrahîm Hathout
 C *****
 C TO CALCULATE THE BUCKLING LOAD OF STAYED COLUMNS IN 3-DIMENSION
 C BY THE FINITE ELEMENT METHOD
 C *****

```

  *****
  *
  * NOTATIONS
  *
  * M = NUMBER OF ELEMENTS
  * N = NUMBER OF NODES
  * NDF = NUMBER DEGREE OF FREEDOM
  * NBS = NUMBER OF ELEMENTS WITH BENDING STIFFNESS
  * NKG = NUMBER OF ELEMENTS WITH SIGNIFICANT AXIAL LOAD
  * NM = NUMBER OF BUCKLING LOADS REQUIRED
  * NN = DIMENSION OF THE PROBLEM
  * IVC = VARIABLE CORRELATION TABLE
  * CN = CO-ORDINATE OF NODAL POINTS
  * D22 = OUTER DIAMETER
  * D11 = INNER DIAMETER
  * E = MODULUS OF ELASTICITY
  * G = MODULUS OF RIGIDITY
  * AA = CROSS SECTIONAL AREA
  * MI = MOMENT OF INERTIA
  * DC = DIRECTION COSINES
  * XL = EIGEN VALUE
  * X = EIGEN VECTOR
  * XX = CRITICAL LOAD
  * REF = THE RELATIVE EFFICIENCY ( CRITICAL LOAD/WEIGHT)
  * MK = MASTER STIFFNESS MATRIX
  * LGTH = LENGTH OF ELEMENT
  * GLK1 = MASTER ELASTIC STIFFNESS MATRIX
  * GLK2 = MASTER GEOMETRIC STIFFNESS MATRIX
  * GLK1V = VECTOR CONTAIN ELEMENTS OF M.E.S. MATRIX TO TRANSFER THIS
  * MATRIX FROM DOUBLE TO SINGLE DIMENSION
  * GLK2V = VECTOR CONTAIN ELEMENTS OF M.G.S. MATRIX TO TRANSFER THIS
  * MATRIX FROM DOUBLE TO SINGLE DIMENSION
  * ALPHA1 (FOR GENERAL MEMBER) = ANGLE BETWEEN HORIZONTAL AND PRINCIPAL
  * CROSS SECTION AXES
  * ALPHA1 (FOR VERTICAL MEMBER) = ANGLE FROM GLOBAL Z TO LOCAL X3.
  * POSITIVE IF TOWARD GLOBAL X AXIS
  *****
  
```

0001
 0002
 0003
 0004
 0005
 0006
 0007
 0008
 0009
 0010
 0011
 0012
 0013
 0014
 0015
 0016
 0017
 0018
 0019
 0020
 0021
 0022
 0023
 0024
 0025
 0026
 0027
 0028
 0029

```

  DIMENSION GLK2V(10000),MI(50),XL(100),X(10000),XX(100)
  DIMENSION DC(50,4),MK(100,100),MN(50,2),AA(50),E(50),G(50)
  DIMENSION ALPHA1(50),GLK1(100,100),GLK2(100,100),GLK1V(10000)
  DIMENSION D22(50),D11(50),LGTH(50),IVC(50,12)
  DIMENSION CN(10,30,4),REF(100)
  REAL MK, LGTH, MI
  PI = 4.0 * ATAN(1.0)
  NPROR = 0
  LOLA = 1
  MDLY = 1
  NONA1 = 0
  C1 ***** INPUT DATA *****
  READ(5,10) M,N,NDF,NN,NKG,NBS,NM
  FORMAT(7I3)
  10
  C READ MEMBER END NODES (IN NUMERICAL ORDER BY MEMBER)
  C READ(5,20) ((MN(I,J),J=1,2),I=1,M)
  C FORMAT(2I3)
  C READ VC TABLE (BY MEMBER, IN SAME ORDER AS MEMBER END NODES)
  C READ(5,30) ((IVC(I,J),J=1,12),I=1,M)
  C 30 FORMAT(12I4)
  C READ OUTER AND INNER DIAMETERS (IN NUMERICAL ORDER BY MEMBER)
  C 49 READ (5,50) NUM,MS,MF,DO
  C 50 FORMAT (3I3,F10.0)
  C IF (NUM .EQ. 0) GO TO 55
  C DO 51 I=MS,MF
  C 51 D22(I)=DO
  C GO TO 49
  C 55 READ (5,50) NUM,MS,MF,DI
  C IF (NUM .EQ. 0) GO TO 60
  C DO 57 I=MS,MF
  C 57 D11(I)=DI
  C GO TO 55
  C READ MODULI OF ELASTICITY (IN NUMERICAL ORDER BY MEMBER)
  C 60 READ (5,50) NUM,MS,MF,EM
  
```

FORTRAN IV G LEVEL 21

MAIN

DATE = 76338

05/12/43

```

0030      IF(NUM.EQ.0) GO TO 75
0031      DO 62 I=MS,MF
0032      62 E(I)=EM
0033      GO TO 60
0034      75 READ(5,50)NUM,MS,MF,ALPHA
0035      IF(NUM.EQ.0.0) GO TO 70
0036      DO 72 I=MS,MF
0037      72 ALPHA(I)=ALPHA
0038      GO TO 75
0039      70 READ(5,50)NUM,MS,MF,GM
0040      IF(NUM.EQ.0) GO TO 555
0041      DO 71 I=MS,MF
0042      71 G(I)=GM
0043      GO TO 70
C      READ COORDINATES (IN NUMERICAL ORDER BY NODE, X THEN Y THEN Z COORD.)
0044      555 DO 455 K=1,LOLA
0045      READ(5,40) ((CN(K,I,J),J=1,NP),I=1,N)
0046      40 FORMAT(2F12.6)
0047      455 CONTINUE
0048      IDOXY=NBS+1
0049      DO 456 LC=1,LOLA
0050      NIS=30
0051      NOS=NIS+1
0052      554 READ(5,298) DM
0053      298 FORMAT(F10.7)
0054      DO 1010 I=IDCDY,NIS
0055      D22(I)=DM
0056      1010 D11(I)=0.0
0057      READ(5,298) DM
0058      DO 1011 I=NOS,M
0059      D22(I)=DM
0060      1011 D11(I)=C.0
C2**** CALCULATE MEMBER PROPERTIES*****
C      MCMENT OF INERTIA
0061      DO 67 I=1,NBS
0062      MI(I)=PI*(D22(I)**4-D11(I)**4)/64.0
0063      67 CONTINUE
0064      NBS1=NBS+1
0065      DO 68 I=NBS1,M
0066      68 MI(I)=0.0
C      AFEA.LENGTH.DIRECTION COSINES
0067      DO 80 I=1,M
0068      AA(I)=PI*(D22(I)**2-D11(I)**2)/4.
0069      80 CONTINUE
0070      DO 110 I=1,M
0071      K=MN(I,1)
0072      LO=MN(I,2)
0073      SUM=0.
0074      DO 90 J=1,NN
0075      SUM=SUM+(CN(LC,LO,J)-CN(LC,K,J))**2
0076      90 CONTINUE
0077      LGTH(I)=SQRT(SUM)
0078      DO 100 J=1,NN
0079      OC(I,J)=(CN(LC,LO,J)-CN(LC,K,J))/LGTH(I)
0080      100 CONTINUE
0081      110 CONTINUE
C3**** WRITE INPUT DATA AND MECHANICAL PROPERTIES*****
0082      NPROB=NPROB+1
0083      WRITE (6,118) NPROB
0084      118 FORMAT(////.10X,14HPROBLEM NUMBER,14./)
0085      WRITE (6,119)
0086      119 FORMAT(/.10X,25HUNITS ARE INCHES AND KIPS./)
0087      WRITE (6,120)
0088      120 FORMAT (10X,6HNO. OF,5X,6HNO. OF,5X,10HDEGREES OF,5X,9HDIMENSION,5
1X,19HNO. OF MEMBERS WITH,5X,6HNO. OF)
0089      WRITE (6,130)
0090      130 FORMAT (10X,7HMEMBERS,4X,5HNCDES,7X,7HFREEDCM,7X,10HOF PROBLEM,6X,
12HKG,5X,1MI,11X,5HMCDES)
0091      WRITE (6,140) M,N,NDF,NN,NKG,NBS,NM
0092      140 FORMAT(10X,14.2X,13.8X,13.13X,12.13X,13.4X,13.12X,12./)
0093      WRITE (6,150)
0094      150 FORMAT (10X,6HMEMBER,5X,9HENC NODES,5X,5HOUTER,5X,5HINNER,5X,7HMOD
1ULUS,10X,7HMODULUS,5X,4HAREA,5X,6HCMCFNT,7X,5HLENGTH)
0095      WRITE (6,160)
0096      160 FORMAT (35X,5HDIAM.,5X,5HDIAM.,5X,9HOF ELAST.,5X,10HOF RIGIDTY,
110X,10HOF INERTIA)
0097      WRITE(6,170)((I,(MN(I,J),J=1,2),D22(I),D11(I),E(I),G(I),AA(I),
1MI(I),LGTH(I),I=1,M)

```

FORTRAN IV G LEVEL 21

MAIN

DATE = 76338

05/12/43

```

0098      170 FORMAT(11X,I3,7X,I3,2X,I3,5X,FA,7,4X,F6,3,6X,F7,1,7X,F7,1,5X,
0099      180 FORMAT(//,6HMEMBER,34X,3HVC-TABLE,/)
0100      WRITE(6,190)
0101      190 FORMAT(11X,I3,12X,I3,2X,I3,7X,I3,2X,I3,2X,I3,2X,I3,2X,I3,2X,I3,2X,I3,2X,/)
0102      WRITE(6,200)
0103      200 FORMAT(//,10X,6H-NODE ,5X,11H-COORDINATES,5X,3H X ,9X,3H Y ,9X,
0104      13H Z )
0105      DO 707 I=1,N
0106      WRITE(6,210) I,(CN(LC,I,J),J=1,NN)
0107      210 FORMAT(11X,I3,20X,F8,3,4X,F9,3,4X,FA,3,/)
0108      707 CONTINUE
0109      WRITE(6,220)
0110      220 FORMAT(//,30X,6HMEMBER,5X,7H-ALPHA1,/)
0111      DO 747 I=1,M
0112      WRITE(6,230) I,ALPHA1(I)
0113      230 FORMAT(31X,I3,7X,F9,3)
0114      747 CONTINUE
0115      C*****MASTER ELASTIC STIFFNESS MATRIX*****
0116      CALL SLAKM(M,MI,AA,F,G,LGTH,DC,NDF,IVC,GLK1,ALPHA1)
0117      C*****MASTER GEOMETRIC STIFFNESS MATRIX*****
0118      CALL GECKM (MKG,LGTH,DC,NDF,IVC,ALPHA1,GLK2)
0119      C*****CALCULATE INVERSE OF EIGENVALUES AND THE EIGENVECTORS*****
0120      CALL APRAY (2,NDF,NDF,100,100,GLK1V,GLK1)
0121      CALL ARRAY (2,NDF,NDF,100,100,GLK2V,GLK2)
0122      CALL NFOOT (NDF,GLK2V,GLK1V,XL,X)
0123      C*****CALCULATE AND WRITE EIGENVALUES*****
0124      WRITE(6,762)
0125      762 FORMAT(//,15X,13HCRITICAL LOAD,/)
0126      DO 763 I=1,NM
0127      XX(I)=1.0/XL(I)
0128      763 WRITE (6,764) XX(I)
0129      764 FORMAT(15X,F15,6,/)
0130      C*****WRITE EIGENVECTORS*****
0131      WRITE(6,765)
0132      765 FORMAT(//,25X,12HEIGENVECTORS,/)
0133      DO 766 I=1,NDF
0134      IP=I+NDF
0135      IKP=I+2*NDF
0136      WRITE(6,767) I,X(I),X(IP),X(IKP)
0137      767 FORMAT(12X,I3,10X,F18,15,10X,F18,15,10X,F18,15,/)
0138      766 CONTINUE
0139      CALL UCDDY (M,NRS,NM,AA,LGTH,XX,WT,FEF)
0140      WRITE(6,496)
0141      496 FORMAT(//,15X,13HCRITICAL LOAD,9X,10HTHE WEIGHT,11X,23HTHE RELAT
0142      IVE EFFICIENCY,/)
0143      DO 8000 I=1,NM
0144      WRITE(6,470) XX(I),WT,REF(I)
0145      470 FORMAT(15X,F11,6,10X,F11,6,10X,F15,9,/)
0146      8000 CONTINUE
0147      NONA1=NCNA1+1
0148      IF (NONA1.EQ.MOLY) GO TO 456
0149      GO TO 554
0150      456 CONTINUE
0151      WRITE(6,303)
0152      303 FORMAT(//,20X,35HTHE MASTER ELASTIC STIFFNESS MATRIX,/)
0153      CALL PMOUT(GLK1,99,99,1,100,100)
0154      WRITE(6,304)
0155      304 FORMAT(//,20X,37HTHE MASTER GEOMETRIC STIFFNESS MATRIX,/)
0156      CALL PMOUT (GLK2,99,99,1,100,100)
0157      STOP
0158      END

```

FORTRAN IV G LEVEL 21

ELAKM

DATE = 76338

05/12/43

```

0001      SUBROUTINE ELAKM (N,MI,AA,E,C,EL,DC,NDF,IVC,MK,ALPHA)
C*****
C      THIS SUBROUTINE WILL TRY TO CALCULATE THE MASTER ELASTIC STIFFNESS M.
C*****
0002      DIMENSION AA(50),E(50),G(50),EL(50),DC(50,4),IVC(50,12)
0003      DIMENSION MK(100,100),MI(50),ALPHA(50),EKG(12,12),T(12,12)
0004      DIMENSION U(12,12),V(12,12),EKL(12,12)
0005      REAL MI,MK
0006      DO 104 I=1,NDF
0007      DO 104 J=1,NDF
0008      104 MK(I,J)=0.0
0009      DO 100 K=1,M
0010      PI=4.0*ATAN(1.0)
0011      ALPHA=ALPHA(K)*PI/180.
0012      CX=DC(K,1)
0013      CY=DC(K,2)
0014      CZ=DC(K,3)
0015      DO 1 I=1,12
0016      DO 1 J=1,12
0017      1 T(I,J)=0.0
0018      T(1,1)=CX
0019      T(1,2)=CY
0020      T(1,3)=CZ
0021      IF(CX+CZ)8,9,8
0022      8 ELONE=SQRT(CX**2+CZ**2)
0023      T(2,1)=(-CX*CY*COS(ALPHA)-CZ*SIN(ALPHA))/ELONE
0024      T(2,2)=SQRT(CX**2+CZ**2)*COS(ALPHA)
0025      T(2,3)=(-CY*CZ*COS(ALPHA)+CX*SIN(ALPHA))/ELONE
0026      T(3,1)=(CX*CY*SIN(ALPHA)-CZ*COS(ALPHA))/ELONE
0027      T(3,2)=-SQRT(CX**2+CZ**2)*SIN(ALPHA)
0028      T(3,3)=(CY*CZ*SIN(ALPHA)+CX*COS(ALPHA))/ELONE
0029      GO TO 10
0030      9 T(2,1)=-CY*CCS(ALPHA)
0031      T(2,3)=CY*SIN(ALPHA)
0032      T(3,1)=SIN(ALPHA)
0033      T(3,3)=COS(ALPHA)
0034      10 DN2 I=4.6
0035      DO 2J=4.6
0036      JJ=J-3
0037      II=I-3
0038      2 T(I,J)=T(II,JJ)
0039      DO 3 I=7.9
0040      DO 3 J=7.9
0041      II=I-3
0042      JJ=J-3
0043      3 T(I,J)=T(II,JJ)
0044      DO 4 I=10.12
0045      DO 4 J=10.12
0046      II=I-3
0047      JJ=J-3
0048      4 T(I,J)=T(II,JJ)
0049      DO 5 I=1,12
0050      DO 5 J=1,12
0051      5 EKL(I,J)=0.0
0052      EKL(1,1)=E(K)*AA(K)/EL(K)
0053      EKL(1,7)=-EKL(1,1)
0054      EKL(2,2)=12*E(K)*MI(K)/EL(K)**3
0055      EKL(2,6)=-6*E(K)*MI(K)/EL(K)**2
0056      EKL(2,8)=-EKL(2,2)
0057      EKL(2,12)=-EKL(2,6)
0058      EKL(3,3)=12*E(K)*MI(K)/EL(K)**3
0059      EKL(3,5)=-6*E(K)*MI(K)/EL(K)**2
0060      EKL(3,9)=-EKL(3,3)
0061      EKL(3,11)=-EKL(3,5)
0062      EKL(4,4)=2.0*G(K)*MI(K)/EL(K)
0063      EKL(4,10)=-EKL(4,4)
0064      EKL(5,5)=4*E(K)*MI(K)/EL(K)
0065      EKL(5,9)=-EKL(3,11)
0066      EKL(5,11)=-2*E(K)*MI(K)/EL(K)
0067      EKL(6,6)=4*E(K)*MI(K)/EL(K)
0068      EKL(6,8)=-EKL(2,6)
0069      EKL(6,12)=2*E(K)*MI(K)/EL(K)
0070      EKL(7,7)=EKL(1,1)
0071      EKL(8,8)=-EKL(2,8)
0072      EKL(8,12)=-EKL(2,12)
0073      EKL(9,9)=-EKL(3,9)
0074      EKL(9,11)=-EKL(3,11)
0075      EKL(10,10)=-EKL(4,10)

```

FORTRAN IV G _LEVEL 21

ELAKN

DATE = 76338

05/12/43

```

0076      EKL(11.11)=EKL(5.5)
0077      EKL(12.12)=EKL(6.6)
0078      DO 6 I=2.12
0079      I I=I-1
0080      DO 6 J=1.11
0081      6 FKL(I,J)=EKL(J,I)
0082      CALL TRANS (T,U.12.12)
0083      CALL MULT (U,EKL,V.12.12.12)
0084      CALL MULT (V,T,EKG.12.12.12)
0085      DO 101 I=1.12
0086      IL=IVC(K,I)
0087      IF(IL.EQ.0) GO TO 101
0088      DO 102 J=1.12
0089      IN=IVC(K,J)
0090      IF(IN.EQ.0) GO TO 102
0091      IL1=IABS(IL)
0092      IN1=IABS(IN)
0093      JJ=IL1/IL
0094      KK=IN1/IN
0095      MK(IL1.IN1)=MK(IL1.IN1)+JJ*KK*EKG(I,J)
0096      102 CONTINUE
0097      101 CONTINUE
0098      100 CONTINUE
0099      RETURN
0100      END.

```

FORTRAN IV G LEVEL 2)

GECKM

DATE = 76338

05/12/43

```

0001      SUBROUTINE GECKM (NKG,EL,DC,NDF,IVC,ALPHA1,MK)
C*****
C      THIS SUBROUTINE WILL TRY TO CALCULATE THE MASTER GEOMETRIC STIFFNESS MATRIX
C*****
0002      DIMENSION EL(50),DC(50,4),IVC(50,12),GKL(12,12),GKG(12,12)
0003      DIMENSION T(12,12),ALPHA1(50),U(12,12),V(12,12),MK(100,100)
0004      REAL MK
0005      DO 104 I=1,NDF
0006      DO 104 J=1,NDF
0007      104 MK(I,J)=0.0
0008      DO 100 K=1,NKG
0009      PI=4.0*ATAN(1.0)
0010      ALPHA=ALPHA1(K)*PI/180.
0011      CX=DC(K,1)
0012      CY=DC(K,2)
0013      CZ=DC(K,3)
0014      DO 1 I=1,12
0015      DO 1 J=1,12
0016      1 T(I,J)=0.0
0017      T(1,1)=CX
0018      T(1,2)=CY
0019      T(1,3)=CZ
0020      IF(CX+CZ)8,9,8
0021      8 ELONE=SQRT(CX**2+CZ**2)
0022      T(2,1)=(-CX*CY*COS(ALPHA)-CZ*SIN(ALPHA))/ELONE
0023      T(2,2)=SQRT(CX**2+CZ**2)*COS(ALPHA)
0024      T(2,3)=(-CY*CZ*COS(ALPHA)+CX*SIN(ALPHA))/ELONE
0025      T(3,1)=(CX*CY*SIN(ALPHA)-CZ*COS(ALPHA))/ELONE
0026      T(3,2)=-SQRT(CX**2+CZ**2)*SIN(ALPHA)
0027      T(3,3)=(CY*CZ*SIN(ALPHA)+CX*COS(ALPHA))/ELONE
0028      GO TO 10
0029      9 T(2,1)=-CY*COS(ALPHA)
0030      T(2,3)=CY*SIN(ALPHA)
0031      T(3,1)=SIN(ALPHA)
0032      T(3,3)=COS(ALPHA)
0033      10 DO2 I=4,6
0034      DO 2 J=4,6
0035      JJ=J-3
0036      II=I-3
0037      2 T(I,J)=T(II,JJ)
0038      DO 3 I=7,9
0039      DO 3 J=7,9
0040      II=I-3
0041      JJ=J-3
0042      3 T(I,J)=T(II,JJ)
0043      DO 4 I=10,12
0044      DO 4 J=10,12
0045      II=I-3
0046      JJ=J-3
0047      4 T(I,J)=T(II,JJ)
0048      DO 5 I=1,12
0049      DO 5 J=1,12
0050      5 GKL(I,J)=0.0
0051      GKL(2,2)=6.0/(5.0*EL(K))
0052      GKL(2,6)=0.10
0053      GKL(2,8)=-GKL(2,2)
0054      GKL(2,12)=GKL(2,6)
0055      GKL(3,3)=GKL(2,2)
0056      GKL(3,5)=-GKL(2,6)
0057      GKL(3,9)=GKL(2,8)
0058      GKL(3,11)=GKL(3,5)
0059      GKL(5,5)=2.0*EL(K)/15.0
0060      GKL(5,9)=GKL(2,6)
0061      GKL(5,11)=-EL(K)/30.0
0062      GKL(6,6)=GKL(5,5)
0063      GKL(6,8)=GKL(3,5)
0064      GKL(6,12)=GKL(5,11)
0065      GKL(8,8)=GKL(2,2)
0066      GKL(8,12)=GKL(3,5)
0067      GKL(9,9)=GKL(2,2)
0068      GKL(9,11)=GKL(2,6)
0069      GKL(11,11)=GKL(5,5)
0070      GKL(12,12)=GKL(6,6)
0071      DO 6 I=2,12
0072      II=I-1
0073      DO 6 J=1,11
0074      6 GKL(I,J)=GKL(J,I)
0075      CALL TRANS (T,U,12,12,12)

```

FORTRAN IV G LEVEL 21

GECKM

DATE = 76338

05/12/43

```
0076 CALL MULT (U,GKL,V,12,12,12)
0077 CALL MULT (V,T,GKG,12,12,12)
0078 DO 101 I=1,12
0079 IL=IVC(K,I)
0080 IF(IL.EQ.0) GO TO 101
0081 DO 102 J=1,12
0082 IN=IVC(K,J)
0083 IF(IN.EQ.0) GO TO 102
0084 IL1=IABS(IL)
0085 IN1=IABS(IN)
0086 JJ=IL1/IL
0087 KK=IN1/IN
0088 MK(IL1,IN1)=MK(IL1,IN1)+JJ*KK*CKG(I,J)
0089 102 CONTINUE
0090 101 CONTINUE
0091 100 CONTINUE
0092 RETURN
0093 END
```

FORTRAN IV G LEVEL 21

DODY

DATE = 76338

05/12/43

```

0001      SUBROUTINE DODY (M,NBS,NM,A,EL,XX,WT,REF)
C*****
C      THIS SUBROUTINE WILL TRY TO CALCULATE THE WEIGHT AND RELATIVE EFFICIENCY
C*****
0002      DIMENSION V(50),A(50),EL(50),XX(100),REF(100)
0003      RHO=.283
0004      DO 100 I=1,NBS
0005      V(I)=A(I)*EL(I)
0006      100 CONTINUE
0007      NBS1=NBS+1
0008      DO 200 I=NBS1,M
0009      V(I)=A(I)*EL(I)
0010      200 CONTINUE
0011      VT=0.0
0012      DO 300 J=1,M
0013      VT=VT+V(J)
0014      300 CONTINUE
0015      WT=VT*RHO
0016      DO 400 K=1,NM
0017      REF(K)=1000.0*(XX(K)/WT)
0018      400 CONTINUE
0019      RETURN
0020      END

```


BIBLIOGRAPHY

1. Chu, K. H., and Berge, S. S., "Analysis and Design of struts with Tension Ties", Journal of Structural Division, ASCE, Vol.89, No. ST1, Proc. Paper 3414, Feb. 1963, pp.127-163.
2. Mauch, H. R., and Felton, L. P., "Optimum Design of Columns Supported by Tension Ties", Journal of the Structural Division, ASCE, Vol.93, No.ST3, Proc. Paper 5281, June 1967, pp.210-220.
3. Ellis, J. S., "The R.M.C. Design-Build-Test Projects", Engineering Education, American Society for Engineering Education, Vol.62, No.3, Dec. 1971, pp1294-296.
4. Pearson, K. M., "The Behavior of a Stayed Column with Varying Stay Tension and Cross Member Length", Thesis presented to the Royal Military College of Canada, Kingston, Ontario, Canada, in 1971, in partial fulfillment of the requirements for the degree of Bachelor of Engineering.
5. Smith, R.J., McCaffrey, G.T., and Ellis, J. S., "Buckling of a Single Crossarm Stayed Column", Journal of Structural Division, ASCE, Vol.101, No.ST1, Proc. Paper 11071, Jan. 1975, pp.249-268.
6. Temple, M. C., "Buckling of Stayed Columns", accepted for publication by the Journal of the Structural Division, ASCE.
7. Temple, M. C., Stability of Columns with Biplanar Bracing, Ph.D. Thesis, Civil Engineering Dept., University of Toronto, 1970.
8. Timoshenko, S. P., Theory of Elastic Stability, Second Edition, McGraw-Hill Book Company, Inc., 1961.
9. Gregory, M., Elastic Instability, First Edition, E. and F.N. Spon Ltd., London, 1967.
10. Gere, J. M., and Weaver, J.r, Matrix Algebra for Engineers, First Edition, D. Van Nostrand Company, Inc., 1965.
11. Horne, M. R., and Merchant, W., The Stability of Frames, First Edition, Pergamon Press, 1965.

12. Majid, K. I., Non-linear Structures, First Edition, Published in the USA by Wiley-Interscience Division, 1972.
13. Martin, H. C., "On the Derivation of Stiffness Matrices for Analysis of Large Deflection and Stability Problems", Proceedings of the First Air Force Conference on Matrix Methods in Structural Mechanics, AFFDL-TR-66-80, November, 1965.
14. Mallett, R. H., and Marcal, P.V., "Finite Element Analysis on Nonlinear Structures", Proceedings, ASCE, Journal of the Structures Division, Vol.94, No.ST9, September 1968.
15. Berke, L., and Mallett, R. H., "Automated Large Deflection and Stability Analysis of Three-Dimensional Bar Structures", Proceedings, Structures Technology for Large Radio and Radal Telescope Systems, MIT Press, 1969.
16. Martin, H. C., and Carey, G. F., "Introduction to Finite Element Analysis, First Edition, McGraw-Hill Book Company, Inc., 1973.
17. Martin, H. C., Finite Elements and The Analysis of Geometrically Nonlinear Problems, in "Recent Advances in Matrix Mehtods in Structural Analysis and Design", R. H. Gallagher, S. Y. Yamada and J. T. Oden (eds.), Proc., Japan-U.S. Seminar Matrix Methods Struct. Analysis and Design, Tokyo, August 25-30, 1969, University of Alabama Press, 1970.
18. Przemieniecki, J. S., "Theory of Matrix Structural Analysis", First Edition, McGraw-Hill Book Co., 1968.
19. Gerstle, K. H., "Basic Structural Analysis", Prentice-Hall, Inc. Englewood Cliffs, New Jersey, 1974.
20. IBM Application program, (360A-CM-03X), System/360 Scientific Subroutine Package, H20-0205-3, Version III, Programmer's Manual.
21. F. K. Bogner, R. L. Fox and L. A. Schmit, Jr., "The Generation of Iner-Element-Compatible Stiffness and Mass Matrices by the Use of Interpolation Formulas", Matrix Method in Structure Mechanics, AFFDL-TR-66-80, November, 1966.
22. Prof. Monforton, G.R., Ph.D. 1976, Private Communication

VITA AUCTORIS

The author was born in Shebeen-El-Kom, Egypt, on October 25, 1950. He obtained his secondary education from Lotfy El-Sayed School at Giza, graduating in 1968.

In September 1968 he entered the Faculty of Engineering, Cairo University, Giza. In July 1973 he received the B.Sc. degree in Civil Engineering from that university with general appreciation Distinction with Honor Degree. During his studies in Cairo University he was granted financial aid as a reward.

In the period 1973 to 1975 he worked as a Teaching Assistant in the Structural Engineering Department at Cairo University.

He came to Canada in September 1975 and started doing his graduate work in Civil Engineering at the University of Windsor.